Doctoral Thesis

Charge Redistribution Near the Surfaces of Superconductors

(超伝導体における表面電荷)

EZEKIEL SAMBO JOSHUA
Graduate School of Science, Hokkaido University
Department of Physics

March, 2020

Contents

Acknowledgements

My first sincere gratitude goes to my supervisor, Professor Takafumi Kita, for his invaluable support and illuminating discussions. Through his inspiration I have learnt how to learn, unlearn and re-learn.

I would like to thank Professor Migaku Oda and Professor Koji Nemoto for their comments and suggestions in the process of the review of this thesis.

I am truly indebted to Dr. Hikaru Ueki for everything. I can not thank him enough for his collaboration and immense help.

I would like to also thank Mr. Wataru Kohno for his collaboration and for not withholding his very critical opinions regarding the study which led to this thesis and also Ms. Marie Ohuchi for her collaboration and many insightful discussions and comments. I would also like to thank all members of the Condensed Matter Theory II Laboratory (Kita Group) for their support and encouragements.

I would like to say a big thank you to my adorable wife Zipporah and my son Hideki for their love and cheer.

I thankfully acknowledge the financial support received from the Ministry of Education, Culture, Sports, Science, and Technology (MEXT) of Japan, through the . Above all, thanks to the Almighty who makes all things possible.

The computations in this thesis were carried out using the facilities of the Supercomputer Center, the Institute for Solid State Physics, the University of Tokyo.

Dedication

To my parents, for teaching me how to live before their passing.

1 Introduction

1.1 Forces acting on charged particles

From the viewpoint of fundamental physics, electrostatic charge redistribution implies the action of certain forces on charged particles. For instance, in normal metals[1], semiconductors[2] as well as in superconductors[3, 4, 5], the magnetic Lorentz force

$$\mathbf{F}_{\text{Lorentz}} = (q\mathbf{v} \times \mathbf{B}), \tag{1.1}$$

where $\mathbf{B}$, $\mathbf{v}$ and q are the magnetic field, particle velocity and charge (charge distribution), respectively, results in the Hall effect. However, exclusively in superconductors, besides the Lorentz force which is included as a necessary ingredient in London's phenomenological theory of superconductivity, other forces are expected to be present even in the absence of external or spontaneous magnetic fields, namely; the pair-potential (Δ) gradient (PPG) force[6, 7, 8]

$$\mathbf{F}_{\text{PPG}} \propto \frac{\partial \Delta}{\partial \boldsymbol{r}}, \tag{1.2}$$

which originates from the spatial variation of the pair potential, and another force originating from the pressure due to the slope of the density of states (DOS) in the normal states at the Fermi level[9, 10, 11]

$$\mathbf{F}_{\text{SDOS}} \propto \frac{N'(\mu_n)}{N(\mu_n)}. \tag{1.3}$$

Where $N'(\mu_n)/N(\mu_n)$ is the slope of DOS in the normal states at the Fermi level between the normal and the superconducting regions. These three forces bring about electron-hole asymmetry which induces the redistribution of charged particles in both the Meissner and the vortex state in type-II superconductors and are also expected in the presence of surfaces and interfaces. Charge redistribution in superconductors occurs in order to balance the electrochemical potential between the normal regions and the superconducting regions. For a complete understanding of the mechanism of electric charging in superconductors, it is imperative to account for all three forces within a microscopic theory.

1.2 Augmented quasiclassical equations

Quite recently, the augmented quasiclassical equations incorporating the three-force-terms were derived, with the standard Eilenberger equations[12, 13] as the leading-order contributions and the force terms as first-order quantum corrections in terms of the quasiclassical parameter $\delta \equiv (k_{\text{F}}\xi_0)^{-1} \ll 1$, where k_{F} is the Fermi wave number and ξ_0 is the coherence length at zero temperature[4, 7, 11], and are expressed in the Matsubara formalism as

$$\begin{aligned}&\left[i\varepsilon_n\hat{\tau}_3 - \hat{\Delta}\hat{\tau}_3, \hat{g}\right] + i\hbar\boldsymbol{v}_\mathrm{F}\cdot\boldsymbol{\partial}\hat{g}\\&\quad + \frac{i\hbar}{2}\left\{\boldsymbol{\partial}\hat{\Delta}\hat{\tau}_3, \boldsymbol{\partial}_{\boldsymbol{p}_\mathrm{F}}\hat{g}\right\} - \frac{i\hbar}{2}\left\{\boldsymbol{\partial}_{\boldsymbol{p}_\mathrm{F}}\hat{\Delta}\hat{\tau}_3, \boldsymbol{\partial}\hat{g}\right\}\\&\qquad + \frac{i\hbar}{2}e\boldsymbol{v}_\mathrm{F}\cdot\left(\boldsymbol{B}\times\frac{\partial}{\partial\boldsymbol{p}_\mathrm{F}}\right)\{\hat{\tau}_3, \hat{g}(\varepsilon_n, \boldsymbol{p}_\mathrm{F}, \boldsymbol{r})\} = \hat{0},\end{aligned} \tag{1.4}$$

where $\check{g} = \check{g}(\varepsilon_n, \boldsymbol{p}_\mathrm{F}, \boldsymbol{r})$ is the quasiclassical Green's function, $\check{\Delta} = \check{\Delta}(\boldsymbol{p}_\mathrm{F}, \boldsymbol{r})$ is the pair potential, ε_n is the Matsubara energy, $\boldsymbol{v}_\mathrm{F}$ is the Fermi velocity, and $\boldsymbol{p}_\mathrm{F}$ is the Fermi momentum. Matrix $\check{\tau}_3$ denotes

$$\check{\tau}_3 = \begin{bmatrix}\hat{\tau}_3 & \hat{0}\\ \hat{0} & \hat{\tau}_3\end{bmatrix}, \quad \hat{\tau}_3 = \begin{bmatrix}\underline{\sigma}_0 & 0\\ 0 & -\underline{\sigma}_0\end{bmatrix}, \tag{1.5}$$

with $[\hat{a}, \hat{b}] \equiv \hat{a}\hat{b} - \hat{b}\hat{a}$, and $\{\hat{a}, \hat{b}\} \equiv \hat{a}\hat{b} + \hat{b}\hat{a}$.

1.2.1 Meissner state charging

In the presence of a very weak magnetic field $\boldsymbol{B}$ (below the lower critical field), superconductors show perfect diamagnetic behaviours. Furthermore, the Lorentz force acting on equilibrium supercurrents induces the redistribution of charge towards the surface of the sample and a Hall electric field emerges. This goes on until a time when the electric field due to the surface charge balances the the magnetic Lorentz force acting on supercurrents and equilibrium is reached. The induced electric field in the Meissner state $\boldsymbol{E}_M$ is given by [5, 14]

$$\boldsymbol{E}_M = \boldsymbol{B}\times\underline{R}_H\boldsymbol{j}_s \tag{1.6}$$

Where $\underline{R}_H$ is the Hall coefficient and $\boldsymbol{j}_s$ is the current flowing along the edge of the sample. This expression for the electric field agrees reasonably with the prediction of London theory. Moreover, in the case of anisotropic superconductors, the information about the electronic band structure is contained in the expression for the Hall coefficient given by [14]

$$\underline{R}_\mathrm{H} \equiv \frac{1}{2eN(0)}\left\langle\frac{\partial}{\partial\boldsymbol{p}_F}(1-Y)\boldsymbol{v}_F\right\rangle_F \langle\boldsymbol{v}_F(1-Y)\boldsymbol{v}_F\rangle_F^{-1}, \tag{1.7}$$

where $Y \equiv Y(\boldsymbol{p}_F, T)$ is the Yosida function and is expressed as

$$Y(\boldsymbol{p}_F, T) = 1 - 2\pi k_\mathrm{B}\mathrm{T}\sum_{n=-\infty}^{\infty}\frac{|\Delta|^2\phi\bar{\phi}}{2(|\varepsilon_n|^2 + |\Delta|^2\phi\bar{\phi})^{3/2}} \tag{1.8}$$

Here ϕ is the basis function of the energy gap, k_B and T denoting the Boltzmann constant and temperature, respectively. The electric field induced in the Meissner state shows a sign change with temperature dependence[14] for materials with anisotropic Fermi surface and energy gap and also at specific doping levels, due to the Fermi surface curvature. The Fermi surface curvature and gap anisotropy result in the anisotropic redistribution of thermally excited quasiparticles, hence the sign change. Fermi surface and gap anisotropies are therefore very crucial to understanding both the magnitude and sign of electric charge in superconductors.

1.2.2 Vortex charging

The augmented quasiclassical equations have been used in the study of electric charging of a single superconducting vortex and also for the charging of the Abrikosov lattice system [8, 5, 11, 15, 16, 17]. It has been shown that in the vortex core of an isotropic type-II superconductor the PPG force gives up to 10 to 10^2 times larger contribution to charging effect compared to the Lorentz force[8]. Even more recently, Ueki *et al.* found that the SDOS pressure gives the dominant contribution near the transition temperature, while the PPG force dominates as the temperature approaches zero[11]. Masaki studied the charged and uncharged vortices in a chiral p-wave superconductor based on the augmented quasiclassical equations. He pointed out that the vortex-core charge is dominated by the contribution of the angular derivative terms in the PPG force terms[15]. Using a simplified picture of a system consisting of a vortex core in the normal state, surrounded by a superconducting material, Khomskii *et al.* showed that a finite difference in chemical potential $\delta\mu \neq 0$ between the normal and the superconducting subsystems results in the the redistribution of charge[9, 10].

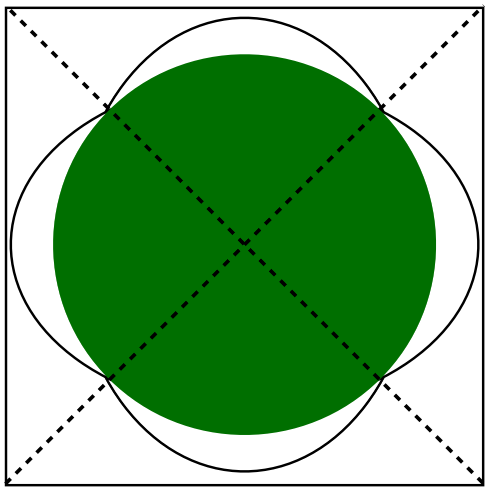

Figure 1: A schematic of the gap structure for the $d_{x^2-y^2}$ pairing state with gap nodal lines (diagonal dashed lines).

1.3 Surface systems

In the context of surface charging, Furusaki *et al.* studied spontaneous surface charging in chiral p-wave superconductors based on the Bogoliubov–de Gennes equations. They found two contributions, one contribution originates from the Lorentz force due to the spontaneous edge currents, while the other contribution has topological origin and is related to the intrinsic angular momentum of the Cooper pairs[18]. Emig *et al.* also showed using a phenomenological analysis on the basis of Ginzburg–Landau theory that the presence of surfaces in d-wave superconductors can induce charge inhomogeneity due to the suppression of the energy gap[19].

In a $d_{x^2-y^2}$-wave superconductor (the gap structure for the $d_{x^2-y^2}$ pairing state is shown in Fig. 1) with a specularly reflective surface cut along the [110] direction i.e. along the nodal lines, the order parameter is suppressed [20, 21, 22] near the surface and vanishes at the surface due to a change in its sign along the classical quasiparticle trajectories. This sign change also results in the formation of zero energy states (ZES) near (at) the edges of these materials[26, 25, 23, 24, 27]. ZES in d-wave superconductors are detectable through the observation of zero-bias conductance peaks in the spectra of scanning tunneling spectroscopy at oriented surfaces of the d-wave crystals[28, 29, 30]. Figure 2 shows the normalized conductance measured for grains of cuprate superconductors[31]. Hayashi *et al.* discussed the connection between the Caroli–de Gennes–Matricon states[32] at the vortex core of an s-wave superconductor and the occurrence of electric charge[33]. They concluded that the particle-hole asymmetry inside the vortex core observed through the local density of states (LDOS) implies the corresponding existence of charge at the vortex core. Recently, Masaki also discussed the connection between particle-hole asymmetry and vortex charging in superconductors[15]. Surface charging in d-wave superconductors may also have a similar connection with particle-hole asymmetry in the LDOS, which is expected to appear due to first-order quantum corrections within the augmented quasi-classical theory.

1.4 Motivation

Several studies have been carried out on the charging effect in the vortex state of superconductors based on microscopic theories, these have inspired a lot of experimental efforts leading to a better understanding of the electrodynamics of superconductors in the vortex state. On the other hand, surface charge in superconductors remains unexplored or at best previous studies on surface charge have been mostly based on phenomenological approaches, despite the rich physics inherent at the surfaces of superconductors, especially in systems with anisotropic energy gap and/or Fermi surface. In fact, even in the absence of magnetic fields, surface effects in d-wave superconductors result in the appearance of the PPG force due to the suppression of the pair potential near the surface and the pressure

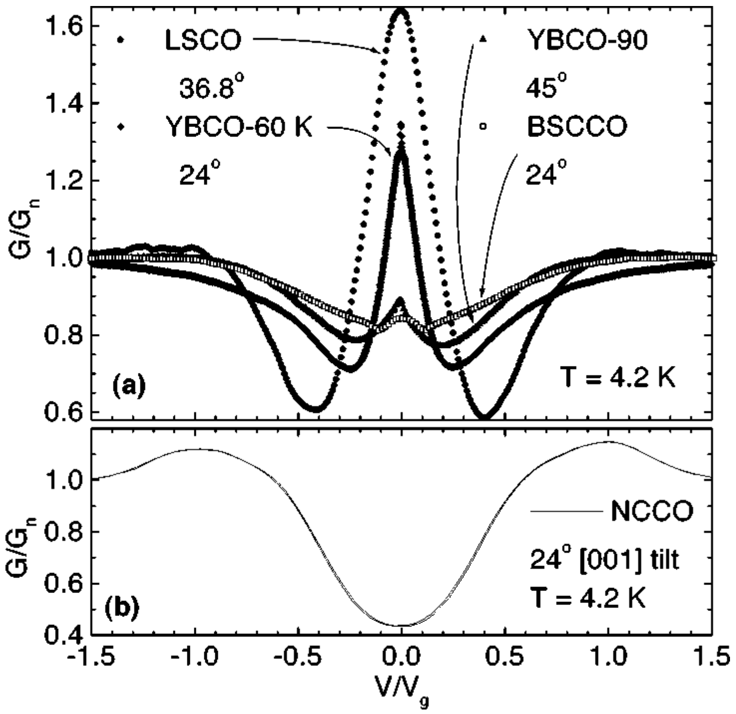

Figure 2: Normalized conductance vs normalized voltage of oriented grain boundaries of cuprate superconductors at $T = 4.2K$.

due to the SDOS at the Fermi level. Hence the presence of oriented surfaces in d-wave superconductors is expected to be accompanied by the redistribution of charged particles.

Experiments by Bok and Klein [34] followed by Morris and Brown [35] successfully circumvented the difficulties encountered in the earlier attempts at the measurement of Hall voltage in superconductors by applying capacitive couplings to the samples. Although, such measurement have not been carried out on materials with gap and Fermi surface anisotropy yet. There is also the possibility of observing qualitative signatures of electric charging by observing electron-hole asymmetry in the local density of states in the tunnelling spectra of superconductors, such as the cuprates.

In this study, we have carried out a microscopic investigation of the spontaneous surface charge on a semi-finite $d_{x^2-y^2}$ superconductor cut along the [110] direction due to the PPG force and the SDOS pressure. Moreover, the SDOS pressure gives the dominant contribution to the surface charge for the realistic electron-fillings $n = 0.8$, 0.9, and 1.15 at all temperatures. We also observe zero energy Andreev bound states at the surface of the d-wave superconductor, which manifest themselves in the zero energy peaks in local density of states within the augmented quasiclassical theory. We further highlight that the particle-hole asymmetry in the local density of states due to the PPG force and the SDOS pressure is a qualitative evidence of electric charging. This particle-hole asymmetry may be observed in experiments.

This thesis is organized as follows. In Sect. 2, we derive the augmented quasiclassical equations of superconductivity in the Matsubara formalism, with the three force terms which are responsible for charging. In Sect. 3, we apply the augmented quasiclassical equations to perform a microscopic study on the spontaneous charge redistribution near the surface of a d-wave superconductor cut along the [110] direction. We also calculate the local density of states within the augmented quasiclassical theory. In Sect. 4, we give a general summary of the content of this thesis, as well as our conclusion.

2 General Augmented Quasiclassical Theory

In this chapter, we review the formulation of the augmented Eilenberger equations in the Matsubara formalism taking into account the three force terms namely; the Lorentz force, the pair potential gradient force and the pressure due to the slope of density of states in the normal states at the Fermi level. For simplicity, we consider the spin-singlet pairing state. To this end, we follow the derivation in earlier works [5, 11, 13].

2.1 Augmented Eilenberger equations

The augmented quasiclassical equations given in the Matsubara formalism are expressed as

$$\begin{aligned}&\left[i\varepsilon_n\hat{\tau}_3-\hat{\Delta}\hat{\tau}_3,\hat{g}\right]+i\hbar\boldsymbol{v}_{\mathrm{F}}\cdot\boldsymbol{\partial}\hat{g}\\&\quad+\frac{i\hbar}{2}\left\{\boldsymbol{\partial}\hat{\Delta}\hat{\tau}_3,\boldsymbol{\partial}_{\boldsymbol{p}_{\mathrm{F}}}\hat{g}\right\}-\frac{i\hbar}{2}\left\{\boldsymbol{\partial}_{\boldsymbol{p}_{\mathrm{F}}}\hat{\Delta}\hat{\tau}_3,\boldsymbol{\partial}\hat{g}\right\}\\&\quad+\frac{i\hbar}{2}e\boldsymbol{v}_{\mathrm{F}}\cdot\left(\boldsymbol{B}\times\frac{\partial}{\partial\boldsymbol{p}_{\mathrm{F}}}\right)\{\hat{\tau}_3,\hat{g}(\varepsilon_n,\boldsymbol{p}_{\mathrm{F}},\boldsymbol{r})\}=\hat{0},\end{aligned}\tag{2.1}$$

where $\check{g}=\check{g}(\varepsilon_n,\boldsymbol{p}_{\mathrm{F}},\boldsymbol{r})$ is the quasiclassical Green's function, $\check{\Delta}=\check{\Delta}(\boldsymbol{p}_{\mathrm{F}},\boldsymbol{r})$ is the superconducting pair potential, ε_n is the Matsubara energy, $\boldsymbol{v}_{\mathrm{F}}$ is the Fermi velocity, and $\boldsymbol{p}_{\mathrm{F}}$ is the Fermi momentum.

The gauge-invariant operator $\boldsymbol{\partial}$ is given by

$$\boldsymbol{\partial}\equiv\begin{cases}\boldsymbol{\nabla} & :\text{ on }\hat{g}\text{ or }\hat{g}^*\\ \boldsymbol{\nabla}-i\dfrac{2e}{\hbar}\boldsymbol{A}(\boldsymbol{r}) & :\text{ on }\hat{f}\\ \boldsymbol{\nabla}+i\dfrac{2e}{\hbar}\boldsymbol{A}(\boldsymbol{r}) & :\text{ on }\hat{f}^*\end{cases},\tag{2.2}$$

Matrix $\check{\tau}_3$ denotes

$$\check{\tau}_3=\begin{bmatrix}\hat{\tau}_3 & \hat{0}\\ \hat{0} & \hat{\tau}_3\end{bmatrix},\quad\hat{\tau}_3=\begin{bmatrix}\underline{\sigma}_0 & 0\\ 0 & -\underline{\sigma}_0\end{bmatrix},\tag{2.3}$$

with $[\hat{a},\hat{b}]\equiv\hat{a}\hat{b}-\hat{b}\hat{a}$ and $\{\hat{a},\hat{b}\}\equiv\hat{a}\hat{b}+\hat{b}\hat{a}$.

The quasiclassical Green's function is defined as

$$\begin{aligned}\hat{g}(\varepsilon_n,\boldsymbol{p}_{\mathrm{F}},\boldsymbol{r})&\equiv\mathrm{P}\int_{-\infty}^{\infty}\frac{d\xi_{\boldsymbol{p}}}{\pi}i\hat{\tau}_3\hat{G}(\varepsilon_n,\boldsymbol{p},\boldsymbol{r})\\&\equiv\begin{bmatrix}\underline{g}(\varepsilon_n,\boldsymbol{p}_{\mathrm{F}},\boldsymbol{r}) & -i\underline{f}(\varepsilon_n,\boldsymbol{p}_{\mathrm{F}},\boldsymbol{r})\\ -i\underline{f}^*(\varepsilon_n,-\boldsymbol{p}_{\mathrm{F}},\boldsymbol{r}) & -\underline{g}^*(\varepsilon_n,-\boldsymbol{p}_{\mathrm{F}},\boldsymbol{r})\end{bmatrix},\end{aligned}\tag{2.4}$$

where P denotes the principal value and $\hat{G}(\varepsilon_n,\boldsymbol{p},\boldsymbol{r})$ is the Green's function of Gorkov's equation. The definition of the Green's function starting from the second quantised field operators and the derivation of Eq. (2.1) is given in Appendix.

2.2 Local density of states

The local density of states (LDOS) can be expressed as

$$N_{\rm s}(\varepsilon,\boldsymbol{r}) \equiv -{\rm Tr}\int \frac{d^3p}{(2\pi\hbar)^3}\frac{1}{2\pi}{\rm Im}\underline{G}^{\rm R}(\varepsilon,\boldsymbol{p},\boldsymbol{r}) \tag{2.5}$$

where $\underline{G}^{\rm R}(\varepsilon,\boldsymbol{p},\boldsymbol{r}) \equiv \underline{G}(\varepsilon_n \to -i\varepsilon+\eta,\boldsymbol{p},\boldsymbol{r})$ is the retarded Green's function with η denoting an infinitesimal positive constant.

We replace the momentum integral using

$$\int \frac{d^3p}{(2\pi\hbar)^3} = \int_{-\infty}^{\infty} d\xi_{\boldsymbol{p}} N(\xi_{\boldsymbol{p}}+\mu-e\Phi(\boldsymbol{r}))\int\frac{d\Omega_{\boldsymbol{p}}}{4\pi}. \tag{2.6}$$

Where the differential $d\Omega_{\boldsymbol{p}}$ is the increment of the solid angle in the momentum space defined based on the structure of the Fermi surface. For example, for a spherical Fermi surface, $d\Omega_{\boldsymbol{p}}$ may be expressed as

$$\int d\Omega_{\boldsymbol{p}} = \int_0^{\pi} d\theta_{\boldsymbol{p}}\sin\theta_{\boldsymbol{p}}\int_0^{2\pi} d\varphi_{\boldsymbol{p}}. \tag{2.7}$$

The LDOS now becomes

$$N_{\rm s}(\varepsilon,\boldsymbol{r}) = -{\rm Tr}\int_{-\infty}^{\infty} d\xi_{\boldsymbol{p}} N(\xi_{\boldsymbol{p}}+\mu-e\Phi(\boldsymbol{r}))\int\frac{d\Omega_{\boldsymbol{p}}}{4\pi}\frac{1}{2\pi}{\rm Im}\underline{G}^{\rm R}(\varepsilon,\boldsymbol{p},\boldsymbol{r}), \tag{2.8}$$

$N(\xi_{\boldsymbol{p}}+\mu-e\Phi(\boldsymbol{r})) \equiv N(\epsilon)$ denotes the normal DOS and is defined by

$$N(\epsilon) \equiv \int \frac{d^3p}{(2\pi\hbar)^3}\delta(\epsilon-\varepsilon_{\boldsymbol{p}}). \tag{2.9}$$

We here make the following important assumptions regarding the variations of the density of states;

(i) the superconducting DOS approaches the normal state DOS as the single-particle energy increases

(ii) the energy variation of the normal DOS is slow.

Consequent upon these assumptions, the superconducting DOS in Eq. (2.8) may be expressed in terms of $\underline{g}$ and $\underline{g}^{(1)}$. To this end, we expand $N(\epsilon)$ at $\epsilon = \mu - e\Phi(\boldsymbol{r})$ as

$$N(\xi_{\boldsymbol{p}}+\mu-e\Phi(\boldsymbol{r})) \approx N(\mu-e\Phi(\boldsymbol{r})) + N'(\mu-e\Phi(\boldsymbol{r}))\xi_{\boldsymbol{p}}. \tag{2.10}$$

Using $N'(\mu_{\rm n})\Delta_0/N(\mu_{\rm n}) = O(\delta)$, $\delta\mu/\Delta_0 = O(\delta)$, and $|e|\Phi/\Delta_0 = O(\delta)$, we obtain

$$N(\mu-e\Phi(\boldsymbol{r})) = N(\mu_{\rm n})[1+O(\delta^2)]. \tag{2.11}$$

Here Δ_0 denotes the energy gap at zero temperature, and $\delta\mu$ is the chemical potential difference between the normal and superconducting states, and is defined by $\delta\mu \equiv \mu -$

$\mu_{\rm n}$ with $\mu_{\rm n}$ denoting the chemical potential in the normal state. Thus, we rewrite the expansion of $N(\xi_{\boldsymbol{p}} + \mu - e\Phi(\boldsymbol{r}))$ as

$$N(\xi_{\boldsymbol{p}} + \mu - e\Phi(\boldsymbol{r})) \approx N(\mu_{\rm n}) + N'(\mu_{\rm n})\xi_{\boldsymbol{p}}. \tag{2.12}$$

Substituting it into Eq. (2.8) and using Eqs. (A.27), (A.30), and (A.32), we obtain the superconducting LDOS as

$$\begin{aligned}
&N_{\rm s}(\varepsilon, \boldsymbol{r}) \\
&\approx \frac{N(\mu_{\rm n})}{2}{\rm Tr}\int\frac{d\Omega_{\boldsymbol{p}}}{4\pi}\Bigg\{{\rm Re}\underline{g}^{\rm R}(\varepsilon, \boldsymbol{p}_{\rm F}, \boldsymbol{r}) + \frac{N'(\mu_{\rm n})}{N(\mu_{\rm n})}\varepsilon{\rm Re}\underline{g}^{\rm R}(\varepsilon, \boldsymbol{p}_{\rm F}, \boldsymbol{r}) \\
&\quad + \frac{1}{2}\frac{N'(\mu_{\rm n})}{N(\mu_{\rm n})}{\rm Im}\left[\underline{\Delta}(\boldsymbol{p}_{\rm F}, \boldsymbol{r})\underline{\bar{f}}^{\rm R}(\varepsilon, \boldsymbol{p}_{\rm F}, \boldsymbol{r}) + \underline{f}^{\rm R}(\varepsilon, \boldsymbol{p}_{\rm F}, \boldsymbol{r})\underline{\bar{\Delta}}(\boldsymbol{p}_{\rm F}, \boldsymbol{r})\right]\Bigg\} \\
&\quad \times \theta(|\tilde{\varepsilon}_{\rm c}| - |\varepsilon|) + N(\varepsilon + \mu - e\Phi(\boldsymbol{r}))\theta(|\varepsilon| - |\tilde{\varepsilon}_{\rm c}|),
\end{aligned} \tag{2.13}$$

where the retarded Green's functions and barred functions in the Keldysh formalism are defined generally by $\underline{g}^{\rm R}(\varepsilon, \boldsymbol{p}_{\rm F}, \boldsymbol{r}) \equiv \underline{g}(\varepsilon_n \to -i\varepsilon + \eta, \boldsymbol{p}_{\rm F}, \boldsymbol{r})$ and $\underline{\bar{g}}^{\rm R}(\varepsilon, \boldsymbol{p}_{\rm F}, \boldsymbol{r}) \equiv \underline{g}^{\rm R*}(-\varepsilon, -\boldsymbol{p}_{\rm F}, \boldsymbol{r})$, respectively. The cutoff energy $\tilde{\varepsilon}_{\rm c} > 0$ is determined such that it satisfies the relation

$$\int_{-\tilde{\varepsilon}_{\rm c}}^{\tilde{\varepsilon}_{\rm c}} N_{\rm s}(\varepsilon, \boldsymbol{r})d\varepsilon = \int_{-\tilde{\varepsilon}_{\rm c}}^{\tilde{\varepsilon}_{\rm c}} N(\varepsilon + \mu - e\Phi)d\varepsilon. \tag{2.14}$$

2.3 Pair potential

Here we express the self-consistency equation for the superconducting pair potential using the quasiclassical Green's function. Using Eqs. (A.17b), (A.20b), and putting

$$\mathcal{V}(|\bar{\boldsymbol{r}}_{12}|) = \int\frac{dp^3}{(2\pi\hbar)^3}\mathcal{V}_p {\rm e}^{i\boldsymbol{p}\cdot\bar{\boldsymbol{r}}_{12}/\hbar}, \tag{2.15}$$

in Eq. (A.15), we obtain $\underline{\Delta}(\boldsymbol{p}, \boldsymbol{r}_{12})$ as

$$\underline{\Delta}(\boldsymbol{p}, \boldsymbol{r}_{12}) = \int\frac{dp'^3}{(2\pi\hbar)^3}\mathcal{V}_{|\boldsymbol{p}-\boldsymbol{p}'|}k_{\rm B}T\sum_{n=-\infty}^{\infty}\underline{F}(\varepsilon_n, \boldsymbol{p}', \boldsymbol{r}_{12}). \tag{2.16}$$

Furthermore, we expand the interaction $\mathcal{V}_{|\boldsymbol{p}-\boldsymbol{p}'|}$ in terms of the surface harmonics $Y_{lm}(\hat{\boldsymbol{p}})$ as

$$\mathcal{V}_{|\boldsymbol{p}-\boldsymbol{p}'|} = \sum_{l=0}^{\infty}\mathcal{V}_l(\boldsymbol{p}, \boldsymbol{p}')\sum_{m=-l}^{l}4\pi Y_{lm}(\hat{\boldsymbol{p}})Y_{lm}^*(\hat{\boldsymbol{p}}'), \tag{2.17}$$

We note here that $l = 0, 1, 2$ corresponds to s-wave, p-wave and d-wave pairing, respectively. Hence, we here assume that only a single l is relevant. Using Eq. (2.6), Eq. (2.16) becomes

$$\begin{aligned}
\underline{\Delta}(\boldsymbol{p}, \boldsymbol{r}) = &\int_{-\infty}^{\infty}d\xi_{\boldsymbol{p}'}N(\xi_{\boldsymbol{p}'} + \mu - e\Phi(\boldsymbol{r}))\int\frac{d\Omega_{\boldsymbol{p}'}}{4\pi} \\
&\times \mathcal{V}_l(\boldsymbol{p}, \boldsymbol{p}')\sum_{m=-l}^{l}4\pi Y_{lm}(\hat{\boldsymbol{p}})Y_{lm}^*(\hat{\boldsymbol{p}}')k_{\rm B}T\sum_{n=-\infty}^{\infty}\underline{F}(\varepsilon_n, \boldsymbol{p}', \boldsymbol{r}).
\end{aligned} \tag{2.18}$$

Assuming a constant and weak-coupling interaction, we can rewrite the interaction potential as $\mathcal{V}_l(\boldsymbol{p}, \boldsymbol{p}') = \mathcal{V}_l^{(\mathrm{eff})}\theta(\varepsilon_\mathrm{c} - |\xi_{\boldsymbol{p}}|)\theta(\varepsilon_\mathrm{c} - |\xi_{\boldsymbol{p}'}|)$, with $\mathcal{V}_l^{(\mathrm{eff})}$ denoting the constant effective potential, and ε_c is the cutoff energy [13]. We can also rewrite Eq. (2.18) as

$$\underline{\Delta}(\boldsymbol{p}, \boldsymbol{r}) = \int_{-\varepsilon_\mathrm{c}}^{\varepsilon_\mathrm{c}} d\xi_{\boldsymbol{p}'} N(\xi_{\boldsymbol{p}'} + \mu - e\Phi(\boldsymbol{r})) \int \frac{d\Omega_{\boldsymbol{p}'}}{4\pi} \times \mathcal{V}_l^{(\mathrm{eff})} \sum_{m=-l}^{l} 4\pi Y_{lm}(\hat{\boldsymbol{p}}) Y_{lm}^*(\hat{\boldsymbol{p}}') k_\mathrm{B}T \sum_{n=-n_\mathrm{c}}^{n_\mathrm{c}} \underline{F}(\varepsilon_n, \boldsymbol{p}', \boldsymbol{r}), \tag{2.19}$$

where the cutoff n_c is determined from $(2n_\mathrm{c} + 1)\pi k_\mathrm{B}T = \varepsilon_\mathrm{c}$ [13]. Using Eqs. (A.27), (A.30), (A.32), and (2.12), we see that only the value at $\boldsymbol{p} = \boldsymbol{p}_\mathrm{F}$ contributes to $\underline{\Delta}(\boldsymbol{p}, \boldsymbol{r})$ as

$$\underline{\Delta}(\boldsymbol{p}_\mathrm{F}, \boldsymbol{r}) \approx -\mathcal{V}_l^{(\mathrm{eff})} N(\mu_\mathrm{n}) \int \frac{d\Omega_{\boldsymbol{p}'}}{4\pi} \sum_{m=-l}^{l} 4\pi Y_{lm}(\hat{\boldsymbol{p}}) Y_{lm}^*(\hat{\boldsymbol{p}}') \times \pi k_\mathrm{B}T \sum_{n=-n_\mathrm{c}}^{n_\mathrm{c}} \left\{ \underline{f}(\varepsilon_n, \boldsymbol{p}'_\mathrm{F}, \boldsymbol{r}) - \frac{i}{2}\frac{N'(\mu_\mathrm{n})}{N(\mu_\mathrm{n})} \left[\underline{\Delta}(\boldsymbol{p}'_\mathrm{F}, \boldsymbol{r}) \underline{\bar{g}}(\varepsilon_n, \boldsymbol{p}'_\mathrm{F}, \boldsymbol{r}) - \underline{g}(\varepsilon_n, \boldsymbol{p}'_\mathrm{F}, \boldsymbol{r}) \underline{\Delta}(\boldsymbol{p}'_\mathrm{F}, \boldsymbol{r}) \right] \right\}, \tag{2.20}$$

where the barred functions in the Matsubara formalism are defined generally by $\underline{\bar{g}}(\varepsilon_n, \boldsymbol{p}_\mathrm{F}, \boldsymbol{r}) \equiv \underline{g}^*(\varepsilon_n, -\boldsymbol{p}_\mathrm{F}, \boldsymbol{r})$. Expanding $\underline{\Delta}(\mathbf{p}_\mathrm{F}, \mathbf{r})$ with respect to the surface harmonics as

$$\underline{\Delta}(\boldsymbol{p}_\mathrm{F}, \boldsymbol{r}) = \sum_{m=-l}^{l} \underline{\Delta}_{lm}(\mathbf{r}) \sqrt{4\pi} Y_{lm}(\hat{\boldsymbol{p}}), \tag{2.21}$$

the self-consistency equation for the pair potential is given by

$$\underline{\Delta}_{lm}(\mathbf{r}) = 2\pi \mathrm{g}_0 k_\mathrm{B}T \sum_{n=0}^{n_\mathrm{c}} \int \frac{d\Omega_\mathbf{p}}{4\pi} \sqrt{4\pi} Y_{lm}^*(\hat{\boldsymbol{p}}) \left\{ \underline{f}(\varepsilon_n, \boldsymbol{p}_\mathrm{F}, \boldsymbol{r}) - \frac{i}{2}\frac{N'(\mu_\mathrm{n})}{N(\mu_\mathrm{n})} \left[\underline{\Delta}(\boldsymbol{p}_\mathrm{F}, \boldsymbol{r}) \underline{\bar{g}}(\varepsilon_n, \boldsymbol{p}_\mathrm{F}, \boldsymbol{r}) - \underline{g}(\varepsilon_n, \boldsymbol{p}_\mathrm{F}, \boldsymbol{r}) \underline{\Delta}(\boldsymbol{p}_\mathrm{F}, \boldsymbol{r}) \right] \right\}, \tag{2.22}$$

where $\mathrm{g}_0 \equiv -\mathcal{V}_l^{(\mathrm{eff})} N(\mu_\mathrm{n})$ denotes the coupling constant. Neglecting the spin magnetism, we write the quasiclassical Green's function in matrix form as $\underline{g} = g\underline{\sigma}_0$. Consequently, the gap equation [Eq. (2.22)] reduces to the self-consistency expression for the pair potential in the Eilenberger equations.

2.4 Expressions for charge density and electric field

To obtain general expressions for the charge density and the induced electric field, we write the charge density using the quasiclassical Green's function. As a starting point, we introduce the electron density $n(\boldsymbol{r})$ as [11, 13]

$$n(\boldsymbol{r}) = k_{\mathrm{B}}T\mathrm{Tr}\sum_{n=-\infty}^{\infty}\underline{G}(\boldsymbol{r},\boldsymbol{r};\varepsilon_n)\mathrm{e}^{-i\varepsilon_n 0_-} = 2\int_{-\infty}^{\infty}d\varepsilon N_{\mathrm{s}}(\varepsilon,\boldsymbol{r})f(\varepsilon), \tag{2.23}$$

where $f(\varepsilon) = 1/\left[\mathrm{e}^{\varepsilon/k_{\mathrm{B}}T}+1\right]$ is the fermion distribution function. Substituting Eq. (2.13) into Eq. (2.23), we rewrite the electron density in terms of $\underline{g}^{\mathrm{R}}$ and $\underline{g}^{\mathrm{R}(1)}$ as

$$\begin{aligned}
n(\boldsymbol{r}) \approx\; & N(\mu_{\mathrm{n}})\mathrm{Tr}\int_{-\tilde{\varepsilon}_{\mathrm{c}}}^{\tilde{\varepsilon}_{\mathrm{c}}}d\varepsilon f(\varepsilon) \\
& \times\int\frac{d\Omega_{\boldsymbol{p}}}{4\pi}\left[\mathrm{Re}\underline{g}^{\mathrm{R}}(\varepsilon,\boldsymbol{p}_{\mathrm{F}},\boldsymbol{r})+\frac{N'(\mu_{\mathrm{n}})}{N(\mu_{\mathrm{n}})}\mathrm{Re}\underline{g}^{\mathrm{R}(1)}(\varepsilon,\boldsymbol{p}_{\mathrm{F}},\boldsymbol{r})\right] \\
& +2\int_{-\infty}^{\infty}d\varepsilon\frac{N(\varepsilon+\mu-e\Phi(\boldsymbol{r}))}{\mathrm{e}^{\varepsilon/k_{\mathrm{B}}T}+1}-2\int_{-\tilde{\varepsilon}_{\mathrm{c}}}^{\tilde{\varepsilon}_{\mathrm{c}}}d\varepsilon\frac{N(\varepsilon+\mu-e\Phi(\boldsymbol{r}))}{\mathrm{e}^{\varepsilon/k_{\mathrm{B}}T}+1},
\end{aligned} \tag{2.24}$$

We also introduce the electron density in the normal state n_{n} as

$$n_{\mathrm{n}} = 2\int_{-\infty}^{\infty}d\varepsilon N(\varepsilon+\mu_{\mathrm{n}})f(\varepsilon), \tag{2.25}$$

where the prefactor of 2 is introduced so as to account for the two possible electron spin states. We can now write the charge density using $\rho(\boldsymbol{r}) = en(\boldsymbol{r}) - en_{\mathrm{n}}$ as

$$\begin{aligned}
\rho(\boldsymbol{r}) \approx\; & eN(\mu_{\mathrm{n}})\mathrm{Tr}\int_{-\tilde{\varepsilon}_{\mathrm{c}}}^{\tilde{\varepsilon}_{\mathrm{c}}}d\varepsilon f(\varepsilon) \\
& \times\int\frac{d\Omega_{\boldsymbol{p}}}{4\pi}\left[\mathrm{Re}\underline{g}^{\mathrm{R}}(\varepsilon,\boldsymbol{p}_{\mathrm{F}},\boldsymbol{r})+\frac{N'(\mu_{\mathrm{n}})}{N(\mu_{\mathrm{n}})}\mathrm{Re}\underline{g}^{\mathrm{R}(1)}(\varepsilon,\boldsymbol{p}_{\mathrm{F}},\boldsymbol{r})\right] \\
& -2e\int_{-\tilde{\varepsilon}_{\mathrm{c}}}^{\tilde{\varepsilon}_{\mathrm{c}}}d\varepsilon N(\varepsilon+\mu-e\Phi(\boldsymbol{r}))f(\varepsilon) \\
& +2e\int_{-\infty}^{\infty}d\varepsilon N(\varepsilon)\left[\frac{1}{\mathrm{e}^{(\varepsilon+e\Phi(\boldsymbol{r})-\delta\mu-\mu_{\mathrm{n}})/k_{\mathrm{B}}T}+1}-\frac{1}{\mathrm{e}^{(\varepsilon-\mu_{\mathrm{n}})/k_{\mathrm{B}}T}+1}\right].
\end{aligned} \tag{2.26}$$

Furthermore, let us carry out a perturbation expansion with respect to the Lorentz and PPG forces as $\underline{g}^{\mathrm{R}} = \underline{g}_0^{\mathrm{R}} + \underline{g}_1^{\mathrm{R}}\cdots$ and $\underline{g}^{\mathrm{R}(1)} = \underline{g}_0^{\mathrm{R}(1)} + \underline{g}_1^{\mathrm{R}(1)}\cdots$ [5, 8, 14], which is expanded up to the first order in terms of the quasiclassical parameter δ below. We also use Eq. (A.32), the $\underline{g}_0^{\mathrm{R}}$ and gap equation (Eq. (2.22)) in the standard Eilenberger equations, and approximate the distribution function, as follows:

$$\begin{aligned}
& \frac{1}{\mathrm{e}^{(\varepsilon+e\Phi(\boldsymbol{r})-\delta\mu-\mu_{\mathrm{n}})/k_{\mathrm{B}}T}+1} \\
& \quad\approx\frac{1}{\mathrm{e}^{(\varepsilon-\mu_{\mathrm{n}})/k_{\mathrm{B}}T}+1}+\frac{d}{d\varepsilon}\frac{1}{\mathrm{e}^{(\varepsilon-\mu_{\mathrm{n}})/k_{\mathrm{B}}T}+1}[e\Phi(\boldsymbol{r})-\delta\mu].
\end{aligned} \tag{2.27}$$

Using them, we obtain a general expression for the charge density, with contributions from the Lorentz force (in the presence of magnetic field), the gradient of the pair potential, and the pressure due to the slope of the density of states as

$$\rho(\boldsymbol{r}) \approx 2\pi k_{\mathrm{B}} T e N(\mu_{\mathrm{n}}) \mathrm{Tr} \sum_{n=0}^{\tilde{n}_{\mathrm{c}}} \int \frac{d\Omega_{\boldsymbol{p}}}{4\pi} \mathrm{Im} \underline{g}_1(\varepsilon_n, \boldsymbol{p}_{\mathrm{F}}, \boldsymbol{r})$$
$$+ e \frac{N'(\mu_{\mathrm{n}})}{N(\mu_{\mathrm{n}})} \int_{-\tilde{\varepsilon}_{\mathrm{c}}}^{\tilde{\varepsilon}_{\mathrm{c}}} d\varepsilon \frac{\varepsilon}{\mathrm{e}^{\varepsilon/k_{\mathrm{B}}T} + 1} [N_{\mathrm{s0}}(\varepsilon, \boldsymbol{r}) - 2N(\mu_{\mathrm{n}})]$$
$$- (-1)^l c e N(\mu_{\mathrm{n}}) \frac{N'(\mu_{\mathrm{n}})}{N(\mu_{\mathrm{n}})} \mathrm{Tr} \sum_{m=-l}^{l} |\underline{\Delta}_{lm}(\boldsymbol{r})|^2$$
$$- 2eN(\mu_{\mathrm{n}})[e\Phi(\boldsymbol{r}) - \delta\mu], \tag{2.28}$$

where the cutoff $\tilde{n}_{\mathrm{c}}$ is obtained from $(2\tilde{n}_{\mathrm{c}} + 1)\pi k_{\mathrm{B}} T = \tilde{\varepsilon}_{\mathrm{c}}$, the coefficient c is defined by

$$c \equiv \int_{-\tilde{\varepsilon}_{\mathrm{c}}}^{\tilde{\varepsilon}_{\mathrm{c}}} d\varepsilon \frac{1}{2\varepsilon} \tanh \frac{\varepsilon}{2k_{\mathrm{B}} T_{\mathrm{c}}}, \tag{2.29}$$

with T_{c} denoting the superconducting transition temperature at zero magnetic field, and $N_{\mathrm{s0}}(\varepsilon, \boldsymbol{r})$ is the LDOS obtained from the standard Eilenberger equations defined by

$$N_{\mathrm{s0}}(\varepsilon, \boldsymbol{r}) \equiv \frac{N(\mu_{\mathrm{n}})}{2} \mathrm{Tr} \int \frac{d\Omega_{\boldsymbol{p}}}{4\pi} \mathrm{Re} \underline{g}_0^{\mathrm{R}}(\varepsilon, \boldsymbol{p}_{\mathrm{F}}, \boldsymbol{r}). \tag{2.30}$$

Using Gauss's law $\boldsymbol{\nabla} \cdot \boldsymbol{E} = \rho/\epsilon_0$, we obtain an equation for the electric field as

$$- \lambda_{\mathrm{TF}}^2 \boldsymbol{\nabla}^2 \boldsymbol{E}(\boldsymbol{r}) + \boldsymbol{E}(\boldsymbol{r})$$
$$= - \frac{\pi k_{\mathrm{B}} T}{e} \boldsymbol{\nabla} \mathrm{Tr} \sum_{n=0}^{\tilde{n}_{\mathrm{c}}} \int \frac{d\Omega_{\boldsymbol{p}}}{4\pi} \mathrm{Im} \underline{g}_1(\varepsilon_n, \boldsymbol{p}_{\mathrm{F}}, \boldsymbol{r})$$
$$- \frac{1}{e} \frac{N'(\mu_{\mathrm{n}})}{N(\mu_{\mathrm{n}})} \int_{-\tilde{\varepsilon}_{\mathrm{c}}}^{\tilde{\varepsilon}_{\mathrm{c}}} d\varepsilon \varepsilon f(\varepsilon) \boldsymbol{\nabla} \frac{N_{\mathrm{s0}}(\varepsilon, \boldsymbol{r})}{N(\mu_{\mathrm{n}})}$$
$$+ (-1)^l \frac{c}{2e} \frac{N'(\mu_{\mathrm{n}})}{N(\mu_{\mathrm{n}})} \boldsymbol{\nabla} \mathrm{Tr} \sum_{m=-l}^{l} |\underline{\Delta}_{lm}(\boldsymbol{r})|^2, \tag{2.31}$$

where $\lambda_{\mathrm{TF}} \equiv \sqrt{\epsilon_0/2e^2 N(\mu_{\mathrm{n}})}$ is the Thomas–Fermi screening length.

2.5 Chemical potential

Using Eq. (2.28), we obtain an expression for the chemical potential μ as follows [11]

$$\mu = \mu_{\mathrm{n}} - \pi k_{\mathrm{B}} T \mathrm{Tr} \sum_{n=0}^{\tilde{n}_{\mathrm{c}}} \int \frac{d\Omega_{\boldsymbol{p}}}{4\pi} \frac{1}{V} \int d^3 r \mathrm{Im} \underline{g}_1(\varepsilon_n, \boldsymbol{p}_{\mathrm{F}}, \boldsymbol{r})$$
$$- \frac{1}{2} \frac{N'(\mu_{\mathrm{n}})}{N(\mu_{\mathrm{n}})} \int_{-\tilde{\varepsilon}_{\mathrm{c}}}^{\tilde{\varepsilon}_{\mathrm{c}}} d\varepsilon \varepsilon f(\varepsilon) \frac{1}{V} \int d^3 r \left[\frac{N_{\mathrm{s0}}(\varepsilon, \boldsymbol{r})}{N(\mu_{\mathrm{n}})} - 2 \right]$$
$$+ \frac{(-1)^l}{2} c \frac{N'(\mu_{\mathrm{n}})}{N(\mu_{\mathrm{n}})} \mathrm{Tr} \sum_{m=-l}^{l} \frac{1}{V} \int d^3 r |\underline{\Delta}_{lm}(\boldsymbol{r})|^2 + e \frac{1}{V} \int d^3 r \Phi(\boldsymbol{r}). \tag{2.32}$$

3 Spontaneous Surface Charge on a $d_{x^2-y^2}$-wave Superconductor

In this chapter, we apply the augmented quasiclassical equations to a quasi-$2D$ superconductor with d-wave pairing. More specifically, we consider a semi-infinite system on $x > 0$ with a single specular interface with vacuum at $x = 0$, cut along the [110] direction. We show that the presence of the [110] surface in a $d_{x^2-y^2}$-wave superconductor is accompanied by the spontaneous accumulation of electric charge due to the appearance of the pair potential gradient force and a second force due to the slope of the density of states in the normal states at the Fermi level. We also calculate the local density of states within the augmented quasiclassical theory, taking into account first-order quantum corrections due to the pair potential gradient (PPG) force and the pressure due to the slope of the density of states (SDOS pressure). We observe zero energy Andreev bound states at the [110] surface, consistent with other theoretical predictions and also in agreement with experiments as a defining characteristic of the d-wave pairing in superconductors. These zero energy bound states appear due to the sign change of the superconducting order parameter of the $d_{x^2-y^2}$ state. We further observe particle-hole asymmetry in the LDOS deviations from the standard Eilenberger solutions. This asymmetry is a qualitative evidence of electric charging at the surface of the superconductor, and may be observed in experiments.

3.1 Formalism

3.1.1 Augmented quasiclassical equations

We consider a time-reversal invariant superconductor, the quasiclassical equations augmented with the pair potential gradient terms are given in the Matsubara formalism by [8, 11]

$$\left[i\varepsilon_n\hat{\tau}_3 - \hat{\Delta}\hat{\tau}_3, \hat{g}\right] + i\hbar\boldsymbol{v}_{\rm F}\cdot\boldsymbol{\nabla}\hat{g} + \frac{i\hbar}{2}\left\{\boldsymbol{\nabla}\hat{\Delta}\hat{\tau}_3, \boldsymbol{\partial}_{\boldsymbol{p}_{\rm F}}\hat{g}\right\} - \frac{i\hbar}{2}\left\{\boldsymbol{\partial}_{\boldsymbol{p}_{\rm F}}\hat{\Delta}\hat{\tau}_3, \boldsymbol{\nabla}\hat{g}\right\} = \hat{0}, \tag{3.1}$$

where $e < 0$ is the electron charge, $\varepsilon_n = (2n+1)\pi k_{\rm B}T$ is the fermion Matsubara energy ($n = 0, \pm 1, \ldots$), $\boldsymbol{v}_{\rm F}$ is the Fermi velocity while $\boldsymbol{p}_{\rm F}$ is the Fermi momentum. The commutators $[\hat{a}, \hat{b}] \equiv \hat{a}\hat{b} - \hat{b}\hat{a}$ and $\{\hat{a}, \hat{b}\} \equiv \hat{a}\hat{b} + \hat{b}\hat{a}$. The functions $\hat{g} = \hat{g}(\varepsilon_n, \boldsymbol{p}_{\rm F}, \boldsymbol{r})$ and $\hat{\Delta} = \hat{\Delta}(\boldsymbol{p}_{\rm F}, \boldsymbol{r})$ are the quasiclassical Green's functions and the pair potential.

We consider the spin-singlet pairing state without spin paramagnetism. The matrices $\hat{g}$, $\hat{\Delta}$ and $\hat{\tau}_3$ are written as

$$\hat{g} = \begin{bmatrix} g & -if \\ i\bar{f} & -\bar{g} \end{bmatrix}, \quad \hat{\Delta} = \begin{bmatrix} 0 & \Delta\phi \\ \Delta\phi & 0 \end{bmatrix}, \quad \hat{\tau}_3 = \begin{bmatrix} 1 & 0 \\ 0 & -1 \end{bmatrix}, \tag{3.2}$$

where real functions $\Delta = \Delta(\boldsymbol{r})$ and $\phi = \phi(\boldsymbol{p}_{\mathrm{F}})$ denote the amplitude of the energy gap and the basis function of the energy gap, and the barred functions in the Matsubara formalism are defined generally by $\bar{X}(\varepsilon, \boldsymbol{p}_{\mathrm{F}}, \boldsymbol{r}) \equiv X^{*}(-\varepsilon, -\boldsymbol{p}_{\mathrm{F}}, \boldsymbol{r})$.

Following the procedure in Ref., we carry out a perturbation expansion of f and g in terms of δ as $f = f_0 + f_1 + \cdots$ and $g = g_o + g_1 + \cdots$. Then the main part in the standard Eilenberger equations [13, 12] are obtained from the leading-order contribution in terms of the quasiclassical parameter as

$$\varepsilon_n f_0 + \frac{1}{2}\hbar \boldsymbol{v}_{\mathrm{F}} \cdot \boldsymbol{\nabla} f_0 = \Delta \phi g_0. \tag{3.3}$$

We also obtain the relations from the normalization condition as

$g_0 = \bar{g}_0 = \mathrm{sgn}(\varepsilon_n)\sqrt{1 - f_0 \bar{f}_0}$[13]. Using Eq. (2.22) and neglecting spin magnetism, the self-consistency equation for the pair potential is expressed as

$$\Delta = 2\pi \mathrm{g}_0 k_{\mathrm{B}} T \sum_{n=0}^{\infty} \langle f_0 \phi \rangle_{\mathrm{F}}, \tag{3.4}$$

where $\langle \cdots \rangle_{\mathrm{F}}$ denotes the Fermi surface average, g_0 denotes the coupling constant responsible for the Cooper pairing, defined by $\mathrm{g}_0 \equiv -N(0) V_l^{(\mathrm{eff})}$ with $V_l^{(\mathrm{eff})}$ and $N(0)$ denoting the constant effective potential and the normal-state density-of-states (DOS) per spin and unit volume at the Fermi level respectively. We obtain the expression for the first-order Green's function g_1 in terms of quasiclassical parameter δ from Eq. (3.1) as

$$\begin{aligned} \boldsymbol{v}_{\mathrm{F}} \cdot \boldsymbol{\nabla} g_1 = & -\frac{i}{2} \boldsymbol{\nabla} \Delta \phi \cdot \frac{\partial f_0}{\partial \boldsymbol{p}_{\mathrm{F}}} - \frac{i}{2} \boldsymbol{\nabla} \Delta \phi \cdot \frac{\partial \bar{f}_0}{\partial \boldsymbol{p}_{\mathrm{F}}} \\ & + \frac{i}{2} \Delta \frac{\partial \phi}{\partial \boldsymbol{p}_{\mathrm{F}}} \cdot \boldsymbol{\nabla} f_0 + \frac{i}{2} \Delta \frac{\partial \phi}{\partial \boldsymbol{p}_{\mathrm{F}}} \cdot \boldsymbol{\nabla} \bar{f}_0. \end{aligned} \tag{3.5}$$

We note that the momentum derivative terms of ϕ come in the g_1 equation for anisotropic superconductors[15].

3.1.2 Local density of states

The LDOS is obtained as[11]

$$\begin{aligned} N_{\mathrm{s}}(\varepsilon, \boldsymbol{r}) = & N(0) \langle \mathrm{Re} g_0^{\mathrm{R}} + \mathrm{Re} g_1^{\mathrm{R}} \rangle_{\mathrm{F}} + N'(0) \varepsilon \langle \mathrm{Re} g_0^{\mathrm{R}} \rangle_{\mathrm{F}} \\ & + \frac{1}{2} N'(0) \Delta \langle \mathrm{Im} f_0^{\mathrm{R}} + \mathrm{Im} \bar{f}_0^{\mathrm{R}} \rangle_{\mathrm{F}}, \end{aligned} \tag{3.6}$$

where the functions $g_{0,1}^{\mathrm{R}}$ and f_0^{R} are the quasiclassical retarded Green's functions which are obtained by solving Eqs. (3.3) and (3.5) with the following transformation:

$g_{0,1}^{\mathrm{R}}(\varepsilon, \boldsymbol{p}_{\mathrm{F}}, \boldsymbol{r}) = g_{0,1}(\varepsilon_n \to -i\varepsilon + \eta, \boldsymbol{p}_{\mathrm{F}}, \boldsymbol{r})$ and $f_0^{\mathrm{R}}(\varepsilon, \boldsymbol{p}_{\mathrm{F}}, \boldsymbol{r}) = f_0(\varepsilon_n \to -i\varepsilon + \eta, \boldsymbol{p}_{\mathrm{F}}, \boldsymbol{r})$, and η is a positive infinitesimal constant (smearing factor).

3.1.3 Electric field equation

Using Eq. (2.31), the electric field is expressed as[11]

$$
\begin{aligned}
-\lambda_{\mathrm{TF}}^2 \nabla^2 \boldsymbol{E}(\boldsymbol{r}) + \boldsymbol{E}(\boldsymbol{r}) = & -\frac{2\pi k_{\mathrm{B}}T}{e}\sum_{n=0}^{\infty}\langle \nabla \mathrm{Im} g_1 \rangle_{\mathrm{F}} \\
& -\frac{1}{e}\frac{N'(0)}{N(0)}\int_{\tilde{\varepsilon}_{\mathrm{c}-}}^{\tilde{\varepsilon}_{\mathrm{c}+}} d\varepsilon f(\varepsilon)\varepsilon \left\langle \nabla \mathrm{Re} g_0^{\mathrm{R}} \right\rangle_{\mathrm{F}} - \frac{c}{e}\frac{N'(0)}{N(0)}\nabla \Delta^2,
\end{aligned}
\tag{3.7}
$$

where $\lambda_{\mathrm{TF}} \equiv \sqrt{1/2\epsilon_0 e^2 N(0)}$ denotes the Thomas–Fermi screening length, and the function $f(\varepsilon) = 1/(\mathrm{e}^{\varepsilon/k_{\mathrm{B}}T} + 1)$ is the Fermi distribution function for electrons. The first term on the RHS of Eq. (A.29) is the PPG term, while the second and third terms are the contributions from the SDOS pressure. Furthermore, it can be seen that the third term depends on the gradient of the amplitude of the pair potential. The parameter c first introduced by Khomskii *et al.*[10] is given by[11]

$$
c \equiv \int_{\tilde{\varepsilon}_{\mathrm{c}-}}^{\tilde{\varepsilon}_{\mathrm{c}+}} d\varepsilon \frac{1}{2\varepsilon}\tanh\frac{\varepsilon}{2k_{\mathrm{B}}T_{\mathrm{c}}},
\tag{3.8}
$$

where T_{c} denotes the superconducting transition temperature at zero magnetic field. The cutoff energies $\tilde{\varepsilon}_{\mathrm{c}\pm}$ are determined by[11]

$$
\int_{\tilde{\varepsilon}_{\mathrm{c}-}}^{\tilde{\varepsilon}_{\mathrm{c}+}} N_{\mathrm{s}}(\varepsilon, \boldsymbol{r}) d\varepsilon = \int_{\tilde{\varepsilon}_{\mathrm{c}-}}^{\tilde{\varepsilon}_{\mathrm{c}+}} N(\varepsilon) d\varepsilon, \quad N_{\mathrm{s}}(\tilde{\varepsilon}_{\mathrm{c}\pm}, \boldsymbol{r}) = N(\tilde{\varepsilon}_{\mathrm{c}\pm}).
\tag{3.9}
$$

3.1.4 Density of states and the chemical potential difference in the homogeneous system

We introduce the normal DOS $N(\varepsilon)$, expressed as

$$
N(\varepsilon) \equiv \int \frac{dp_{\mathrm{x}} dp_{\mathrm{y}}}{(2\pi\hbar)^2}\delta(\varepsilon - \epsilon_{\boldsymbol{p}} + \mu),
\tag{3.10}
$$

where $\epsilon_{\boldsymbol{p}}$ denotes the single particle energy. p_{x} and p_{y} are the x and y-components of the quasiparticle momentum, respectively, while μ is the chemical potential.

The superconducting DOS in the homogeneous system is written using Eq. (2.13) [11]

$$
\begin{aligned}
N_{\mathrm{s}}(\varepsilon) = & N(0)\left\langle \frac{|\varepsilon|}{\sqrt{\varepsilon^2 - \Delta_{\mathrm{bulk}}^2\phi^2}}\theta(|\varepsilon| - \Delta_{\mathrm{bulk}}|\phi|)\right\rangle_{\mathrm{F}} \\
& + N'(0)\left\langle \mathrm{sgn}(\varepsilon)\sqrt{\varepsilon^2 - \Delta_{\mathrm{bulk}}^2\phi^2}\theta(|\varepsilon| - \Delta_{\mathrm{bulk}}|\phi|)\right\rangle_{\mathrm{F}},
\end{aligned}
\tag{3.11}
$$

where Δ_{bulk} denotes the gap amplitude in the bulk.

The chemical potential difference between the normal and superconducting states of the homogeneous system is given by[11]

$$
\delta\mu = -\frac{N'(0)}{N(0)}\int_{\tilde{\varepsilon}_{\mathrm{c}-}}^{\tilde{\varepsilon}_{\mathrm{c}+}} d\varepsilon \varepsilon f(\varepsilon)\left[\frac{N_{\mathrm{s}0}^{\mathrm{bulk}}(\varepsilon)}{N(0)} - 1\right] - c\frac{N'(0)}{N(0)}\Delta_{\mathrm{bulk}}^2,
\tag{3.12}
$$

where $N^{\mathrm{bulk}}_{\mathrm{s0}}(\varepsilon)$ is the LDOS in the bulk obtained from the standard Eilenberger equations as

$$N^{\mathrm{bulk}}_{\mathrm{s0}}(\varepsilon) = N(0)\left\langle \frac{|\varepsilon|}{\sqrt{\varepsilon^2 - \Delta^2_{\mathrm{bulk}}\phi^2}}\theta(|\varepsilon| - \Delta_{\mathrm{bulk}}|\phi|)\right\rangle_{\mathrm{F}}. \tag{3.13}$$

The details of the derivation of Eqs. (3.6), (A.29), (3.11), and (3.12) are available in Ref. [11]

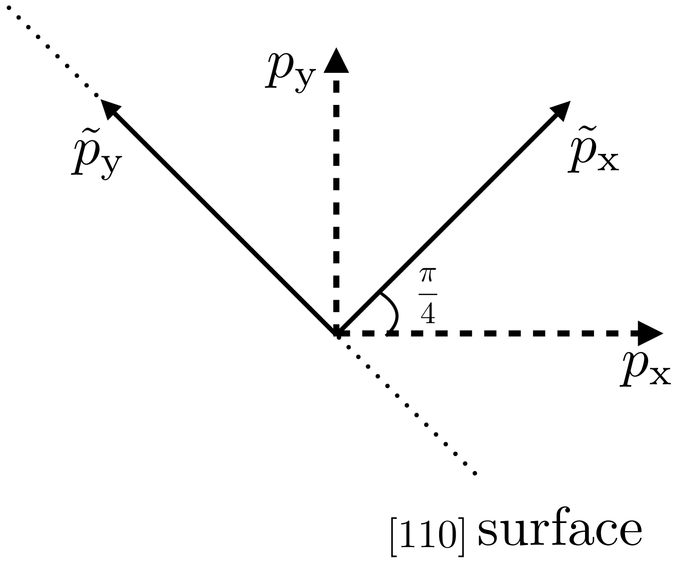

Figure 3: Schematic representation of quasi-particle momenta p_{x} and p_{y} transformed to $\tilde{p}_{\mathrm{x}}$ and $\tilde{p}_{\mathrm{y}}$, respectively by a $\pi/4$ rotation. This rotation gives a [110] surface along the $\tilde{p}_{\mathrm{y}}$ direction.

3.2 Numerical procedures

3.2.1 Model *d*-wave pairing

We here perform numerical calculations for a quasi-two-dimensional semi-finite system with a single specular surface. As a starting point, we introduce the single-particle energy on a two-dimensional square lattice used for high-T_{c} superconductors[36, 37, 14]

$$\begin{aligned}\epsilon_{\boldsymbol{p}} &= -2t(\cos\tilde{p}_{\mathrm{x}} + \cos\tilde{p}_{\mathrm{y}}) + 4t_1(\cos\tilde{p}_{\mathrm{x}}\cos\tilde{p}_{\mathrm{y}} - 1)\\ &\quad + 2t_2(\cos 2\tilde{p}_{\mathrm{x}} + \cos 2\tilde{p}_{\mathrm{y}} - 2),\end{aligned} \tag{3.14}$$

with the dimensionless hopping parameters $t_1/t = 1/6$ and $t_2/t = -1/5$, and the momenta $\tilde{p}_{\mathrm{x}}$ and $\tilde{p}_{\mathrm{y}}$ are given by $\tilde{p}_{\mathrm{x}} = (p_{\mathrm{x}} + p_{\mathrm{y}})/\sqrt{2}$ and $\tilde{p}_{\mathrm{y}} = (p_{\mathrm{y}} - p_{\mathrm{x}})/\sqrt{2}$. We also adopt a model d-wave pairing as $\phi = C(\cos\tilde{p}_{\mathrm{x}} - \cos\tilde{p}_{\mathrm{y}})$, where the real constant C is determined via the normalization condition $\langle\phi^2\rangle_{\mathrm{F}} = 1$.

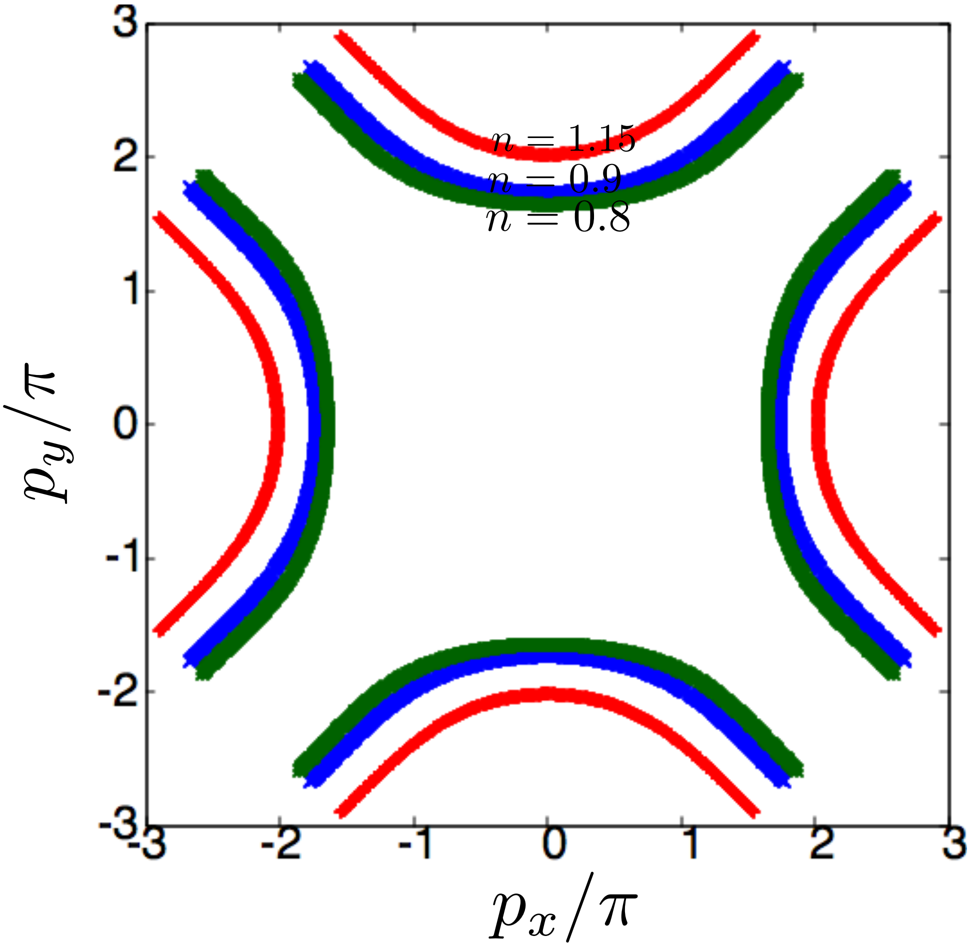

Figure 4: (Color online) Fermi surfaces of $n = 0.8, 0.9$ and 1.15 for the single-particle energy.

3.2.2 Self-consistent solution

We first obtain the self-consistent solutions to the standard Eilenberger equations in Eqs. (3.3) and (3.4) using Riccati method[13, 38, 39, 40]. The relevant boundary conditions used near the bulk is obtained by carrying out a gradient expansion[13] up to the first-order, as shown in appendix. We also assume mirror reflection at the surface such that

$$a(\varepsilon_n, \boldsymbol{p}_{\rm F}, 0) \equiv a(\varepsilon_n, \boldsymbol{p}'_{\rm F}, 0), \tag{3.15}$$

$$\frac{\partial a}{\partial \boldsymbol{p}_{\rm Fx}}(\varepsilon_n, \boldsymbol{p}_{\rm F}, 0) \equiv a(\varepsilon_n, \boldsymbol{p}'_{\rm F}, 0) \tag{3.16}$$

and

$$g_0(\varepsilon_n, \boldsymbol{p}_{\rm F}, 0) \equiv g_0(\varepsilon_n, \boldsymbol{p}'_{\rm F}, 0), \quad f_0(\varepsilon_n, \boldsymbol{p}_{\rm F}, 0) \equiv f_0(\varepsilon_n, \boldsymbol{p}'_{\rm F}, 0), \tag{3.17}$$

where $\boldsymbol{p}_{\rm F}$ and $\boldsymbol{p}'_{\rm F}$ are the Fermi momenta before and after reflection at the surface respectively and are related by[20]

$$\boldsymbol{p}'_{\rm F} = \boldsymbol{p}_{\rm F} - 2\boldsymbol{n}(\boldsymbol{n} \cdot \boldsymbol{p}_{\rm F}), \tag{3.18}$$

with $\boldsymbol{n}$=$-\hat{\boldsymbol{x}}$. We note that we need to solve Eqs. (B.1) and (B.6) (see appendix) by numerical integration towards the $-\hat{\boldsymbol{x}}$ direction for $v_{{\rm F}x} < 0$ from the bulk at $x = x_{\rm c} \gg \xi_0$ to the surface at $x = 0$ and towards the $\hat{\boldsymbol{x}}$ direction for $v_{{\rm F}x} > 0$ from the surface at $x = 0$ to the bulk at $x = x_{\rm c}$. We also use the solutions obtained by the gradient expansion of Eqs. (B.1) and (B.6) up to the first-order in the region of $|v_{{\rm F}x}| \ll \langle v_{\rm F} \rangle_{\rm F}$.

3.2.3 Calculation of surface charging

We next solve Eq. (A.29) to obtain the surface electric field with the boundary conditions where the electric field vanishes at the surface and the first term on the LHS of Eq. (A.29) is neglected near the bulk, using Eq. (3.5) and substituting the Green's functions f_0 and $g_0^{\rm R}$ into Eq. (A.29) accordingly. We obtain the retarded Green's functions with the transformation $\varepsilon_n \to -i\varepsilon + \eta$ and the same procedures as in the calculation of the Matsubara Green's functions. The derivatives $\partial f_0/\partial x$ and $\partial f_0/\partial p_{{\rm F}x}$ in Eq. (3.5) are also shown in appendix. We finally calculate the corresponding charge density using Gauss' law, $\boldsymbol{\nabla} \cdot \boldsymbol{E}(x) = \rho(x)/\epsilon_0$. Furthermore, we calculate the LDOS, by substituting the retarded Green's functions $g_{0,1}^{\rm R}$ and $f_0^{\rm R}$ into Eq. (3.6). We also use $g_1^{\rm R} = 0$ at the bulk as a boundary condition to solve Eq. (3.5). We choose the parameters appropriate for cuprate superconductors as $\delta = 0.05$, $t = 14\Delta_0$, and $\lambda_{\rm TF} = 0.05\xi_0$, where Δ_0 denotes the gap amplitude at zero temperature.

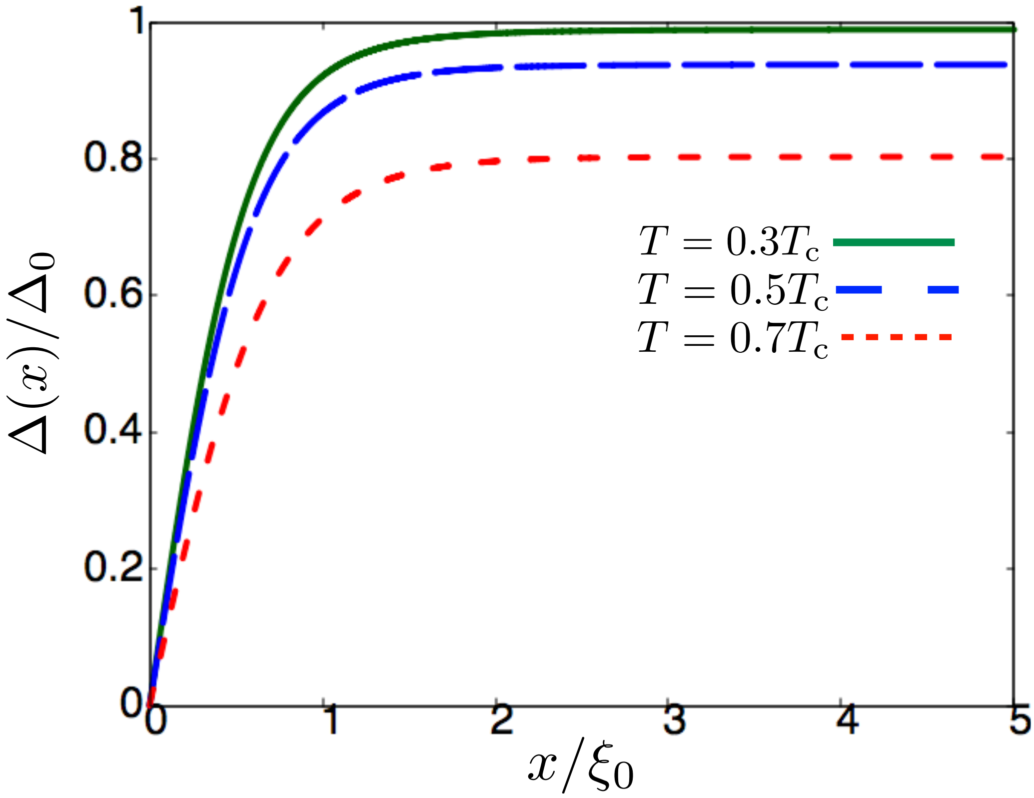

Figure 5: (Color online) Temperature dependences in the self-consistent pair potential for the $d_{x^2-y^2}$-wave state with a smooth [110] surface at $x = 0$. At temperatures $T = 0.3T_c$ (green solid line), $0.5T_c$ (blue long dashed line), and $0.7T_c$ (red short dashed line), for the filling $n = 0.9$.

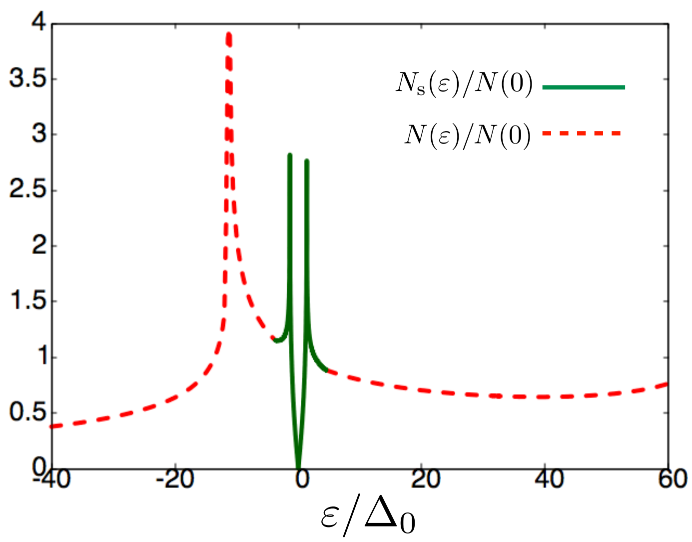

Figure 6: (Color online) Superconducting DOS $N_s(\varepsilon)$ (green solid line) and the normal DOS $N(\varepsilon)$ (red dashed lines) in the homogeneous system at temperature $T = 0.1T_c$, for the filling $n = 0.9$, in units of $N(0)$ over $-40\Delta_0 \leq \varepsilon \leq 60\Delta_0$.

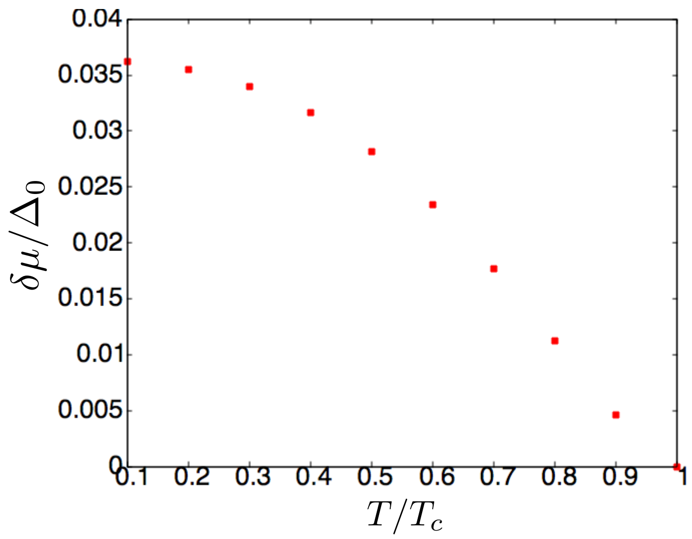

Figure 7: Temperature dependence of the chemical potential difference $\delta\mu$ between the normal and the superconducting states of the homogeneous system at the filling $n = 0.9$.

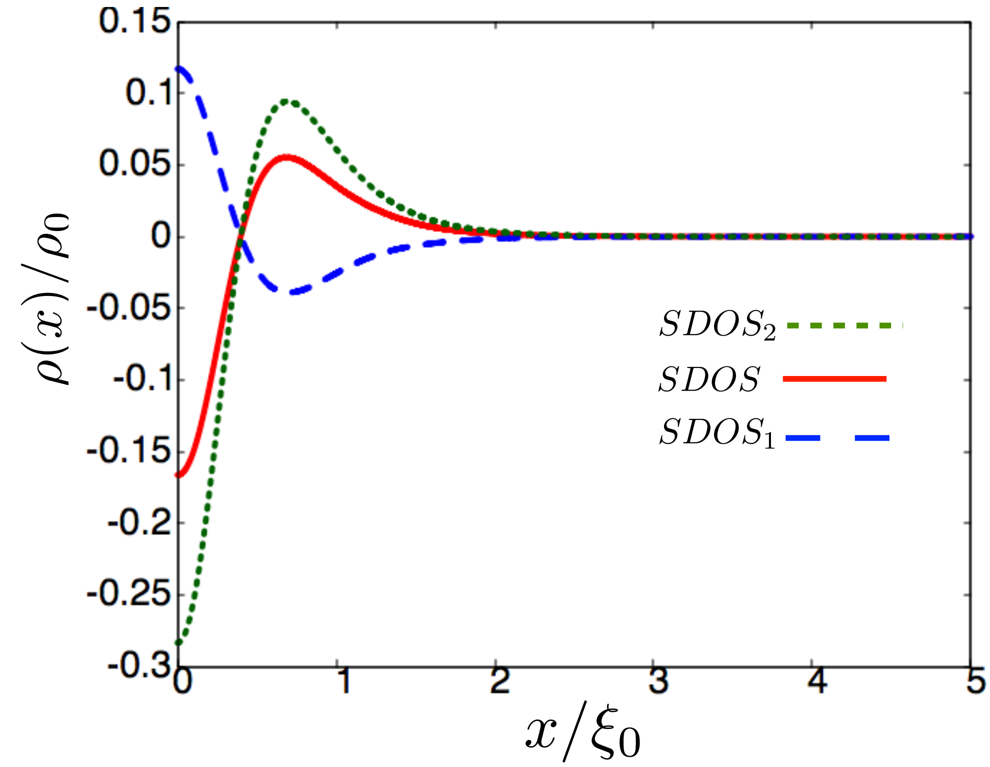

Figure 8: (Color online) Surface charge due to SDOS pressure, in units of $\rho_0 \equiv \varepsilon_0\Delta_0/|e|\xi_0^2$, with $\eta = 0.01$, at temperature $T = 0.5T_c$, for the filling $n = 0.9$, with contributions from the second term in Eq. (A.29) (blue long dashed line), the third term in Eq. (A.29) (green short dashed line). While the total charge density due to the SDOS pressure is given by the red solid line.

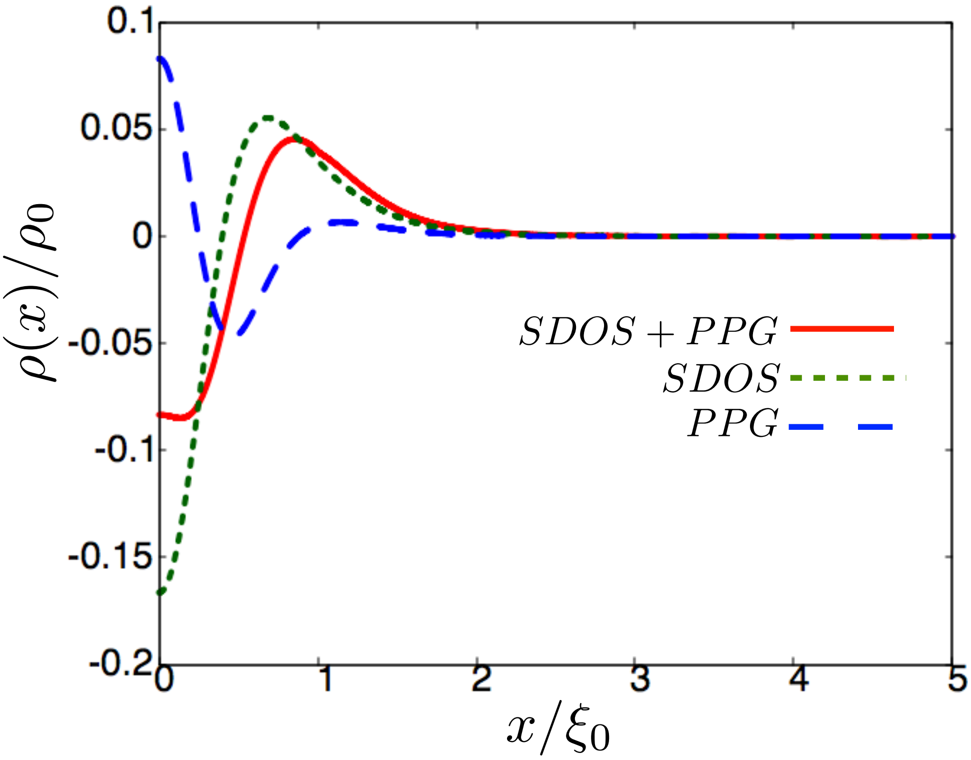

Figure 9: (Color online) Total spontaneous surface charge density (red solid line) due to the PPG force (blue long dashed line) and the SDOS pressure (green short dashed line), in units of $\rho_0 \equiv \varepsilon_0 \Delta_0/|e|\xi_0^2$, at temperature $T = 0.5T_c$, for the filling $n = 0.9$, with $\eta = 0.01$.

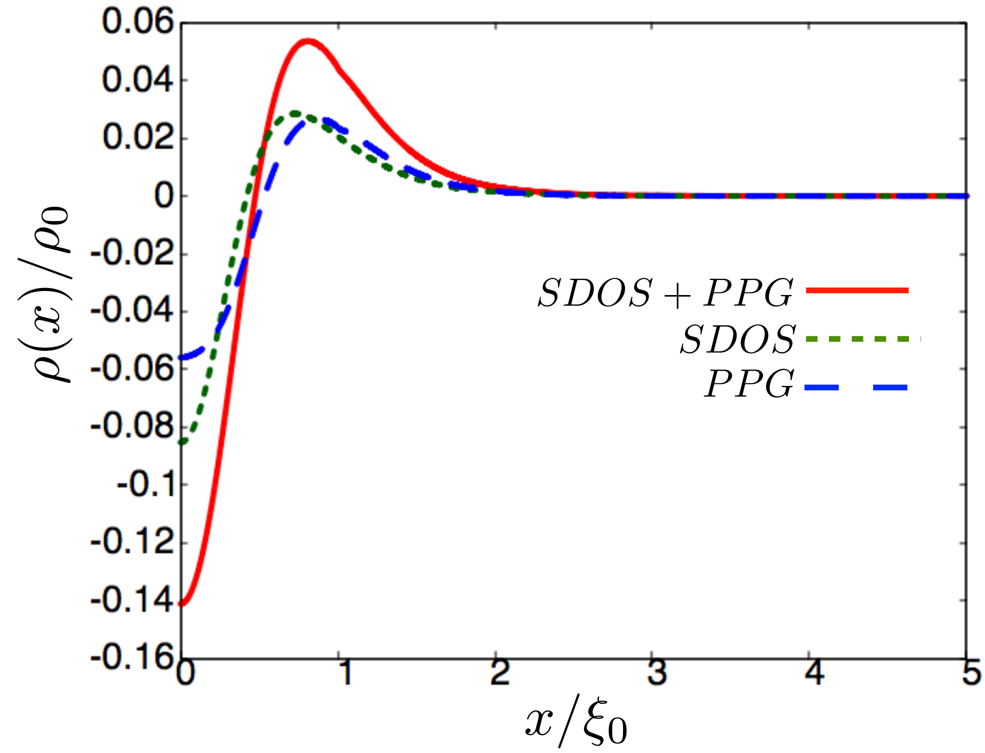

Figure 10: (Color online) Total spontaneous surface charge density (red solid line) due to the PPG force (blue long dashed line) and the SDOS pressure (green short dashed line), in units of $\rho_0 \equiv \varepsilon_0 \Delta_0 / |e| \xi_0^2$, at temperature $T = 0.5T_c$, for the filling $n = 1.15$, with $\eta = 0.01$.

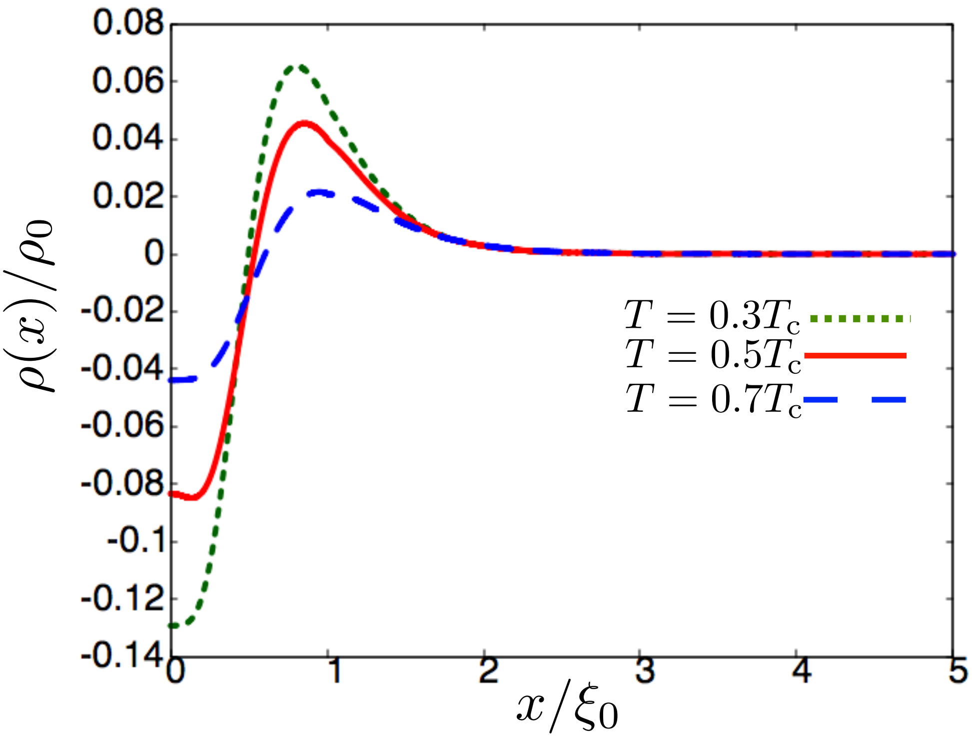

Figure 11: (Colour online) Temperature dependence of the total surface charge induced by the PPG force and SDOS pressure, for the filling $n = 0.9$, in units of $\rho_0 \equiv \varepsilon_0\Delta_0/|e|\xi_0^2$, with $\eta = 0.01$, at temperatures $T = 0.3T_c$ (green short dashed line), $0.5T_c$ (red solid line), and $0.7T_c$ (blue long dashed line).

3.3 Results

We discuss our numerical results as follows. Figure 5 shows the self-consistent gap amplitude for the d-wave paired superconductor with a [110] oriented surface at the filling $n = 0.9$. The pair potential is suppressed around the surface and vanishes at the surface due to a change in its sign around the surface. The slope of pair potential is described by $\xi_1^{-1} = [\Delta(\infty)]^{-1}\lim_{x\to 0}[\Delta(x)/x]$. Although ξ_1 decreases as the temperature is lowered in high-temperature region, it saturates to the finite value as $T \to 0$. Indeed, ξ_1 behaves quite similar to the coherence length incorporating both energy-gap and Fermi-surface anisotropies defined as $\xi_c \equiv [\langle \hbar^2 v_{Fx}^2 \phi^2\rangle_F/\langle\phi^4\rangle_F]^{\frac{1}{2}}\Delta^{-1}(\infty)$. In this sense, the behaviour of pair potential in the surface system is distinguished from the one in the vortex systems in type-II superconductors, which induces vortex-core shrinkage[41, 42].

In Fig. 6 , the superconducting DOS and the normal DOS in the homogeneous system at the filling $n = 0.9$ connect at energies $\varepsilon = \tilde{\varepsilon}_{c+}$ and $\tilde{\varepsilon}_{c-}$. They connect more smoothly taking into account higher order derivatives of the DOS at the Fermi level, but the higher order derivatives contribute little to quantities. Thus, we can perform the following calculations using these cutoff energies $\tilde{\varepsilon}_{c\pm}$.

In Fig. 7, we show the temperature dependence of the chemical potential difference between the normal and superconducting states of the homogeneous system for the filling

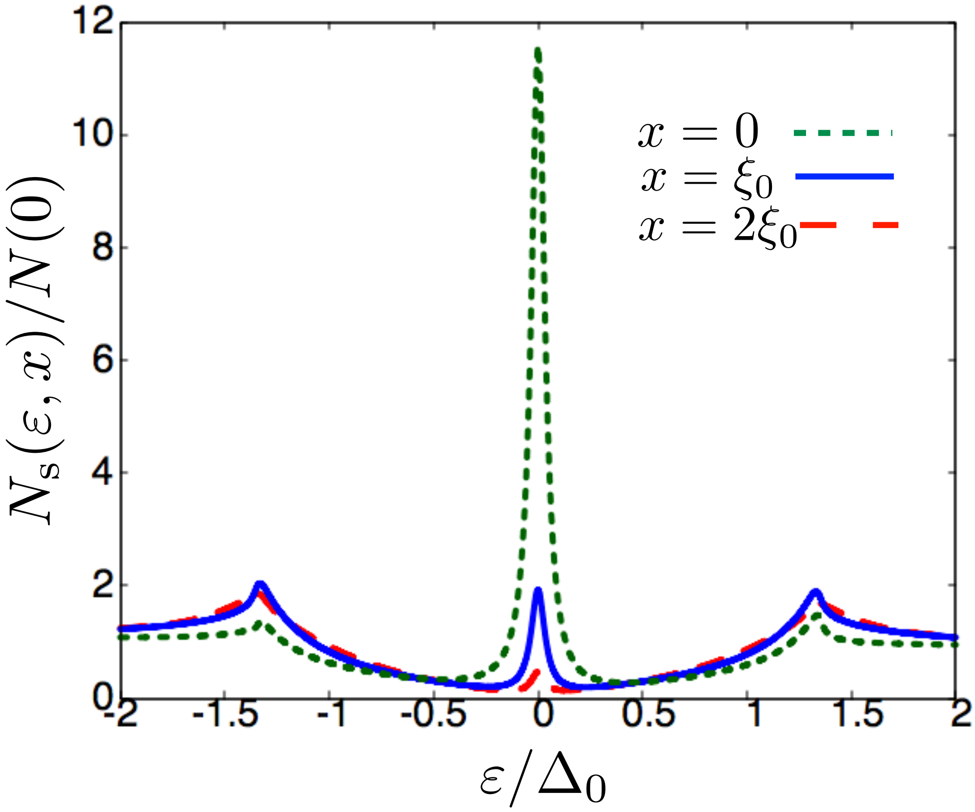

Figure 12: (Color online) LDOS $N_{\mathrm{s}}(\varepsilon, x)$ at $x = 0$ (green short dashes), ξ_0 (blue solid line), and $2\xi_0$ (red long dashes), with $\eta = 0.04$, at temperature $T = 0.1T_{\mathrm{c}}$, for the filling $n = 0.9$.

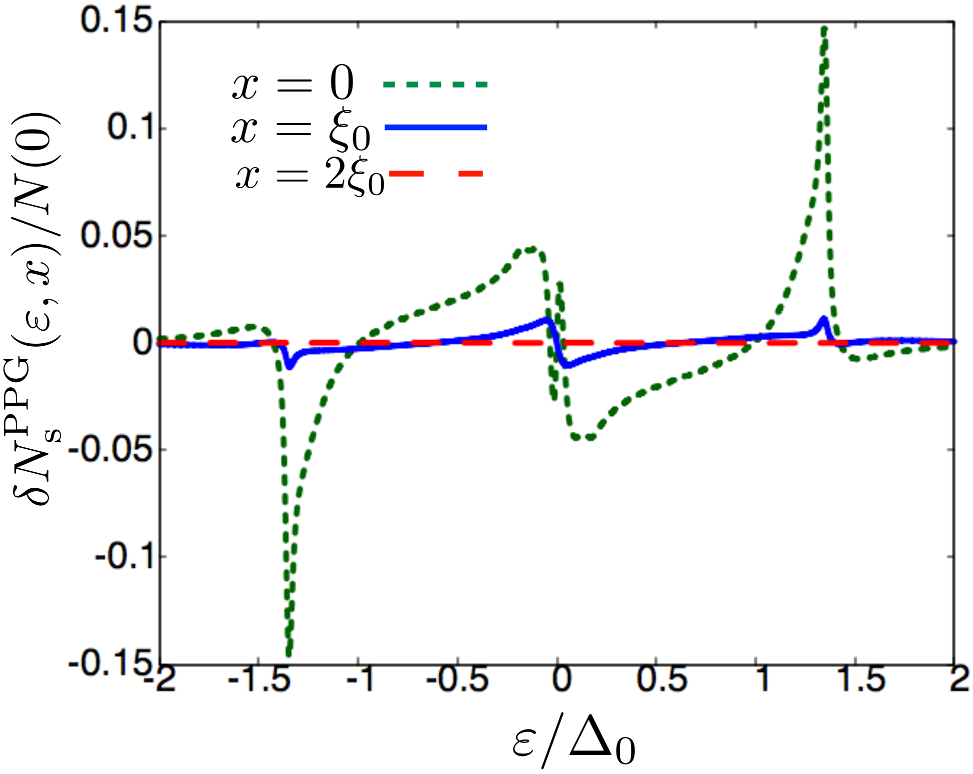

Figure 13: (Color online) Deviation $\delta N_{\mathrm{s}}^{\mathrm{PPG}}(\varepsilon, x)$ from the standard Eilenberger solutions in the LDOS due to quantum corrections from the PPG within the augmented quasiclassical theory, at $x = 0$ (green short dashes), ξ_0 (blue solid line), and $2\xi_0$ (red long dashes), with $\eta = 0.04$, at temperature $T = 0.1T_{\mathrm{c}}$, for the filling $n = 0.9$.

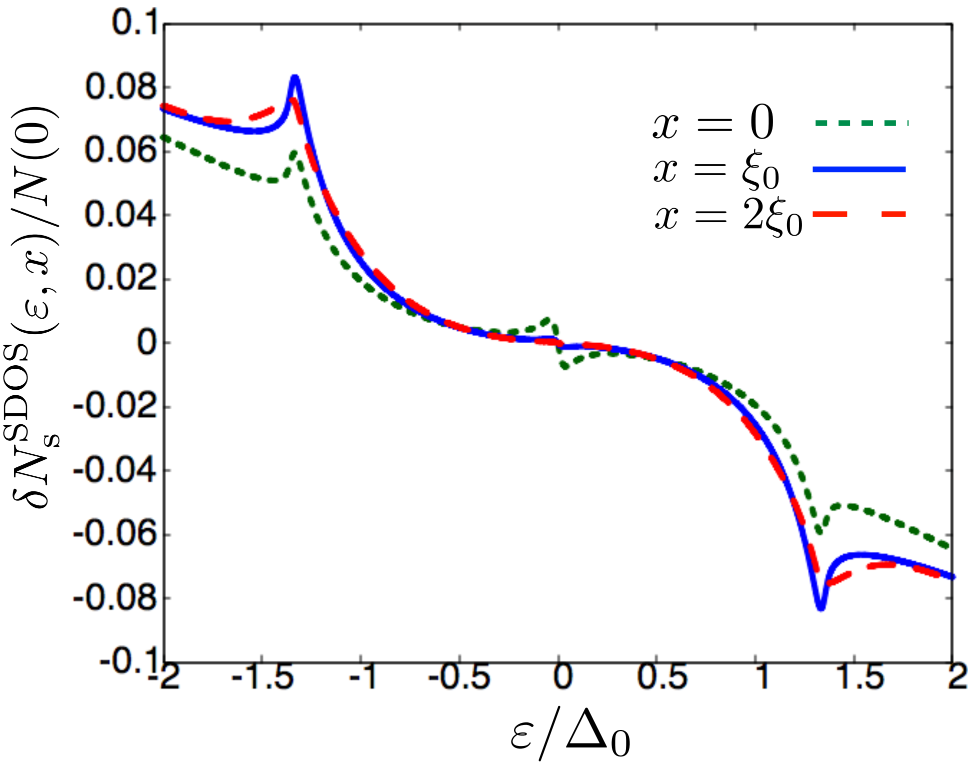

Figure 14: (Color online) Deviation $\delta N_{\mathrm{s}}^{\mathrm{SDOS}}(\varepsilon, x)$ from the standard Eilenberger solutions in the LDOS due to quantum corrections from the SDOS within the augmented quasiclassical theory, at $x = 0$ (green short dashes), ξ_0 (blue solid line), and $2\xi_0$ (red long dashes), with $\eta = 0.04$, at temperature $T = 0.1T_{\mathrm{c}}$, for the filling $n = 0.9$.

$n = 0.9$ due to the SDOS at the Fermi level. Assuming roughly normal metal at the [110] surface, we can explain that the (effective) chemical potential difference between the [110] surface and the bulk is what brings about the redistribution of charged particles.

Figure 8 plots the surface charge density due to the the SDOS pressure for the filling $n = 0.9$. The SDOS pressure charge consists of the second and third terms in Eq. (A.29), which have different signs respectively. As seen in Fig. 8, the third term dominates over the second term and thus the SDOS pressure charge at the surface becomes negative in total. We also confirmed the third term was dominant at all temperature for the fillings $n = 0.8$, 0.9, and 1.15 which are also realistic doping levels. Furthermore, Fig. 9 shows the total surface charge with contributions from the PPG force and the SDOS pressure for the filling $n = 0.9$. The SDOS pressure gives the dominant contribution to the surface charge within our present model at $n = 0.9$. We also confirmed that the SDOS pressure was dominant at not only $n = 0.9$, but also at $n = 0.8$ and $n = 1.15$. Since there is no supercurrents near the surface, there are no phase terms of the pair potential in the PPG force terms which are dominant in vortex systems[15]. Therefore, the contribution from the PPG force to the surface charge becomes small, and the SDOS pressure is dominant in a wide parameter range of the semi-finite system, compared to the vortex system. Figure 10 shows the total surface charge with contributions from the PPG force and the SDOS pressure for the filling $n = 1.15$. The PPG force contribution has the same negative sign as the SDOS pressure contribution, with the SDOS pressure giving the dominant contribution to the total charge.

As shown in Fig. 9 and 10, the sign of the charge density due to the PPG force at $n = 0.9$ is different from the one at $n = 1.15$. To explain this fact, we assume the form of pair potential as $\Delta \simeq \Delta_{\rm bulk} \tanh(x/\xi_1)$ and substitute it into Eq. (C.6) with taking $x \to 0$. By this procedure, we obtain

$$\rho_{\rm PPG}(0) \sim -\frac{2a^{(3)}\hbar^2\epsilon_0\Delta_{\rm bulk}^2}{\xi_1^4 e}\left\langle \phi^2 \frac{dv_{{\rm F}x}}{dp_{{\rm F}x}} \right\rangle_{\rm F}, \tag{3.19}$$

where $\rho_{\rm PPG}$ represents the charge density induced by PPG force and $a^{(3)} \equiv \pi k_{\rm B}T\sum_{n=0}^{\infty}\varepsilon_n^{-3}$. As described in appendix B, this approximation is valid at high temperature near the critical temperature. Relying on this expression, we see that the filling dependence is determined only by $\langle\phi^2 dv_{{\rm F}x}/dp_{{\rm F}x} \simeq\rangle dv_{{\rm F}x}/dp_{{\rm F}x} \propto (\underline{R}_{\rm H}^{\rm (n)})_{xx} = (\underline{R}_{\rm H}^{\rm (n)})_{yy}$, where $\underline{R}_{\rm H}^{\rm (n)}$ is a Hall coefficient in the normal state [14]. Therefore, as shown in Fig. 1 of Ref., charge density caused by PPG force also changes its sign around $n = 1$, which is mainly caused by the change of Fermi-surface curvature.

In Fig. 11, the temperature dependence of the total surface charge for the filling $n = 0.9$ is shown. The total spontaneously induced surface charge increases with a decrease in temperature. This follows the temperature dependence of the slope of the pair potential shown in Fig. 5. One may notice that the second order derivative of $\rho(x \gtrsim 0)$ with respect to x is not monotonic. The second order derivative of $\rho(x=0)$ is given by

$$(\partial^2\rho(x)/\partial x^2)_{x=0} \equiv \rho^{(2)}(0) \propto -[\rho_{\rm SDOS}(0)/\xi_{\rm SDOS}^2 + \rho_{\rm PPG}(0)/\xi_{\rm PPG}^2], \tag{3.20}$$

where $\xi_{\rm SDOS}$ ($\xi_{\rm PPG}$) is defined by the value of x at the first peak of charge density due to the SDOS pressure (PPG force). Thus, not only $\rho_i(0)$ but also ξ_i is necessary when we consider $\rho^{(2)}(0)$. In the present case, although $\rho(0)$ decreases monotonically as temperature decreases, $\rho^{(2)}(0)$ behaves nonmonotonically because of the competition between $\rho_{\rm SDOS}(0)/\xi_{\rm SDOS}^2 < 0$ and $\rho_{\rm PPG}(0)/\xi_{\rm PPG}^2 > 0$.

Figure 12 plots the normalised LDOS for the filling $n = 0.9$ at the regions $x = 0$, ξ_0, and $2\xi_0$. The peak structure appears as we move from the bulk to the surface. Figures 13 and 14 plot the deviations $\delta N_{\rm s}^{\rm PPG}(\varepsilon, x)$ and $\delta N_{\rm s}^{\rm SDOS}(\varepsilon, x)$ from the standard Eilenberger solutions in the LDOS at the filling $n = 0.9$, due to quantum corrections from the PPG force and the SDOS pressure respectively. The deviations $\delta N_{\rm s}^{\rm PPG}(\varepsilon, x)$ and $\delta N_{\rm s}^{\rm SDOS}(\varepsilon, x)$ are defined by

$$\delta N_{\rm s}^{\rm PPG}(\varepsilon, x) = N(0)\langle {\rm Re} g_1^{\rm R}\rangle_{\rm F}, \tag{3.21a}$$

$$\delta N_{\rm s}^{\rm SDOS}(\varepsilon, x) = N'(0)\varepsilon\langle {\rm Re} g_0^{\rm R}\rangle_{\rm F} + \frac{1}{2}N'(0)\Delta\langle {\rm Im} f_0^{\rm R} + {\rm Im} \bar{f}_0^{\rm R}\rangle_{\rm F}. \tag{3.21b}$$

We observe particle-hole asymmetry within the augmented quasiclassical theory. The PPG force and the SDOS pressure change their LDOS peaks near zero energy and around energy gap. This asymmetry indicates the presence of electric charging at the surface. The relation between the charging and the particle-hole asymmetry in the LDOS has already been discussed in the vortex system[15, 33]. Furthermore, multiple turning points appear in the LDOS deviations in the region $|\varepsilon/\Delta_0| \leq 1.5$. At $x = 0$, these sign changes appear due to the presence of small peaks in the LDOS at finite energies both within the standard Eilenberger equations and the LDOS with first-order quantum corrections. In the bulk region, the difference in the coherence peaks of the gap-like structures as well as the difference in the width of the energy gap between the LDOS in the standard Eilenberger solutions and the LDOS in the augmented quasiclassical equations might be the origin of these multiple turning points. Although it remains to be clarified if these multiple turning points have any physical meaning.

3.4 Summary

In summary, we have performed a microscopic calculation on surface charging at a single [110] specularly reflective surface of a d-wave superconductor with a Fermi surface used for cuprate superconductors using the augmented quasiclassical theory. We have shown that despite the absence of supercurrent, charge is spontaneously induced around the surface due to the PPG force and the SDOS pressure. The SDOS pressure gives the dominant contribution for the realistic electron-fillings $n = 0.8$, 0.9, and 1.15 at all temperatures. This differs from the case of the charging of an isolated s-wave vortex carried out by Ueki *et al.*, wherein the SDOS term dominates only near the critical temperature. We also have found that it is important to consider the Fermi surfaces, since the contribution from the SDOS pressure greatly depends on the Fermi surface structure. We have also calculated the LDOS within the augmented quasiclassical theory, taking into account the contributions due to the PPG and the SDOS pressure. At the surface, the LDOS shows a peak structure which signifies the presence of ZES. The bulk region shows a (nodal) gap-like structure which is a characteristic of the superconducting state. We have also shown the existence of particle-hole asymmetry (SDOS gives a strong particle-hole asymmetry) in the LDOS. This asymmetry indicates the presence of electric charge.

Although our present study is restricted to a smooth surface without edge currents, the presence of surface roughness is expected to affect the surface states and may consequently alter the surface charge. In addition, surface imperfections appear in the process of fabricating real samples. It is therefore important to take this into account in theory. It is relatively easier to consider surface roughness within the quasiclassical theory using the random S-matrix theory[44] or by adding a disorder-induced self-energy[45, 46]. Furthermore, in the presence of edge currents, the PPG force contribution to the charging effect may be enhanced due to the appearance of the phase terms of the pair potential. A combination of surface roughness and chirality may reveal very interesting physics.

4 General Summary and Conclusion

In this thesis, on the basis of the augmented quasiclassical equations, we have performed a microscopic study on the spontaneous redistribution charge near the surface of a d-wave superconductor cut along the [110] direction. More specifically, we have shown that even in the absence of supercurrents in the system, in a $d_{x^2-y^2}$-paired superconductor cut along the [110] plane, interesting surface effects appear and are accompanied by the pair potential gradient force and another force due to the slope of density of states in the normal states at the Fermi level. We have shown that these two forces induce spontaneous charging in the model d-wave superconductor. In carrying out our numerical study, we adopt a model d-wave pairing suitable for cuprate superconductors and therefore emphasise that this study can be applied to both hole-doped and electron-doped cuprates.

Furthermore, we have also calculated the local density of states within the augmented quasiclassical theory taking into account the first-order quantum corrections in terms of the quasiclassical parameter, due to the pair potential gradient force and the slope of the density of states. Although it has already been pointed out by Hayashi *et al.* and also recently by Masaki, that particle-hole asymmetry in the local density of states at the vortex core of superconductors shows the presence of electric charge. We have extended this idea to the surface state and have shown that the presence of the pair potential gradient force and the slope of the density of states give rise to an observable local particle-hole asymmetry in the local density of states which varies spatially from bulk to surface. We therefore conclude that this local asymmetry is a qualitative evidence of electric charging at the nodal surface of the d-wave paired superconductor.

Appendix

A Derivation of Augmented Quasiclassical Equations

Here, we give an overview of the derivation of the augmented quasiclassical equations (Eq. (2.1)) in the Matsubara formalism, following earlier works [5, 11, 13]. These elegant equations are useful for a microscopic investigation of the redistribution of charged particles in superconductors. We use the Green's function formalism to derive the Gor'kov equations from which the quasiclassical equations are obtained.

A.1 Matsubara Green's functions and Gor'kov equations

As a starting point, we consider electrons in static electromagnetic fields described by the Hamiltonian given in second quantized form as

$$\begin{aligned}\hat{\mathcal{H}} &= \int d\xi_1 \hat{\psi}^\dagger(\xi_1)\hat{\mathcal{K}}_1\hat{\psi}(\xi_1) \\ &\quad + \frac{1}{2}\int d\xi_1 \int d\xi_2 \mathcal{V}(\boldsymbol{r}_1 - \boldsymbol{r}_2)\hat{\psi}^\dagger(\xi_1)\hat{\psi}^\dagger(\xi_2)\hat{\psi}(\xi_2)\hat{\psi}(\xi_1),\end{aligned} \tag{A.1}$$

where the variable ξ is defined explicitly as $\xi \equiv (\boldsymbol{r}, \alpha)$ with $\boldsymbol{r}$ and α denoting the space and spin degrees of freedom, respectively. $\hat{\psi}^\dagger(\xi)$ and $\hat{\psi}(\xi)$ are the second quantized creation and annihilation operators of the fermion field, respectively, we also use † to denote a Hermitian conjugate, and $\mathcal{V}(\boldsymbol{r}_1 - \boldsymbol{r}_2)$ is the interaction potential. The one-particle operator $\hat{\mathcal{K}}_1$ now contains the vector potential $\boldsymbol{A}_1 \equiv \boldsymbol{A}(\boldsymbol{r}_1)$ and is expressed as

$$\hat{\mathcal{K}}_1 \equiv \frac{1}{2m}\left[-i\hbar\frac{\partial}{\partial \boldsymbol{r}_1} - e\boldsymbol{A}(\boldsymbol{r}_1)\right]^2 + e\Phi(\boldsymbol{r}_1) - \mu, \tag{A.2}$$

where m is the electronic mass, $e < 0$ is the electronic charge, and μ is the chemical potential. $\Phi(\boldsymbol{r})$ and $\boldsymbol{A}(\boldsymbol{r})$ are the static scalar potential and vector potential, respectively, and static electromagnetic fields are expressed here in terms of them as $\boldsymbol{E}(\boldsymbol{r}) = -\boldsymbol{\nabla}\Phi(\boldsymbol{r})$ and $\boldsymbol{B}(\boldsymbol{r}) = \boldsymbol{\nabla} \times \boldsymbol{A}(\boldsymbol{r})$. Furthermore, we introduce the fermion field operators in the Heisenberg representation in the Matsubara formalism as

$$\begin{cases} \hat{\psi}_1(1) \equiv e^{\tau_1\hat{\mathcal{H}}}\hat{\psi}(\xi_1)e^{-\tau_1\hat{\mathcal{H}}} \\ \hat{\psi}_2(1) \equiv e^{\tau_1\hat{\mathcal{H}}}\hat{\psi}^\dagger(\xi_1)e^{-\tau_1\hat{\mathcal{H}}} \end{cases}, \tag{A.3}$$

where the argument 1 can be written in explicit form as $1 \equiv (\xi_1, \tau_1)$, where the variable τ_1 lies in the range $0 \le \tau_1 \le 1/k_\mathrm{B}T$ with k_B and T denoting the Boltzmann constant and temperature, respectively. Using them, we introduce the Matsubara Green's function

$$G_{ij}(1,2) \equiv -\langle T_\tau \hat{\psi}_i(1)\hat{\psi}_{3-j}(2)\rangle, \tag{A.4}$$

The bracket notation $\langle\cdots\rangle$ and the operator T_τ denote the grand-canonical average [13] and "time"-ordering operator, respectively. Particle-field operators under T_τ are placed from left to right in order of decreasing "time" τ. For example

$$T_\tau(\hat{\psi}(\xi_1)\hat{\psi}^\dagger(\xi_2)) \equiv \begin{cases} \hat{\psi}(\xi_1)\hat{\psi}^\dagger(\xi_2) & \tau_1 > \tau_2, \\ -\hat{\psi}^\dagger(\xi_2)\hat{\psi}(\xi_1) & \tau_1 < \tau_2. \end{cases} \tag{A.5}$$

In the RHS, the field operators are placed in the chronological order, and a pre-factor of ± 1 appears, depending on whether the transposition is even or odd.

The elements of $G_{ij}(1,2)$ satisfy the following symmetry relations;

$$G_{ij}(1,2) = -G_{3-j,3-i}(2,1) = G^*_{ji}(\xi_2\tau_1, \xi_1\tau_2), \tag{A.6}$$

where the superscript * denotes complex conjugation operation. The Matsubara Green's function can be expanded as [13]

$$G_{ij}(1,2) = k_{\mathrm{B}}T \sum_{n=-\infty}^{\infty} G_{ij}(\xi_1, \xi_2; \varepsilon_n) e^{-i\varepsilon_n(\tau_1-\tau_2)}, \tag{A.7}$$

where the argument $\varepsilon_n = (2n+1)\pi k_{\mathrm{B}}T$ is the fermion Matsubara energy ($n = 0, \pm 1, \ldots$). Separating the spin variable $\alpha =\uparrow, \downarrow$ from $\xi = (\boldsymbol{r}, \alpha)$, we introduce a new notation for each G_{ij} as

$$G_{11}(\xi_1, \xi_2; \varepsilon_n) = G_{\alpha_1,\alpha_2}(\boldsymbol{r}_1, \boldsymbol{r}_2; \varepsilon_n), \tag{A.8a}$$
$$G_{12}(\xi_1, \xi_2; \varepsilon_n) = F_{\alpha_1,\alpha_2}(\boldsymbol{r}_1, \boldsymbol{r}_2; \varepsilon_n), \tag{A.8b}$$
$$G_{21}(\xi_1, \xi_2; \varepsilon_n) = -\bar{F}_{\alpha_1,\alpha_2}(\boldsymbol{r}_1, \boldsymbol{r}_2; \varepsilon_n), \tag{A.8c}$$
$$G_{22}(\xi_1, \xi_2; \varepsilon_n) = -\bar{G}_{\alpha_1,\alpha_2}(\boldsymbol{r}_1, \boldsymbol{r}_2; \varepsilon_n). \tag{A.8d}$$

Subsequently, we express the spin degrees of freedom as the 2×2 matrix

$$\underline{G}(\boldsymbol{r}_1, \boldsymbol{r}_2; \varepsilon_n) \equiv \begin{bmatrix} G_{\uparrow\uparrow}(\boldsymbol{r}_1, \boldsymbol{r}_2; \varepsilon_n) & G_{\uparrow\downarrow}(\boldsymbol{r}_1, \boldsymbol{r}_2; \varepsilon_n) \\ G_{\downarrow\uparrow}(\boldsymbol{r}_1, \boldsymbol{r}_2; \varepsilon_n) & G_{\downarrow\downarrow}(\boldsymbol{r}_1, \boldsymbol{r}_2; \varepsilon_n) \end{bmatrix}. \tag{A.9}$$

Therefore, the Green's functions $\underline{G}$ and $\underline{F}$ from Eqs. (A.6) and (A.7) have the following symmetry relations;

$$\underline{G}(\boldsymbol{r}_1, \boldsymbol{r}_2; \varepsilon_n) = \underline{G}^\dagger(\boldsymbol{r}_2, \boldsymbol{r}_1; -\varepsilon_n) = \underline{\bar{G}}^{\mathrm{T}}(\boldsymbol{r}_2, \boldsymbol{r}_1; -\varepsilon_n), \tag{A.10a}$$
$$\underline{F}(\boldsymbol{r}_1, \boldsymbol{r}_2; \varepsilon_n) = -\underline{\bar{F}}^\dagger(\boldsymbol{r}_2, \boldsymbol{r}_1; -\varepsilon_n) = -\underline{F}^{\mathrm{T}}(\boldsymbol{r}_2, \boldsymbol{r}_1; -\varepsilon_n), \tag{A.10b}$$

where the superscript $^{\mathrm{T}}$ denotes the transpose. It follows from these symmetry relations that $\underline{\bar{G}}(\boldsymbol{r}_1, \boldsymbol{r}_2; \varepsilon_n) = \underline{G}^*(\boldsymbol{r}_1, \boldsymbol{r}_2; \varepsilon_n)$ and $\underline{\bar{F}}(\boldsymbol{r}_1, \boldsymbol{r}_2; \varepsilon_n) = \underline{F}^*(\boldsymbol{r}_1, \boldsymbol{r}_2; \varepsilon_n)$ hold. Using $\underline{G}$ and $\underline{F}$, we define a 4×4 matrix in Nambu space by

$$\hat{G}(\boldsymbol{r}_1, \boldsymbol{r}_2; \varepsilon_n) \equiv \begin{bmatrix} \underline{G}(\boldsymbol{r}_1, \boldsymbol{r}_2; \varepsilon_n) & \underline{F}(\boldsymbol{r}_1, \boldsymbol{r}_2; \varepsilon_n) \\ -\underline{F}^*(\boldsymbol{r}_1, \boldsymbol{r}_2; \varepsilon_n) & -\underline{G}^*(\boldsymbol{r}_1, \boldsymbol{r}_2; \varepsilon_n) \end{bmatrix}. \tag{A.11}$$

Within the mean-field approximation, the Nambu Green's function satisfy Gor'kov equations [13, 47]

$$\begin{bmatrix} (i\varepsilon_n - \hat{\mathcal{K}}_1)\underline{\sigma}_0 & \underline{0} \\ \underline{0} & (i\varepsilon_n + \hat{\mathcal{K}}_1^*)\underline{\sigma}_0 \end{bmatrix} \hat{G}(\boldsymbol{r}_1, \boldsymbol{r}_2; \varepsilon_n)$$
$$- \int d^3r_3 \hat{\mathcal{U}}_{\rm BdG}(\boldsymbol{r}_1, \boldsymbol{r}_3)\hat{G}(\boldsymbol{r}_3, \boldsymbol{r}_2; \varepsilon_n) = \hat{\delta}(\boldsymbol{r}_1 - \boldsymbol{r}_2), \tag{A.12}$$

where $\underline{\sigma}_0$ and $\underline{0}$ denote the 2×2 unit and zero matrices, respectively. Matrix $\hat{\mathcal{U}}_{\rm BdG}(\boldsymbol{r}_1, \boldsymbol{r}_3)$ denotes

$$\hat{\mathcal{U}}_{\rm BdG}(\boldsymbol{r}_1, \boldsymbol{r}_2) \equiv \begin{bmatrix} \underline{\mathcal{U}}_{\rm HF}(\boldsymbol{r}_1, \boldsymbol{r}_2) & \underline{\Delta}(\boldsymbol{r}_1, \boldsymbol{r}_2) \\ -\underline{\Delta}^*(\boldsymbol{r}_1, \boldsymbol{r}_2) & -\underline{\mathcal{U}}_{\rm HF}^*(\boldsymbol{r}_1, \boldsymbol{r}_2) \end{bmatrix}, \tag{A.13}$$

where matrices $\underline{\mathcal{U}}_{\rm HF}(\boldsymbol{r}_1, \boldsymbol{r}_2)$ and $\underline{\Delta}(\boldsymbol{r}_1, \boldsymbol{r}_2)$ are the Hartree–Fock and pair potential, respectively, and have the following definitions;

$$\underline{\mathcal{U}}_{\rm HF}(\boldsymbol{r}_1, \boldsymbol{r}_2) \equiv \delta(\boldsymbol{r}_1 - \boldsymbol{r}_2)\underline{\sigma}_0 {\rm Tr} \int d^3r_3 \mathcal{V}(\boldsymbol{r}_1 - \boldsymbol{r}_3)$$
$$\times k_{\rm B}T \sum_{n=-\infty}^{\infty} \underline{G}(\boldsymbol{r}_3, \boldsymbol{r}_3; \varepsilon_n) {\rm e}^{-i\varepsilon_n 0_-}$$
$$- \mathcal{V}(\boldsymbol{r}_1 - \boldsymbol{r}_2) k_{\rm B}T \sum_{n=-\infty}^{\infty} \underline{G}(\boldsymbol{r}_1, \boldsymbol{r}_2; \varepsilon_n) {\rm e}^{-i\varepsilon_n 0_-}, \tag{A.14}$$

$$\underline{\Delta}(\boldsymbol{r}_1, \boldsymbol{r}_2) \equiv \mathcal{V}(\boldsymbol{r}_1 - \boldsymbol{r}_2) k_{\rm B}T \sum_{n=-\infty}^{\infty} \underline{F}(\boldsymbol{r}_1, \boldsymbol{r}_2; \varepsilon_n), \tag{A.15}$$

where the quantity 0_- denotes an extra infinitesimal negative constant. Finally, matrix $\hat{\delta}$ on the right-hand side of Eq. (A.12) is defined by

$$\hat{\delta}(\boldsymbol{r}_1 - \boldsymbol{r}_2) \equiv \begin{bmatrix} \delta(\boldsymbol{r}_1 - \boldsymbol{r}_2)\underline{\sigma}_0 & \underline{0} \\ \underline{0} & \delta(\boldsymbol{r}_1 - \boldsymbol{r}_2)\underline{\sigma}_0 \end{bmatrix}. \tag{A.16}$$

A.2 Gor'kov equations in the Wigner representation

We highlight that one of the known fundamental difficulties encountered when applying the original Wigner transform [11, 13, 48] to charged systems is that it breaks gauge invariance with respect to the center-of-mass coordinate. To ameliorate this difficulty, we adopt the technique of gauge-covariant Wigner transform which has been devised for the Matsubara Green's functions defined by

$$\hat{G}(\varepsilon_n, \boldsymbol{p}, \boldsymbol{r}_{12})$$
$$\equiv \int d^3\bar{r}_{12} e^{-i\boldsymbol{p}\cdot\bar{\boldsymbol{r}}_{12}/\hbar} \hat{\Gamma}(\boldsymbol{r}_{12}, \boldsymbol{r}_1)\hat{G}(\boldsymbol{r}_1, \boldsymbol{r}_2; \varepsilon_n)\hat{\Gamma}(\boldsymbol{r}_2, \boldsymbol{r}_{12})$$
$$\equiv \begin{bmatrix} \underline{G}(\varepsilon_n, \boldsymbol{p}, \boldsymbol{r}_{12}) & \underline{F}(\varepsilon_n, \boldsymbol{p}, \boldsymbol{r}_{12}) \\ -\underline{F}^*(\varepsilon_n, -\boldsymbol{p}, \boldsymbol{r}_{12}) & -\underline{G}^*(\varepsilon_n, -\boldsymbol{p}, \boldsymbol{r}_{12}) \end{bmatrix}, \tag{A.17a}$$

with $\boldsymbol{r}_{12} \equiv (\boldsymbol{r}_1 + \boldsymbol{r}_2)/2$ and $\bar{\boldsymbol{r}}_{12} \equiv \boldsymbol{r}_1 - \boldsymbol{r}_2$, its inverse is expressed as

$$\begin{aligned}
&\hat{G}(\boldsymbol{r}_1, \boldsymbol{r}_2; \varepsilon_n) \\
&= \hat{\Gamma}(\boldsymbol{r}_1, \boldsymbol{r}_{12}) \int \frac{d^3p}{(2\pi\hbar)^3} e^{i\boldsymbol{p}\cdot\bar{\boldsymbol{r}}_{12}/\hbar} \hat{G}(\varepsilon_n, \boldsymbol{p}, \boldsymbol{r}_{12}) \hat{\Gamma}(\boldsymbol{r}_{12}, \boldsymbol{r}_2).
\end{aligned} \tag{A.17b}$$

The matrix $\hat{\Gamma}$ is given by

$$\hat{\Gamma}(\boldsymbol{r}_1, \boldsymbol{r}_2) \equiv \begin{bmatrix} \underline{\sigma}_0 e^{iI(\boldsymbol{r}_1,\boldsymbol{r}_2)} & \underline{0} \\ \underline{0} & \underline{\sigma}_0 e^{-iI(\boldsymbol{r}_1,\boldsymbol{r}_2)} \end{bmatrix}. \tag{A.18}$$

Where the function $I(\boldsymbol{r}_1, \boldsymbol{r}_2)$ is the line integral expressed as

$$I(\boldsymbol{r}_1, \boldsymbol{r}_2) \equiv \frac{e}{\hbar} \int_{\boldsymbol{r}_2}^{\boldsymbol{r}_1} \boldsymbol{A}(\boldsymbol{s}) \cdot d\boldsymbol{s}, \tag{A.19}$$

with $\boldsymbol{s}$ denoting a straight-line path from $\boldsymbol{r}_2$ to $\boldsymbol{r}_1$. Similarly, we rewrite the mean-field potential in Eq. (A.13) as

$$\begin{aligned}
&\hat{\mathcal{U}}_{\mathrm{BdG}}(\boldsymbol{p}, \boldsymbol{r}_{12}) \\
&\equiv \int d^3\bar{r}_{12} e^{-i\boldsymbol{p}\cdot\bar{\boldsymbol{r}}_{12}/\hbar} \hat{\Gamma}(\boldsymbol{r}_{12}, \boldsymbol{r}_1) \hat{\mathcal{U}}_{\mathrm{BdG}}(\boldsymbol{r}_1, \boldsymbol{r}_2) \hat{\Gamma}(\boldsymbol{r}_2, \boldsymbol{r}_{12}) \\
&\equiv \begin{bmatrix} \underline{\mathcal{U}}_{\mathrm{HF}}(\boldsymbol{p}, \boldsymbol{r}_{12}) & \underline{\Delta}(\boldsymbol{p}, \boldsymbol{r}_{12}) \\ -\underline{\Delta}^*(-\boldsymbol{p}, \boldsymbol{r}_{12}) & -\underline{\mathcal{U}}^*_{\mathrm{HF}}(-\boldsymbol{p}, \boldsymbol{r}_{12}) \end{bmatrix},
\end{aligned} \tag{A.20a}$$

It has an inverse which can be written

$$\begin{aligned}
&\hat{\mathcal{U}}_{\mathrm{BdG}}(\boldsymbol{r}_1, \boldsymbol{r}_2) \\
&= \hat{\Gamma}(\boldsymbol{r}_1, \boldsymbol{r}_{12}) \int \frac{d^3p}{(2\pi\hbar)^3} e^{i\boldsymbol{p}\cdot\bar{\boldsymbol{r}}_{12}/\hbar} \hat{\mathcal{U}}_{\mathrm{BdG}}(\boldsymbol{p}, \boldsymbol{r}_{12}) \hat{\Gamma}(\boldsymbol{r}_{12}, \boldsymbol{r}_2).
\end{aligned} \tag{A.20b}$$

The quantities $\underline{\mathcal{U}}_{\mathrm{HF}}(\boldsymbol{p}, \boldsymbol{r}_{12})$ and $\underline{\Delta}(\boldsymbol{p}, \boldsymbol{r}_{12})$ satisfy the following symmetry relations $\underline{\mathcal{U}}_{\mathrm{HF}}(\boldsymbol{p}, \boldsymbol{r}_{12}) = \underline{\mathcal{U}}^{\dagger}_{\mathrm{HF}}(\boldsymbol{p}, \boldsymbol{r}_{12})$ and $\underline{\Delta}(\boldsymbol{p}, \boldsymbol{r}_{12}) = -\underline{\Delta}^{\mathrm{T}}(-\boldsymbol{p}, \boldsymbol{r}_{12})$. Furthermore, we consider the next-to-leading-order contribution in the expansion in terms of the quasiclassical parameter. We hereby obtain Gor'kov equations in the Wigner representation as (see Appendices A.3 and A.4 below for the derivation of the kinetic-energy and self-energy terms in the Wigner representation, respectively)

$$\begin{aligned}
&\left\{ i\varepsilon_n \hat{1} - \left[\xi_{\boldsymbol{p}} - i\frac{\hbar \boldsymbol{v}}{2} \cdot \boldsymbol{\partial} - \frac{\hbar^2 \boldsymbol{\partial}^2}{8m^*} - \frac{i\hbar}{2} e\boldsymbol{E}(\boldsymbol{r}) \cdot \frac{\partial}{\partial \boldsymbol{p}} \right] \hat{\tau}_3 \right\} \hat{G}(\varepsilon_n, \boldsymbol{p}, \boldsymbol{r}) \\
&\quad - \hat{\Delta}(\boldsymbol{p}, \boldsymbol{r}) \circ \hat{G}(\varepsilon_n, \boldsymbol{p}, \boldsymbol{r}) \\
&\quad + \frac{i\hbar}{8} e\boldsymbol{v} \cdot \left[\boldsymbol{B}(\boldsymbol{r}) \times \frac{\partial}{\partial \boldsymbol{p}} \right] \left[3\hat{G}(\varepsilon_n, \boldsymbol{p}, \boldsymbol{r}) + \hat{\tau}_3 \hat{G}(\varepsilon_n, \boldsymbol{p}, \boldsymbol{r}) \hat{\tau}_3 \right] = \hat{1},
\end{aligned} \tag{A.21}$$

where $\xi_{\boldsymbol{p}}$ is defined by $\xi_{\boldsymbol{p}} \equiv \varepsilon_{\boldsymbol{p}} + e\Phi(\boldsymbol{r}) - \mu$ with $\varepsilon_{\boldsymbol{p}}$ denoting the single-particle energy, m^* is the effective mass defined by $m^* \equiv p/v$, $\hat{1}$ denotes the 4×4 unit matrix, $\hat{\tau}_3$ is defined by

$$\hat{\tau}_3 \equiv \begin{bmatrix} \underline{\sigma}_0 & \underline{0} \\ \underline{0} & -\underline{\sigma}_0 \end{bmatrix}, \tag{A.22}$$

$\boldsymbol{\partial}$ is given by

$$\boldsymbol{\partial} \equiv \begin{cases} \dfrac{\partial}{\partial \boldsymbol{r}} & : \text{on } \underline{G} \text{ or } \underline{G}^* \\ \dfrac{\partial}{\partial \boldsymbol{r}} - i\dfrac{2e}{\hbar}\boldsymbol{A}(\boldsymbol{r}) & : \text{on } \underline{F} \\ \dfrac{\partial}{\partial \boldsymbol{r}} + i\dfrac{2e}{\hbar}\boldsymbol{A}(\boldsymbol{r}) & : \text{on } \underline{F}^* \end{cases}, \tag{A.23}$$

and the operator $\circ$ is also defined as

$$\hat{a}(\boldsymbol{p}, \boldsymbol{r}) \circ \hat{b}(\boldsymbol{p}, \boldsymbol{r}) \equiv \hat{a}(\boldsymbol{p}, \boldsymbol{r}) \exp\left[\frac{i\hbar}{2}\left(\overleftarrow{\boldsymbol{\partial}} \cdot \overrightarrow{\boldsymbol{\partial}}_{\boldsymbol{p}} - \overleftarrow{\boldsymbol{\partial}}_{\boldsymbol{p}} \cdot \overrightarrow{\boldsymbol{\partial}}\right)\right] \hat{b}(\boldsymbol{p}, \boldsymbol{r}). \tag{A.24}$$

Taking the Hermitian conjugate of Eq. (A.21), use the symmetries $\hat{\mathcal{U}}^\dagger_{\rm BdG}(\boldsymbol{p}, \boldsymbol{r}) = \hat{\mathcal{U}}_{\rm BdG}(\boldsymbol{p}, \boldsymbol{r})$ and $\hat{G}^\dagger(\varepsilon_n, \boldsymbol{p}, \boldsymbol{r}) = \hat{G}(-\varepsilon_n, \boldsymbol{p}, \boldsymbol{r})$, and replace $\varepsilon_n \to -\varepsilon_n$ to obtain

$$\begin{aligned} &\hat{G}(\varepsilon_n, \boldsymbol{p}, \boldsymbol{r}) \left\{ i\varepsilon_n \hat{1} - \hat{\tau}_3 \left[\xi_{\boldsymbol{p}} + i\frac{\hbar \boldsymbol{v}}{2} \cdot \boldsymbol{\partial} - \frac{\hbar^2 \boldsymbol{\partial}^2}{8m^*} + \frac{i\hbar}{2} e\boldsymbol{E}(\boldsymbol{r}) \cdot \frac{\partial}{\partial \boldsymbol{p}} \right] \right\} \\ &\quad - \hat{G}(\varepsilon_n, \boldsymbol{p}, \boldsymbol{r}) \circ \hat{\Delta}(\boldsymbol{p}, \boldsymbol{r}) \\ &\quad - \frac{i\hbar}{8} e\boldsymbol{v} \cdot \left[\boldsymbol{B}(\boldsymbol{r}) \times \frac{\partial}{\partial \boldsymbol{p}} \right] \left[3\hat{G}(\varepsilon_n, \boldsymbol{p}, \boldsymbol{r}) + \hat{\tau}_3 \hat{G}(\varepsilon_n, \boldsymbol{p}, \boldsymbol{r}) \hat{\tau}_3 \right] = \hat{1}. \end{aligned} \tag{A.25}$$

Next we operate $\hat{\tau}_3$ on the left- and right-hand sides of Eq. (A.25), and subtracting from Eq. (A.21) and also adding to Eq. (A.21). We arrive at the following:

$$\begin{aligned} &\left[i\varepsilon_n \hat{\tau}_3 - \hat{\Delta}(\boldsymbol{p}, \boldsymbol{r}) \hat{\tau}_3, \hat{\tau}_3 \hat{G}(\varepsilon_n, \boldsymbol{p}, \boldsymbol{r}) \right]_\circ + i\hbar \boldsymbol{v} \cdot \boldsymbol{\partial} \hat{\tau}_3 \hat{G}(\varepsilon_n, \boldsymbol{p}, \boldsymbol{r}) \\ &+ i\hbar e \boldsymbol{E} \cdot \frac{\partial}{\partial \boldsymbol{p}} \hat{\tau}_3 \hat{G}(\varepsilon_n, \boldsymbol{p}, \boldsymbol{r}) + \frac{i\hbar}{2} e\boldsymbol{v} \cdot \left(\boldsymbol{B} \times \frac{\partial}{\partial \boldsymbol{p}} \right) \left\{ \hat{\tau}_3, \hat{\tau}_3 \hat{G}(\varepsilon_n, \boldsymbol{p}, \boldsymbol{r}) \right\} \\ &= \hat{0}, \end{aligned} \tag{A.26a}$$

$$\begin{aligned} &\frac{1}{2} \left\{ i\varepsilon_n \hat{\tau}_3 - \hat{\Delta}(\boldsymbol{p}, \boldsymbol{r}) \hat{\tau}_3, \hat{\tau}_3 \hat{G}(\varepsilon_n, \boldsymbol{p}, \boldsymbol{r}) \right\}_\circ - \xi_{\boldsymbol{p}} \hat{\tau}_3 \hat{G}(\varepsilon_n, \boldsymbol{p}, \boldsymbol{r}) - \hat{1} \\ &+ \frac{\hbar^2 \boldsymbol{\partial}^2}{8m^*} \hat{\tau}_3 \hat{G}(\varepsilon_n, \boldsymbol{p}, \boldsymbol{r}) + \frac{i\hbar}{8} e\boldsymbol{v} \cdot \left(\boldsymbol{B} \times \frac{\partial}{\partial \boldsymbol{p}} \right) \left[\hat{\tau}_3, \hat{\tau}_3 \hat{G}(\varepsilon_n, \boldsymbol{p}, \boldsymbol{r}) \right] \\ &= \hat{0}, \end{aligned} \tag{A.26b}$$

with $[\hat{a}, \hat{b}] \equiv \hat{a}\hat{b} - \hat{b}\hat{a}$, $[\hat{a}, \hat{b}]_\circ \equiv \hat{a} \circ \hat{b} - \hat{b} \circ \hat{a}$, $\{\hat{a}, \hat{b}\} \equiv \hat{a}\hat{b} + \hat{b}\hat{a}$, and $\{\hat{a}, \hat{b}\}_\circ \equiv \hat{a} \circ \hat{b} + \hat{b} \circ \hat{a}$. Now, in terms of Eq. (A.17a), we introduce the quasiclassical Green's function

$$\begin{aligned} \hat{g}(\varepsilon_n, \boldsymbol{p}_{\rm F}, \boldsymbol{r}) &\equiv {\rm P}\int_{-\infty}^{\infty} \frac{d\xi_{\boldsymbol{p}}}{\pi} i\hat{\tau}_3 \hat{G}(\varepsilon_n, \boldsymbol{p}, \boldsymbol{r}) \\ &\equiv \begin{bmatrix} \underline{g}(\varepsilon_n, \boldsymbol{p}_{\rm F}, \boldsymbol{r}) & -i\underline{f}(\varepsilon_n, \boldsymbol{p}_{\rm F}, \boldsymbol{r}) \\ -i\underline{f}^*(\varepsilon_n, -\boldsymbol{p}_{\rm F}, \boldsymbol{r}) & -\underline{g}^*(\varepsilon_n, -\boldsymbol{p}_{\rm F}, \boldsymbol{r}) \end{bmatrix}, \end{aligned} \tag{A.27}$$

where P denotes the principal value. It follows that the upper elements $\underline{g}$ and $\underline{f}$ satisfy $\underline{g}(\varepsilon_n, \boldsymbol{p}_{\rm F}, \boldsymbol{r}) = -\underline{g}^\dagger(-\varepsilon_n, \boldsymbol{p}_{\rm F}, \boldsymbol{r})$, $\underline{f}(\varepsilon_n, \boldsymbol{p}_{\rm F}, \boldsymbol{r}) = -\underline{f}^{\rm T}(-\varepsilon_n, -\boldsymbol{p}_{\rm F}, \boldsymbol{r})$. To derive the equation for $\hat{g}$ from Eq. (A.26a), we express $\boldsymbol{\partial}_{\boldsymbol{p}} = \boldsymbol{\partial}_{\boldsymbol{p}_\parallel} + \boldsymbol{v}(\partial/\partial\xi)$ with $\boldsymbol{p}_\parallel$ denoting the component on the energy surface $\xi = \xi_{\boldsymbol{p}}$, set $\boldsymbol{p} = \boldsymbol{p}_{\rm F}$ except for the argument of $\hat{G}$, integrate Eq. (A.26a) over $-\varepsilon_{\rm c} \leq \xi_{\boldsymbol{p}} \leq \varepsilon_{\rm c}$, and use $\boldsymbol{v} \times \boldsymbol{\partial}_{\boldsymbol{p}_\parallel} = \boldsymbol{v} \times \boldsymbol{\partial}_{\boldsymbol{p}}$ and

$$\mathrm{P}\int_{-\infty}^{\infty} d\xi_{\boldsymbol{p}} \frac{\partial}{\partial \xi_{\boldsymbol{p}}} \hat{G}(\varepsilon_n, \boldsymbol{p}, \boldsymbol{r}) = \hat{0}. \tag{A.28}$$

Neglecting terms with $e\boldsymbol{E}\cdot\boldsymbol{\partial}_{\boldsymbol{p}_\parallel}$ and taking the limit $\varepsilon_{\rm c} \to \infty$, we obtain the augmented quasiclassical equations with the Lorentz force and the pair potential gradient terms as

$$\begin{aligned} &\left[i\varepsilon_n\hat{\tau}_3 - \hat{\Delta}(\boldsymbol{p}_{\rm F}, \boldsymbol{r})\hat{\tau}_3, \hat{g}(\varepsilon_n, \boldsymbol{p}_{\rm F}, \boldsymbol{r})\right]_\circ + i\hbar\boldsymbol{v}_{\rm F}\cdot\boldsymbol{\partial}\hat{g}(\varepsilon_n, \boldsymbol{p}_{\rm F}, \boldsymbol{r}) \\ &\quad + \frac{i\hbar}{2} e\boldsymbol{v}_{\rm F}\cdot\left(\boldsymbol{B}\times\frac{\partial}{\partial\boldsymbol{p}_{\rm F}}\right)\{\hat{\tau}_3, \hat{g}(\varepsilon_n, \boldsymbol{p}_{\rm F}, \boldsymbol{r})\} = \hat{0}. \end{aligned} \tag{A.29}$$

Applying the same procedure to Eq. (A.29), we obtain the equation for

$$\hat{g}^{(1)}(\varepsilon_n, \boldsymbol{p}_{\rm F}, \boldsymbol{r}) \equiv \mathrm{P}\int_{-\infty}^{\infty} \frac{d\xi_{\boldsymbol{p}}}{\pi} i\left[\xi_{\boldsymbol{p}}\hat{\tau}_3\hat{G}(\varepsilon_n, \boldsymbol{p}, \boldsymbol{r}) + \hat{1}\right] \tag{A.30}$$

as

$$\begin{aligned} \hat{g}^{(1)}(\varepsilon_n, \boldsymbol{p}_{\rm F}, \boldsymbol{r}) &= \frac{1}{2}\left\{i\varepsilon_n\hat{\tau}_3 - \hat{\Delta}(\boldsymbol{p}_{\rm F}, \boldsymbol{r})\hat{\tau}_3, \hat{g}(\varepsilon_n, \boldsymbol{p}_{\rm F}, \boldsymbol{r})\right\}_\circ \\ &\quad + \frac{\hbar^2\boldsymbol{\partial}^2}{8m^*}\hat{g}(\varepsilon_n, \boldsymbol{p}_{\rm F}, \boldsymbol{r}) + \frac{i\hbar}{8} e\boldsymbol{v}_{\rm F}\cdot\left(\boldsymbol{B}\times\frac{\partial}{\partial\boldsymbol{p}_{\rm F}}\right)[\hat{\tau}_3, \hat{g}(\varepsilon_n, \boldsymbol{p}_{\rm F}, \boldsymbol{r})]. \end{aligned} \tag{A.31}$$

We then neglect the second and third terms in Eq. (A.31) to take the leading order as

$$\hat{g}^{(1)}(\varepsilon_n, \boldsymbol{p}_{\rm F}, \boldsymbol{r}) \approx \frac{1}{2}\left\{i\varepsilon_n\hat{\tau}_3 - \hat{\Delta}(\boldsymbol{p}_{\rm F}, \boldsymbol{r})\hat{\tau}_3, \hat{g}(\varepsilon_n, \boldsymbol{p}_{\rm F}, \boldsymbol{r})\right\}. \tag{A.32}$$

It is important to note that Eq. (A.32) is useful for evaluating the terms of the slope of density of states within the augmented quasiclassical theory. It accounts for the deviations in the local density of states from the standard Eilenberger solutions.

A.3 Kinetic-Energy Terms in the Wigner Representation

Here we show how to simplify the kinetic-energy terms contained in the Gor'kov equation [Eq. (A.12)] in the Wigner representation [Eq. (A.17b)]. To this end, we introduce the following functions

$$\mathcal{E}_1(u) \equiv \int_0^1 d\eta \mathrm{e}^{\eta u} = \frac{\mathrm{e}^u - 1}{u} = \sum_{n=1}^{\infty}\frac{u^{n-1}}{n!}, \tag{A.33}$$

$$\mathcal{E}_2(u) \equiv \int_0^1 d\eta \int_0^\eta d\zeta \mathrm{e}^{\zeta u} = \frac{\mathrm{e}^u - 1 - u}{u^2} = \sum_{n=2}^{\infty}\frac{u^{n-2}}{n!}, \tag{A.34}$$

These functions are used to rewrite the phase factors which appear in in Eq. (A.17b) as follows;

$$I(\boldsymbol{r}_1,\boldsymbol{r}_{12}) = \frac{e}{\hbar}\mathcal{E}_1\left(\frac{\bar{\boldsymbol{r}}_{12}}{2}\cdot\frac{\partial}{\partial\boldsymbol{r}_{12}}\right)\mathbf{A}(\mathbf{r}_{12})\cdot\frac{\bar{\boldsymbol{r}}_{12}}{2}, \tag{A.35a}$$

$$I(\boldsymbol{r}_{12},\boldsymbol{r}_2) = \frac{e}{\hbar}\mathcal{E}_1\left(-\frac{\bar{\boldsymbol{r}}_{12}}{2}\cdot\frac{\partial}{\partial\boldsymbol{r}_{12}}\right)\mathbf{A}(\mathbf{r}_{12})\cdot\frac{\bar{\boldsymbol{r}}_{12}}{2}. \tag{A.35b}$$

Next, we use $\partial/\partial\boldsymbol{r}_1 = \partial/\partial\bar{\boldsymbol{r}}_{12} + (1/2)\partial/\partial\boldsymbol{r}_{12}$ and Eq. (A.35) to rewrite $(\partial/\partial\boldsymbol{r}_1)I(\boldsymbol{r}_1,\boldsymbol{r}_{12})$ and $(\partial/\partial\boldsymbol{r}_1)I(\boldsymbol{r}_{12},\boldsymbol{r}_2)$ in the form

$$\begin{aligned}\frac{\partial}{\partial\boldsymbol{r}_1}I(\boldsymbol{r}_1,\boldsymbol{r}_{12}) &= \frac{e}{\hbar}\boldsymbol{A}(\boldsymbol{r}_1) - \frac{e}{2\hbar}\boldsymbol{A}(\boldsymbol{r}_{12}) \\ &\quad - \frac{e}{4\hbar}\left[2\mathcal{E}_1\left(\frac{\bar{\boldsymbol{r}}_{12}}{2}\cdot\frac{\partial}{\partial\boldsymbol{r}_{12}}\right) - \mathcal{E}_2\left(\frac{\bar{\boldsymbol{r}}_{12}}{2}\cdot\frac{\partial}{\partial\boldsymbol{r}_{12}}\right)\right]\boldsymbol{B}(\boldsymbol{r}_{12})\times\bar{\boldsymbol{r}}_{12},\end{aligned} \tag{A.36a}$$

$$\frac{\partial}{\partial\boldsymbol{r}_1}I(\boldsymbol{r}_{12},\boldsymbol{r}_2) = \frac{e}{2\hbar}\boldsymbol{A}(\boldsymbol{r}_{12}) - \frac{e}{4\hbar}\mathcal{E}_2\left(-\frac{\bar{\boldsymbol{r}}_{12}}{2}\cdot\frac{\partial}{\partial\boldsymbol{r}_{12}}\right)\boldsymbol{B}(\boldsymbol{r}_{12})\times\bar{\boldsymbol{r}}_{12}. \tag{A.36b}$$

Next, we consider the kinetic-energy terms in Eq. (A.12),

$$\begin{aligned}&\begin{bmatrix}\hat{\mathcal{K}}_1\underline{\sigma}_0 & \underline{0} \\ \underline{0} & -\hat{\mathcal{K}}_1^*\underline{\sigma}_0\end{bmatrix}\hat{G}(\boldsymbol{r}_1,\boldsymbol{r}_2;\varepsilon_n) \\ &\qquad = \begin{bmatrix}\hat{\mathcal{K}}_1\underline{G}(\boldsymbol{r}_1,\boldsymbol{r}_2;\varepsilon_n) & \hat{\mathcal{K}}_1\underline{F}(\boldsymbol{r}_1,\boldsymbol{r}_2;\varepsilon_n) \\ \hat{\mathcal{K}}_1^*\underline{F}^*(\boldsymbol{r}_1,\boldsymbol{r}_2;\varepsilon_n) & \hat{\mathcal{K}}_1^*\underline{G}^*(\boldsymbol{r}_1,\boldsymbol{r}_2;\varepsilon_n)\end{bmatrix}.\end{aligned} \tag{A.37}$$

Substituting Eq. (A.17b) and using $\partial/\partial\boldsymbol{r}_1 = \partial/\partial\bar{\boldsymbol{r}}_{12} + (1/2)\partial/\partial\boldsymbol{r}_{12}$ and Eq. (A.36), we can transform each submatrix on the right-hand side as

$$\begin{aligned}\hat{\mathcal{K}}_1\underline{G}(\boldsymbol{r}_1,\boldsymbol{r}_2;\varepsilon_n) &\approx \mathrm{e}^{iI(\boldsymbol{r}_1,\boldsymbol{r}_{12})+iI(\boldsymbol{r}_{12},\boldsymbol{r}_2)}\int\frac{d^3p}{(2\pi\hbar)^3}\mathrm{e}^{i\boldsymbol{p}\cdot\bar{\mathbf{r}}_{12}/\hbar} \\ &\times\left\{\frac{p^2}{2m} + e\Phi(\boldsymbol{r}_{12}) - \mu - \frac{i\hbar}{2}\frac{\boldsymbol{p}}{m}\cdot\frac{\partial}{\partial\boldsymbol{r}_{12}} - \frac{\hbar^2}{8m}\frac{\partial^2}{\partial\boldsymbol{r}_{12}^2}\right. \\ &\left. - \frac{i\hbar}{2}e\frac{\boldsymbol{p}}{m}\cdot\left[\boldsymbol{B}(\boldsymbol{r}_{12})\times\frac{\partial}{\partial\boldsymbol{p}}\right] - \frac{i\hbar}{2}e\boldsymbol{E}(\boldsymbol{r}_{12})\cdot\frac{\partial}{\partial\boldsymbol{p}}\right\}\underline{G}(\varepsilon_n,\boldsymbol{p},\boldsymbol{r}_{12}),\end{aligned} \tag{A.38a}$$

$$\begin{aligned}\hat{\mathcal{K}}_1\underline{F}(\boldsymbol{r}_1,\boldsymbol{r}_2;\varepsilon_n) &\approx \mathrm{e}^{iI(\boldsymbol{r}_1,\boldsymbol{r}_{12})-iI(\boldsymbol{r}_{12},\boldsymbol{r}_2)}\int\frac{d^3p}{(2\pi\hbar)^3}\mathrm{e}^{i\boldsymbol{p}\cdot\bar{\mathbf{r}}_{12}/\hbar} \\ &\times\left\{\frac{p^2}{2m} + e\Phi(\boldsymbol{r}_{12}) - \mu - \frac{i\hbar}{2}\frac{\boldsymbol{p}}{m}\cdot\left[\frac{\partial}{\partial\boldsymbol{r}_{12}} - i\frac{2e}{\hbar}\boldsymbol{A}(\boldsymbol{r}_{12})\right]\right. \\ &- \frac{\hbar^2}{8m}\left[\frac{\partial}{\partial\boldsymbol{r}_{12}} - i\frac{2e}{\hbar}\boldsymbol{A}(\boldsymbol{r}_{12})\right]^2 - \frac{i\hbar}{4}e\frac{\boldsymbol{p}}{m}\cdot\left[\boldsymbol{B}(\boldsymbol{r}_{12})\times\frac{\partial}{\partial\boldsymbol{p}}\right] \\ &\left. - \frac{i\hbar}{2}e\boldsymbol{E}(\boldsymbol{r}_{12})\cdot\frac{\partial}{\partial\boldsymbol{p}}\right\}\underline{F}(\varepsilon_n,\boldsymbol{p},\boldsymbol{r}_{12}),\end{aligned} \tag{A.38b}$$

$$\hat{\mathcal{K}}_1^* \underline{F}^*(\boldsymbol{r}_1, \boldsymbol{r}_2; \varepsilon_n) \approx \mathrm{e}^{-iI(\boldsymbol{r}_1, \boldsymbol{r}_{12}) + iI(\boldsymbol{r}_{12}, \boldsymbol{r}_2)} \int \frac{d^3p}{(2\pi\hbar)^3} \mathrm{e}^{i\boldsymbol{p}\cdot\bar{\mathbf{r}}_{12}/\hbar}$$
$$\left\{ \frac{p^2}{2m} + e\Phi(\boldsymbol{r}_{12}) - \mu - \frac{i\hbar}{2}\frac{\boldsymbol{p}}{m} \cdot \left[\frac{\partial}{\partial \boldsymbol{r}_{12}} + i\frac{2e}{\hbar}\boldsymbol{A}(\boldsymbol{r}_{12}) \right] \right.$$
$$- \frac{\hbar^2}{8m}\left[\frac{\partial}{\partial \boldsymbol{r}_{12}} + i\frac{2e}{\hbar}\boldsymbol{A}(\boldsymbol{r}_{12}) \right]^2 + \frac{i\hbar}{4}e\frac{\boldsymbol{p}}{m} \cdot \left[\boldsymbol{B}(\boldsymbol{r}_{12}) \times \frac{\partial}{\partial \boldsymbol{p}} \right]$$
$$\left. - \frac{i\hbar}{2}e\boldsymbol{E}(\boldsymbol{r}_{12}) \cdot \frac{\partial}{\partial \boldsymbol{p}} \right\} \underline{F}^*(\varepsilon_n, -\boldsymbol{p}, \boldsymbol{r}_{12}), \tag{A.38c}$$

$$\hat{\mathcal{K}}_1^* \underline{G}^*(\boldsymbol{r}_1, \boldsymbol{r}_2; \varepsilon_n) \approx \mathrm{e}^{-iI(\boldsymbol{r}_1, \boldsymbol{r}_{12}) - iI(\boldsymbol{r}_{12}, \boldsymbol{r}_2)} \int \frac{d^3p}{(2\pi\hbar)^3} \mathrm{e}^{i\boldsymbol{p}\cdot\bar{\mathbf{r}}_{12}/\hbar}$$
$$\times \left\{ \frac{p^2}{2m} + e\Phi(\boldsymbol{r}_{12}) - \mu - \frac{i\hbar}{2}\frac{\boldsymbol{p}}{m} \cdot \frac{\partial}{\partial \boldsymbol{r}_{12}} - \frac{\hbar^2}{8m}\frac{\partial^2}{\partial \boldsymbol{r}_{12}^2} \right.$$
$$\left. + \frac{i\hbar}{2}e\frac{\boldsymbol{p}}{m} \cdot \left[\boldsymbol{B}(\boldsymbol{r}_{12}) \times \frac{\partial}{\partial \boldsymbol{p}} \right] - \frac{i\hbar}{2}e\boldsymbol{E}(\boldsymbol{r}_{12}) \cdot \frac{\partial}{\partial \boldsymbol{p}} \right\} \underline{G}^*(\varepsilon_n, -\boldsymbol{p}, \boldsymbol{r}_{12}). \tag{A.38d}$$

For clarity we note that the following approximations were used in arriving at Eq. (A.38).

(i) We have neglected spatial derivatives of both $\boldsymbol{E}$ and $\boldsymbol{B}$, which amounts to setting $\mathcal{E}_1 \to 1$ and $\mathcal{E}_2 \to 1/2$.

(ii) We have also neglected the second-order terms in $\boldsymbol{\partial}_{\boldsymbol{r}_{12}}$, $\boldsymbol{E}$, and $\boldsymbol{B}$ except that of $\boldsymbol{\partial}^2_{\boldsymbol{r}_{12}}$.

(iii) We have expanded Φ around $\boldsymbol{r}_{12}$ up to the first order in $\bar{\boldsymbol{r}}_{12}$ as $\Phi(\boldsymbol{r}_1) \approx \Phi(\boldsymbol{r}_{12}) - \boldsymbol{E}(\boldsymbol{r}_{12}) \cdot \bar{\boldsymbol{r}}_{12}/2$.

By following these procedures, we obtain the kinetic-energy terms of the Gor'kov equation [Eq. (A.12)] in the Wigner representation as

$$\int d^3\bar{r}_{12} \mathrm{e}^{-i\boldsymbol{p}\cdot\bar{\boldsymbol{r}}_{12}/\hbar}$$
$$\times \hat{\Gamma}(\boldsymbol{r}_{12}, \boldsymbol{r}_1) \begin{bmatrix} \hat{\mathcal{K}}_1 \underline{\sigma}_0 & \underline{0} \\ \underline{0} & -\hat{\mathcal{K}}_1^* \underline{\sigma}_0 \end{bmatrix} \hat{G}(\boldsymbol{r}_1, \boldsymbol{r}_2; \varepsilon_n) \hat{\Gamma}(\boldsymbol{r}_2, \boldsymbol{r}_{12})$$
$$= \left[\frac{p^2}{2m} + e\Phi(\boldsymbol{r}_{12}) - \mu - \frac{i\hbar}{2}\frac{\boldsymbol{p}}{m} \cdot \boldsymbol{\partial}_{12} - \frac{\hbar^2}{8m}\boldsymbol{\partial}_{12}^2 \right.$$
$$\left. - \frac{i\hbar}{2}e\boldsymbol{E}(\boldsymbol{r}_{12}) \cdot \frac{\partial}{\partial \boldsymbol{p}} \right] \hat{\tau}_3 \hat{G}(\varepsilon_n, \boldsymbol{p}, \boldsymbol{r}_{12})$$
$$- \frac{i\hbar}{8}e\frac{\boldsymbol{p}}{m} \cdot \left[\boldsymbol{B}(\boldsymbol{r}_{12}) \times \frac{\partial}{\partial \boldsymbol{p}} \right] \left[3\hat{G}(\varepsilon_n, \boldsymbol{p}, \boldsymbol{r}_{12}) + \hat{\tau}_3 \hat{G}(\varepsilon_n, \boldsymbol{p}, \boldsymbol{r}_{12}) \hat{\tau}_3 \right]. \tag{A.39}$$

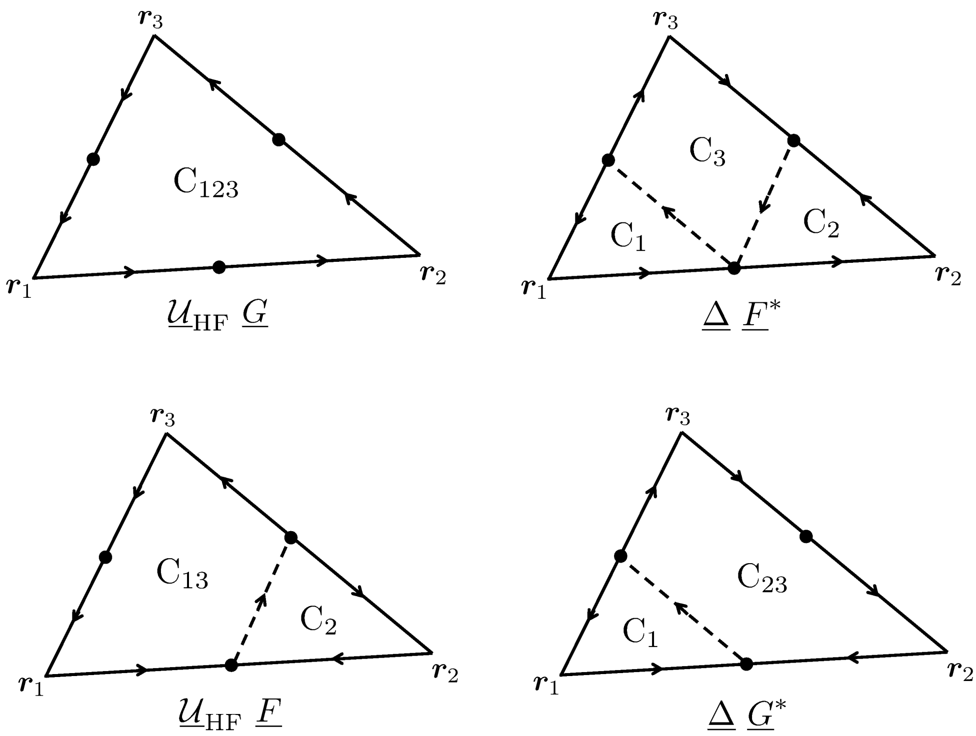

Figure 15: Schematics of the paths of the phase integrals.

A.4 Self-Energy Terms in the Wigner Representation

Here we evaluate the self-energy terms in Eq. (A.12). To this end, we substitute Eqs. (A.17b) and (A.20b) into Eq. (A.12) and rewrite the expression as

$$\int d^3r_3 \hat{\mathcal{U}}_{\rm BdG}(\boldsymbol{r}_1,\boldsymbol{r}_3)\hat{G}(\boldsymbol{r}_3,\boldsymbol{r}_2;\varepsilon_n) = \\ \begin{bmatrix} \underline{J}(\boldsymbol{r}_1,\boldsymbol{r}_2;\varepsilon_n) - \underline{K}(\boldsymbol{r}_1,\boldsymbol{r}_2;\varepsilon_n) & \underline{L}(\boldsymbol{r}_1,\boldsymbol{r}_2;\varepsilon_n) - \underline{M}(\boldsymbol{r}_1,\boldsymbol{r}_2;\varepsilon_n) \\ \underline{L}^*(\boldsymbol{r}_1,\boldsymbol{r}_2;\varepsilon_n) - \underline{M}^*(\boldsymbol{r}_1,\boldsymbol{r}_2;\varepsilon_n) & \underline{J}^*(\boldsymbol{r}_1,\boldsymbol{r}_2;\varepsilon_n) - \underline{K}^*(\boldsymbol{r}_1,\boldsymbol{r}_2;\varepsilon_n) \end{bmatrix}, \tag{A.40}$$

with the matrices $\underline{J}(\boldsymbol{r}_1,\boldsymbol{r}_2;\varepsilon_n)$, $\underline{K}(\boldsymbol{r}_1,\boldsymbol{r}_2;\varepsilon_n)$, $\underline{L}(\boldsymbol{r}_1,\boldsymbol{r}_2;\varepsilon_n)$, and $\underline{M}(\boldsymbol{r}_1,\boldsymbol{r}_2;\varepsilon_n)$ defined in integral form by

$$\underline{J}(\boldsymbol{r}_1,\boldsymbol{r}_2;\varepsilon_n) \equiv \int d^3r_3 \underline{\mathcal{U}}_{\rm HF}(\boldsymbol{r}_1,\boldsymbol{r}_3)\underline{G}(\boldsymbol{r}_3,\boldsymbol{r}_2;\varepsilon_n), \tag{A.41a}$$

$$\underline{K}(\boldsymbol{r}_1,\boldsymbol{r}_2;\varepsilon_n) \equiv \int d^3r_3 \underline{\Delta}(\boldsymbol{r}_1,\boldsymbol{r}_3)\underline{F}^*(\boldsymbol{r}_3,\boldsymbol{r}_2;\varepsilon_n), \tag{A.41b}$$

$$\underline{L}(\boldsymbol{r}_1,\boldsymbol{r}_2;\varepsilon_n) \equiv \int d^3r_3 \underline{\mathcal{U}}_{\rm HF}(\boldsymbol{r}_1,\boldsymbol{r}_3)\underline{F}(\boldsymbol{r}_3,\boldsymbol{r}_2;\varepsilon_n), \tag{A.41c}$$

$$\underline{M}(\boldsymbol{r}_1,\boldsymbol{r}_2;\varepsilon_n) \equiv \int d^3r_3 \underline{\Delta}(\boldsymbol{r}_1,\boldsymbol{r}_3)\underline{G}^*(\boldsymbol{r}_3,\boldsymbol{r}_2;\varepsilon_n). \tag{A.41d}$$

Firstly, let us consider Eq. (A.41a). Putting Eqs. (A.17b) and (A.20b) into Eq. (A.41a), we arrive at the matrix $\underline{J}(\boldsymbol{r}_1, \boldsymbol{r}_2; \varepsilon_n)$ as

$$\underline{J}(\boldsymbol{r}_1, \boldsymbol{r}_2; \varepsilon_n) = \mathrm{e}^{iI(\boldsymbol{r}_1,\boldsymbol{r}_{12})+iI(\boldsymbol{r}_{12},\boldsymbol{r}_2)} \int \frac{d^3p}{(2\pi\hbar)^3} \int \frac{d^3p'}{(2\pi\hbar)^3} \int d^3r_3 \\ \times \mathrm{e}^{i\phi_{123}+i\boldsymbol{p}\cdot\bar{\boldsymbol{r}}_{13}/\hbar+i\boldsymbol{p}'\cdot\bar{\boldsymbol{r}}_{32}/\hbar} \underline{\mathcal{U}}_{\mathrm{HF}}(\boldsymbol{p}, \boldsymbol{r}_{13}) \underline{G}(\varepsilon_n, \boldsymbol{p}', \boldsymbol{r}_{32}), \tag{A.42}$$

where the phase integral ϕ_{123} is expressed as

$$\phi_{123} \equiv \frac{e}{\hbar} \oint_{C_{123}} \boldsymbol{A}(\boldsymbol{s}) \cdot d\boldsymbol{s}, \tag{A.43}$$

with the paths of the phase integral, C_{123} given in Fig. 15. Applying Stokes theorem and approximating $\boldsymbol{B}(\boldsymbol{r}) \approx \boldsymbol{B}(\boldsymbol{r}_{12})$, and noting Fig. 15, the phase integral ϕ_{123} is also expressed as

$$\phi_{123} = \frac{e}{\hbar} \int_{S_{123}} \boldsymbol{B}(\boldsymbol{r}) \cdot d\boldsymbol{S} \approx \frac{e}{2\hbar} \boldsymbol{B}(\boldsymbol{r}_{12}) \cdot (\bar{\boldsymbol{r}}_{32} \times \bar{\boldsymbol{r}}_{13}). \tag{A.44}$$

By the same procedure used in the standard Wigner transformation, [?] we obtain the matrix $\underline{J}(\boldsymbol{r}_1, \boldsymbol{r}_2; \varepsilon_n)$ with $\underline{\mathcal{U}}_{\mathrm{HF}}(\boldsymbol{p}, \boldsymbol{r}_{12})$ and $\underline{G}(\varepsilon_n, \boldsymbol{p}, \boldsymbol{r}_{12})$ in the Wigner representation as

$$\underline{J}(\boldsymbol{r}_1, \boldsymbol{r}_2; \varepsilon_n) \approx \mathrm{e}^{iI(\boldsymbol{r}_1,\boldsymbol{r}_{12})+iI(\boldsymbol{r}_{12},\boldsymbol{r}_2)} \int \frac{d^3p}{(2\pi\hbar)^3} \mathrm{e}^{i\boldsymbol{p}\cdot\bar{\boldsymbol{r}}_{12}/\hbar} \underline{\mathcal{U}}_{\mathrm{HF}}(\boldsymbol{p}, \boldsymbol{r}_{12}) \\ \times \mathrm{e}^{(i\hbar/2)e\boldsymbol{B}(\boldsymbol{r}_{12})\cdot(\overleftarrow{\boldsymbol{\partial}}_{\boldsymbol{p}} \times \overrightarrow{\boldsymbol{\partial}}_{\boldsymbol{p}})} \mathrm{e}^{(i\hbar/2)\overleftarrow{\boldsymbol{\partial}}_{12}\cdot\overrightarrow{\boldsymbol{\partial}}_{\boldsymbol{p}} - (i\hbar/2)\overleftarrow{\boldsymbol{\partial}}_{\boldsymbol{p}}\cdot\overrightarrow{\boldsymbol{\partial}}_{12}} \underline{G}(\varepsilon_n, \boldsymbol{p}, \boldsymbol{r}_{12}), \tag{A.45}$$

where the left (right) arrow on each differential operator denotes that it acts on the left potential (right Green's function), appropriately.

We next consider Eq. (A.41b), substituting Eqs. (A.17b) and (A.20b) into Eq. (A.41d). Then, we can express $\underline{K}(\boldsymbol{r}_1, \boldsymbol{r}_2; \varepsilon_n)$ as

$$\underline{K}(\boldsymbol{r}_1, \boldsymbol{r}_2; \varepsilon_n) = \mathrm{e}^{iI(\boldsymbol{r}_1,\boldsymbol{r}_{12})+iI(\boldsymbol{r}_{12},\boldsymbol{r}_2)} \int \frac{d^3p}{(2\pi\hbar)^3} \int \frac{d^3p'}{(2\pi\hbar)^3} \int d^3r_3 \\ \times \mathrm{e}^{i(\phi_1+\phi_2+\phi_3)-2iI(\boldsymbol{r}_{13},\boldsymbol{r}_{12})-2iI(\boldsymbol{r}_{12},\boldsymbol{r}_{32})+i\boldsymbol{p}\cdot\bar{\boldsymbol{r}}_{13}/\hbar+i\boldsymbol{p}'\cdot\bar{\boldsymbol{r}}_{32}/\hbar} \\ \times \underline{\Delta}(\boldsymbol{p}, \boldsymbol{r}_{13}) \underline{F}^*(\varepsilon_n, -\boldsymbol{p}', \boldsymbol{r}_{32}), \tag{A.46}$$

where the phase integrals $\phi_1 + \phi_2 + \phi_3$ are defined by

$$\phi_1 + \phi_2 + \phi_3 \\ \equiv \frac{e}{\hbar} \oint_{C_1} \boldsymbol{A}(\boldsymbol{s}) \cdot d\boldsymbol{s} + \frac{e}{\hbar} \oint_{C_2} \boldsymbol{A}(\boldsymbol{s}) \cdot d\boldsymbol{s} + \frac{e}{\hbar} \oint_{C_3} \boldsymbol{A}(\boldsymbol{s}) \cdot d\boldsymbol{s}. \tag{A.47}$$

Noting the integral paths C_1, C_2, and C_3 given in Fig. 15, we see that $\phi_1 + \phi_2 + \phi_3 = 0$. Thus, the matrix $\underline{K}(\boldsymbol{r}_1, \boldsymbol{r}_2; \varepsilon_n)$ with $\underline{\Delta}(\boldsymbol{p}, \boldsymbol{r}_{12})$ and $\underline{F}^*(\varepsilon_n, \boldsymbol{p}, \boldsymbol{r}_{12})$ in the Wigner representation is given as

$$\underline{K}(\boldsymbol{r}_1, \boldsymbol{r}_2; \varepsilon_n) \approx \mathrm{e}^{iI(\boldsymbol{r}_1,\boldsymbol{r}_{12})+iI(\boldsymbol{r}_{12},\boldsymbol{r}_2)} \int \frac{d^3p}{(2\pi\hbar)^3} \mathrm{e}^{i\boldsymbol{p}\cdot\bar{\boldsymbol{r}}_{12}/\hbar} \\ \times \underline{\Delta}(\boldsymbol{p}, \boldsymbol{r}_{12}) \mathrm{e}^{(i\hbar/2)\overleftarrow{\boldsymbol{\partial}}_{12}\cdot\overrightarrow{\boldsymbol{\partial}}_{\boldsymbol{p}} - (i\hbar/2)\overleftarrow{\boldsymbol{\partial}}_{\boldsymbol{p}}\cdot\overrightarrow{\boldsymbol{\partial}}_{12}} \underline{F}^*(\varepsilon_n, -\boldsymbol{p}, \boldsymbol{r}_{12}). \tag{A.48}$$

Finally, we calculate $\underline{L}(\boldsymbol{r}_1, \boldsymbol{r}_2; \varepsilon_n)$ and $\underline{M}(\boldsymbol{r}_1, \boldsymbol{r}_2; \varepsilon_n)$. Substituting Eqs. (A.17b) and (A.20b) into Eqs. (A.41c) and (A.41d), the matrices $\underline{L}(\boldsymbol{r}_1, \boldsymbol{r}_2; \varepsilon_n)$ and $\underline{M}(\boldsymbol{r}_1, \boldsymbol{r}_2; \varepsilon_n)$ are given as

$$\underline{L}(\boldsymbol{r}_1, \boldsymbol{r}_2; \varepsilon_n) = \mathrm{e}^{iI(\boldsymbol{r}_1, \boldsymbol{r}_{12}) - iI(\boldsymbol{r}_{12}, \boldsymbol{r}_2)} \int \frac{d^3p}{(2\pi\hbar)^3} \int \frac{d^3p'}{(2\pi\hbar)^3} \int d^3r_3 \\ \times \mathrm{e}^{i(\phi_{13}+\phi_2) - 2iI(\boldsymbol{r}_{32}, \boldsymbol{r}_{12}) + i\boldsymbol{p}\cdot\bar{\boldsymbol{r}}_{13}/\hbar + i\boldsymbol{p}'\cdot\bar{\boldsymbol{r}}_{32}/\hbar} \underline{\mathcal{U}}_{\mathrm{HF}}(\boldsymbol{p}, \boldsymbol{r}_{13}) \underline{F}(\varepsilon_n, \boldsymbol{p}', \boldsymbol{r}_{32}), \tag{A.49}$$

$$\underline{M}(\boldsymbol{r}_1, \boldsymbol{r}_2; \varepsilon_n) = \mathrm{e}^{iI(\boldsymbol{r}_1, \boldsymbol{r}_{12}) - iI(\boldsymbol{r}_{12}, \boldsymbol{r}_2)} \int \frac{d^3p}{(2\pi\hbar)^3} \int \frac{d^3p'}{(2\pi\hbar)^3} \int d^3r_3 \\ \times \mathrm{e}^{i(\phi_1+\phi_{23}) - 2iI(\boldsymbol{r}_{13}, \boldsymbol{r}_{12}) + i\boldsymbol{p}\cdot\bar{\boldsymbol{r}}_{13}/\hbar + i\boldsymbol{p}'\cdot\bar{\boldsymbol{r}}_{32}/\hbar} \underline{\Delta}(\boldsymbol{p}, \boldsymbol{r}_{13}) \underline{G}^*(\varepsilon_n, -\boldsymbol{p}', \boldsymbol{r}_{32}), \tag{A.50}$$

with the phase integrals $\phi_{13} + \phi_2$ and $\phi_1 + \phi_{23}$ expressed as

$$\phi_{13} + \phi_2 \equiv \frac{e}{\hbar} \oint_{C_{13}} \boldsymbol{A}(\boldsymbol{s}) \cdot d\boldsymbol{s} + \frac{e}{\hbar} \oint_{C_2} \boldsymbol{A}(\boldsymbol{s}) \cdot d\boldsymbol{s}, \tag{A.51}$$

$$\phi_1 + \phi_{23} \equiv \frac{e}{\hbar} \oint_{C_1} \boldsymbol{A}(\boldsymbol{s}) \cdot d\boldsymbol{s} + \frac{e}{\hbar} \oint_{C_{23}} \boldsymbol{A}(\boldsymbol{s}) \cdot d\boldsymbol{s}. \tag{A.52}$$

Following the same procedure as used for Eq. (A.44), we perform the phase integration $\phi_{13} + \phi_2$ and $\phi_1 + \phi_{23}$ as

$$\phi_{13} + \phi_2 \approx \frac{e}{4\hbar} \boldsymbol{B}(\boldsymbol{r}_{12}) \cdot (\bar{\boldsymbol{r}}_{32} \times \bar{\boldsymbol{r}}_{13}), \tag{A.53}$$

$$\phi_{23} + \phi_1 \approx -\frac{e}{4\hbar} \boldsymbol{B}(\boldsymbol{r}_{12}) \cdot (\bar{\boldsymbol{r}}_{32} \times \bar{\boldsymbol{r}}_{13}). \tag{A.54}$$

We therefore obtain the matrices $\underline{L}(\boldsymbol{r}_1, \boldsymbol{r}_2; \varepsilon_n)$ and $\underline{M}(\boldsymbol{r}_1, \boldsymbol{r}_2; \varepsilon_n)$ with the potentials and Green's functions given in the Wigner representation as

$$\underline{L}(\boldsymbol{r}_1, \boldsymbol{r}_2; \varepsilon_n) \approx \mathrm{e}^{iI(\boldsymbol{r}_1, \boldsymbol{r}_{12}) - iI(\boldsymbol{r}_{12}, \boldsymbol{r}_2)} \int \frac{d^3p}{(2\pi\hbar)^3} \mathrm{e}^{i\boldsymbol{p}\cdot\bar{\boldsymbol{r}}_{12}/\hbar} \\ \times \underline{\mathcal{U}}_{\mathrm{HF}}(\boldsymbol{p}, \boldsymbol{r}_{12}) \mathrm{e}^{(i\hbar/4)e\boldsymbol{B}(\mathrm{r}_{12})\cdot(\overleftarrow{\boldsymbol{\partial}}_{\boldsymbol{p}} \times \overrightarrow{\boldsymbol{\partial}}_{\boldsymbol{p}})} \\ \times \mathrm{e}^{(i\hbar/2)\overleftarrow{\boldsymbol{\partial}}_{12}\cdot\overrightarrow{\boldsymbol{\partial}}_{\boldsymbol{p}} - (i\hbar/2)\overleftarrow{\boldsymbol{\partial}}_{\boldsymbol{p}}\cdot\overrightarrow{\boldsymbol{\partial}}_{12}} \underline{F}(\varepsilon_n, \boldsymbol{p}, \boldsymbol{r}_{12}), \tag{A.55}$$

$$\underline{M}(\boldsymbol{r}_1, \boldsymbol{r}_2; \varepsilon_n) \approx \mathrm{e}^{iI(\boldsymbol{r}_1, \boldsymbol{r}_{12}) - iI(\boldsymbol{r}_{12}, \boldsymbol{r}_2)} \int \frac{d^3p}{(2\pi\hbar)^3} \mathrm{e}^{i\boldsymbol{p}\cdot\bar{\boldsymbol{r}}_{12}/\hbar} \\ \times \underline{\Delta}(\boldsymbol{p}, \boldsymbol{r}_{12}) \mathrm{e}^{-(i\hbar/4)e\boldsymbol{B}(\mathrm{r}_{12})\cdot(\overleftarrow{\boldsymbol{\partial}}_{\boldsymbol{p}} \times \overrightarrow{\boldsymbol{\partial}}_{\boldsymbol{p}})} \\ \times \mathrm{e}^{(i\hbar/2)\overleftarrow{\boldsymbol{\partial}}_{12}\cdot\overrightarrow{\boldsymbol{\partial}}_{\boldsymbol{p}} - (i\hbar/2)\overleftarrow{\boldsymbol{\partial}}_{\boldsymbol{p}}\cdot\overrightarrow{\boldsymbol{\partial}}_{12}} \underline{G}^*(\varepsilon_n, -\boldsymbol{p}, \boldsymbol{r}_{12}). \tag{A.56}$$

Finally, we use Eqs. (A.45), (A.48), (A.55), and (A.56) in Eq. (A.40) to obtain the self-energy terms of the Gor'kov equation (A.12) in the Wigner representation. Furthermore, we carry out an expansion of the Hartree–Fock potential formally as $\underline{\mathcal{U}}_{\mathrm{HF}}(\boldsymbol{p}, \boldsymbol{r}) = \mathcal{U}_{\mathrm{HF}}(\boldsymbol{p})\underline{\sigma}_0 + O(\underline{\Delta}^2(\boldsymbol{p}, \boldsymbol{r}))$ with $\mathcal{U}_{\mathrm{HF}}(\boldsymbol{p})$ as the Hartree–Fock potential in the homogeneous normal state, and neglecting all the terms of the product of two momenta derivatives of the superconducting pair potential and the Green's function such as $\partial\underline{\Delta}/\partial\boldsymbol{p}\times\partial\underline{G}/\partial\boldsymbol{p}$ and $\partial\underline{\Delta}/\partial\boldsymbol{p}\times\partial\underline{F}/\partial\boldsymbol{p}$. Based on this proceedure, we now rewrite the self-energy terms in the Wigner representation as

$$
\begin{aligned}
&\int d^3\bar{r}_{12}\mathrm{e}^{-i\boldsymbol{p}\cdot\bar{\boldsymbol{r}}_{12}} \\
&\quad\times\hat{\Gamma}(\boldsymbol{r}_{12},\boldsymbol{r}_1)\int d^3r_3\hat{\mathcal{U}}_{\mathrm{BdG}}(\boldsymbol{r}_1,\boldsymbol{r}_3)\hat{G}(\boldsymbol{r}_3,\boldsymbol{r}_2;\varepsilon_n)\hat{\Gamma}(\boldsymbol{r}_2,\boldsymbol{r}_{12}) \\
&\approx\hat{\Delta}(\boldsymbol{p},\boldsymbol{r}_{12})\circ\hat{G}(\varepsilon_n,\boldsymbol{p},\boldsymbol{r}_{12})+\mathcal{U}_{\mathrm{HF}}(\boldsymbol{p})\hat{\tau}_3\circ\hat{G}(\varepsilon_n,\boldsymbol{p},\boldsymbol{r}_{12}) \\
&\quad+\frac{i\hbar}{8}e\boldsymbol{B}(\boldsymbol{r}_{12})\cdot\Bigg\{\left(\boldsymbol{v}-\frac{\boldsymbol{p}}{m}\right) \\
&\qquad\times\frac{\partial}{\partial\boldsymbol{p}}\left[3\hat{G}(\varepsilon_n,\boldsymbol{p},\boldsymbol{r}_{12})+\hat{\tau}_3\hat{G}(\varepsilon_n,\boldsymbol{p},\boldsymbol{r}_{12})\hat{\tau}_3\right]\Bigg\},
\end{aligned}
\tag{A.57}
$$

where quantity $\boldsymbol{v}$ is the normal state velocity and is expressed as

$$
\boldsymbol{v}=\frac{\partial\varepsilon_{\boldsymbol{p}}}{\partial\boldsymbol{p}},\quad\varepsilon_{\boldsymbol{p}}=\frac{p^2}{2m}+\mathcal{U}_{\mathrm{HF}}(\boldsymbol{p}).\tag{A.58}
$$

B Boundary conditions based on gradient expansion

In this section, we derive the boundary conditions required for solving the standard Eilenberger equations. We start from the Riccati form of Eq. (3.3)[13, 38, 39, 40].

$$
v_{\mathrm{F}x}\frac{\partial a}{\partial x}=-2\varepsilon_n a-\Delta\phi a^2+\Delta\phi,\tag{B.1}
$$

where a=$a(\varepsilon_n,\boldsymbol{p}_{\mathrm{F}},x)$ is the Riccati parameter and is related to f_0 and g_0 as

$$
f_0=\frac{2a}{1+a\bar{a}},\quad g_0=\frac{1-a\bar{a}}{1+a\bar{a}}.\tag{B.2}
$$

We carry out a gradient expansion[13] of Eq. (3.3) using

$$
a\approx a^{(0)}+a^{(1)},\tag{B.3}
$$

which gives

$$
\begin{aligned}
a^{(0)}&=\frac{\Delta\phi}{\varepsilon_n+\sqrt{\varepsilon_n^2+\Delta^2\phi^2}},\\
a^{(1)}&=-\frac{v_{\mathrm{F}x}}{2\sqrt{\varepsilon_n^2+\Delta^2\phi^2}}\frac{\partial a^{(0)}}{\partial x},\\
\frac{\partial a^{(0)}}{\partial x}&=-\frac{a^{(0)2}}{\sqrt{\varepsilon_n^2+\Delta^2\phi^2}}\frac{d\Delta}{dx}\phi+\frac{a^{(0)}}{\Delta}\frac{d\Delta}{dx}.
\end{aligned}
\tag{B.4}
$$

The derivatives $\partial f_0/\partial x$ and $\partial f_0/\partial p_{\mathrm{F}x}$ in Eq. (3.5) are expressed as

$$\frac{\partial f_0}{\partial x} = \frac{2}{(1+a\bar{a})^2}\left(\frac{\partial a}{\partial x} - a^2\frac{\partial \bar{a}}{\partial x}\right),$$
$$\frac{\partial f_0}{\partial p_{\mathrm{F}x}} = \frac{2}{(1+a\bar{a})^2}\left(\frac{\partial a}{\partial p_{\mathrm{F}x}} - a^2\frac{\partial \bar{a}}{\partial p_{\mathrm{F}x}}\right). \tag{B.5}$$

$\partial a/\partial x$ is obtained from Eq. (B.1), and $\partial a/\partial p_{\mathrm{F}x}$ is given by solving the following equation:

$$\begin{aligned} v_{\mathrm{F}x}\frac{\partial}{\partial x}\frac{\partial a}{\partial p_{\mathrm{F}x}} &= -2\varepsilon_n\frac{\partial a}{\partial p_{\mathrm{F}x}} - \Delta\frac{\partial \phi}{\partial p_{\mathrm{F}x}}a^2 \\ &- 2\Delta\phi a\frac{\partial a}{\partial p_{\mathrm{F}x}} + \Delta\frac{\partial \phi}{\partial p_{\mathrm{F}x}} - \frac{\partial v_{\mathrm{F}x}}{\partial p_{\mathrm{F}x}}\frac{\partial a}{\partial x}, \end{aligned} \tag{B.6}$$

where the boundary condition for Eq. (B.6) used near the bulk is given by

$$\begin{aligned} \frac{\partial a}{\partial p_{\mathrm{F}x}} &\approx \frac{\partial a^{(0)}}{\partial p_{\mathrm{F}x}} + \frac{\partial a^{(1)}}{\partial p_{\mathrm{F}x}}, \\ \frac{\partial a^{(0)}}{\partial p_{\mathrm{F}x}} &= -\frac{a^{(0)2}}{\sqrt{\varepsilon_n^2+\Delta^2\phi^2}}\Delta\frac{\partial \phi}{\partial p_{\mathrm{F}x}} + \frac{a^{(0)}}{\phi}\frac{\partial \phi}{\partial p_{\mathrm{F}x}}, \\ \frac{\partial a^{(1)}}{\partial p_{\mathrm{F}x}} &= \frac{v_{\mathrm{F}x}\Delta^2\phi}{4(\varepsilon_n^2+\Delta^2\phi^2)^2}\frac{\partial \phi}{\partial p_{\mathrm{F}x}}\frac{\partial a^{(0)}}{\partial x} \\ &- \frac{1}{2\sqrt{\varepsilon_n^2+\Delta^2\phi^2}}\left(\frac{\partial v_{\mathrm{F}x}}{\partial p_{\mathrm{F}x}}\frac{\partial a^{(0)}}{\partial x} + v_{\mathrm{F}x}\frac{\partial^2 a^{(0)}}{\partial x\partial p_{\mathrm{F}x}}\right), \\ \frac{\partial^2 a^{(0)}}{\partial x\partial p_{\mathrm{F}x}} &= \frac{a^{(0)2}}{(\varepsilon_n^2+\Delta^2\phi^2)^{3/2}}\Delta^2\phi^2\frac{d\Delta}{dx}\frac{\partial \phi}{\partial p_{\mathrm{F}x}} \\ &- 2\frac{a^{(0)}}{\sqrt{\varepsilon_n^2+\Delta^2\phi^2}}\frac{\partial a^{(0)}}{\partial x}\Delta\frac{\partial \phi}{\partial p_{\mathrm{F}x}} \\ &- \frac{a^{(0)2}}{\sqrt{\varepsilon_n^2+\Delta^2\phi^2}}\frac{d\Delta}{dx}\frac{\partial \phi}{\partial p_{\mathrm{F}x}} + \frac{\partial a^{(0)}}{\partial x}\frac{1}{\phi}\frac{\partial \phi}{\partial p_{\mathrm{F}x}}. \end{aligned} \tag{B.7a}$$

C Derivation of Eq. (3.19)

In this section, we derive Eq. (3.19). Equation (3.19) is derived by the following procedures: (i) expand quasiclassical Green's functions in terms of pair potential [13] up to third order based on the assumptions $|\Delta(x)| \ll \Delta_0, \hbar v_{\mathrm{F}x}(\partial^n\Delta/\partial x^n) = O(\Delta^{n+1})$, which is valid near T_{c}, (ii) substitute expanded Green's functions into the first term of Eq. (A.29), (iii) neglect the Thomas–Fermi term of Eq. (7). Here, we consider the solutions when $\varepsilon_n > 0$.

First, we expand Green's functions with respect to Δ as

$$f_0 = \sum_{\nu=1}^{\infty} f_0^{(\nu)},\ \ g_0 = 1 + \sum_{\nu=2}^{\infty} g_0^{(\nu)}, \tag{C.1}$$

with initial conditions $f_0^{(0)} = 0$, $g_0^{(0)} = 1$, and $g_0^{(1)} = 0$, and give the following recursive condition from Eilenberger equations:

$$f_0^{(\nu)} = \left[\frac{\Delta\phi g_0^{(\nu-1)}}{\varepsilon_n} - \frac{\hbar v_{Fx}}{2\varepsilon_n} \frac{\partial f_0^{(\nu-1)}}{\partial x} \right], \tag{C.2}$$

where we assumed $\hbar v_{Fx} \partial\Delta/\partial x = O(\Delta^2)$. Using Eq. (C.2) with initial conditions and normalization condition $g_0^2 = 1 - f_0^2 \bar{f}_0^2$, $f_0^{(\nu)}$ and $g_0^{(\nu)}$ up to third order are derived as follows

$$f_0^{(1)} = \frac{\Delta\phi}{\varepsilon_n}, \ f_0^{(2)} = -\frac{\hbar\phi v_{Fx}}{2\varepsilon_n^2} \frac{\partial\Delta}{\partial x},$$

$$f_0^{(3)} = -\left[\frac{(\Delta\phi)^2}{2\varepsilon_n^3} - \frac{(\hbar v_{Fx})^2}{4\varepsilon_n^3} \frac{\partial^2}{\partial x^2} \right] \Delta\phi, \tag{C.3a}$$

$$g_0^{(2)} = -\frac{(\Delta\phi)^2}{2\varepsilon_n^2}, \ g_0^{(3)} = 0. \tag{C.3b}$$

where we used $\mathrm{Im}\Delta = 0$.

The equation for $\partial \mathrm{Im} g_1/\partial x$, which is included in the electric field equation in Eq. (A.29), is given by

$$\frac{\partial \mathrm{Im} g_1}{\partial x} = \frac{-\hbar^2}{4\varepsilon_n^3} \left[\left(2\phi^2 \frac{\partial v_{Fx}}{\partial p_{Fx}} + v_{Fx}\phi \frac{\partial \phi}{\partial p_{Fx}} \right) \frac{\partial\Delta}{\partial x} \frac{\partial^2\Delta}{\partial x^2} - v_{Fx}\phi \frac{\partial\phi}{\partial p_{Fx}} \Delta \frac{\partial^3\Delta}{\partial x^3} \right]. \tag{C.4}$$

If we only consider the PPG force, the electric field equation is given by the first term of Eq. (A.29). Thus, within the present approximation, electric field by PPG force is given by

$$\begin{aligned} &\Big(-\lambda_{TF}^2 \frac{\partial^2}{\partial x^2} + 1 \Big) E_{PPGx}(x) \\ &\simeq \frac{\hbar^2 a^{(3)}}{2e} \left[\left(2\Big\langle \phi^2 \frac{\partial v_{Fx}}{\partial p_{Fx}} \Big\rangle_F + \Big\langle v_{Fx}\phi \frac{\partial\phi}{\partial p_{Fx}} \Big\rangle_F \right) \frac{\partial\Delta}{\partial x} \frac{\partial^2\Delta}{\partial x^2} \right. \\ &\left. - \Big\langle v_{Fx}\phi \frac{\partial\phi}{\partial p_{Fx}} \Big\rangle_F \Delta \frac{\partial^3\Delta}{\partial x^3} \right], \end{aligned} \tag{C.5}$$

where E_{PPGx} represents the x-component of electric field induced by PPG force $a^{(3)} \equiv \pi k_B T \sum_{0 \le n \le n_c} \varepsilon_n^{-3}$. Neglecting the term related to Thomas–Fermi screening length with assumption $\lambda_{TF} \ll \xi_0$, we obtain the approximated charge density as

$$\begin{aligned} \rho_{PPG}(x) \simeq \frac{\hbar^2 a^{(3)}\epsilon_0}{2e} &\left[\left(2\Big\langle \phi^2 \frac{\partial v_{Fx}}{\partial p_{Fx}} \Big\rangle_F + \Big\langle v_{Fx}\phi \frac{\partial\phi}{\partial p_{Fx}} \Big\rangle_F \right) \frac{\partial^2\Delta}{\partial x^2} \frac{\partial^2\Delta}{\partial x^2} \right. \\ &\left. + 2\Big\langle \phi^2 \frac{\partial v_{Fx}}{\partial p_{Fx}} \Big\rangle_F \frac{\partial\Delta}{\partial x} \frac{\partial^3\Delta}{\partial x^3} - \Big\langle v_{Fx}\phi \frac{\partial\phi}{\partial p_{Fx}} \Big\rangle_F \Delta \frac{\partial^4\Delta}{\partial x^4} \right]. \end{aligned} \tag{C.6}$$

where $\rho_{\rm PPG}(x) \equiv \epsilon_0(\partial E_{{\rm PPG}x}/\partial x)$. Therefore, $\rho_{\rm PPG}(x)$ is expressible only in terms of $\Delta^{(n)}(x)$ in high-temperature region where the present approximation is valid. Substituting the pair potential assumed as $\Delta(x) \simeq \Delta_{\rm bulk}\tanh(x/\xi_1)$ into Eq. (C.6) and taking the limit $x \to 0$, we arrive at Eq. (3.19).

D Local density of states in the augmented quasiclassical theory

Here we derive the expressions which are relevant to our numerical calculation of the local density of states within the augmented quasiclassical theory.

D.1 Riccati equation

We write the Riccati-type equation in Keldysh formalism as,

$$v_{{\rm F}x}\frac{\partial a^{\rm R}}{\partial x} = -2(-i\varepsilon+\eta)a^{\rm R} - \Delta\phi a^{{\rm R}2} + \Delta\phi \tag{D.1}$$

Separating the real and imaginary parts we get,

$$v_{{\rm F}x}\frac{\partial {\rm Re}a^{\rm R}}{\partial x} = -2\eta{\rm Re}a^{\rm R} - 2\varepsilon{\rm Im}a^{\rm R} - \Delta\phi({\rm Re}a^{{\rm R}2} - {\rm Im}a^{{\rm R}2}) + \Delta\phi \tag{D.2a}$$

and

$$v_{{\rm F}x}\frac{\partial {\rm Im}a^{\rm R}}{\partial x} = 2\varepsilon{\rm Re}a^{\rm R} - 2\eta{\rm Im}a^{\rm R} - 2\Delta\phi{\rm Re}a^{\rm R}{\rm Im}a^{\rm R} \tag{D.2b}$$

Similarly,

$$-v_{{\rm F}x}\frac{\partial \bar{a}^{\rm R}}{\partial x} = -2(-i\varepsilon+\eta)\bar{a}^{\rm R} - \Delta\phi \bar{a}^{{\rm R}2} + \Delta\phi \tag{D.3}$$

This gives,

$$-v_{{\rm F}x}\frac{\partial {\rm Re}\bar{a}^{\rm R}}{\partial x} = -2\eta{\rm Re}\bar{a}^{\rm R} + 2\varepsilon{\rm Im}\bar{a}^{\rm R} - \Delta\phi({\rm Re}\bar{a}^{{\rm R}2} - {\rm Im}\bar{a}^{{\rm R}2}) + \Delta\phi \tag{D.4a}$$

$$-v_{{\rm F}x}\frac{\partial {\rm Im}\bar{a}^{\rm R}}{\partial x} = 2\varepsilon{\rm Re}\bar{a}^{\rm R} + 2\eta{\rm Im}\bar{a}^{\rm R} + 2\Delta\phi{\rm Re}\bar{a}^{\rm R}{\rm Im}\bar{a}^{\rm R} \tag{D.4b}$$

D.2 Green's functions

We use the Riccati parameters to calculate the Green's functions as follows,

$$g_0^{\rm R} = \frac{1-a^{\rm R}\bar{a}^{\rm R}}{1+a^{\rm R}\bar{a}^{\rm R}}, \quad f_0^{\rm R} = \frac{2a^{\rm R}}{1+a^{\rm R}\bar{a}^{\rm R}} \tag{D.5}$$

$$
\begin{aligned}
a^{\mathrm{R}}\bar{a}^{\mathrm{R}} &= (\mathrm{Re}a^{\mathrm{R}} + i\mathrm{Im}a^{\mathrm{R}})(\mathrm{Re}\bar{a}^{\mathrm{R}} - i\mathrm{Im}\bar{a}^{\mathrm{R}}) \\
&= (\mathrm{Re}a^{\mathrm{R}}\mathrm{Re}\bar{a}^{\mathrm{R}} + \mathrm{Im}a^{\mathrm{R}}\mathrm{Im}\bar{a}^{\mathrm{R}}) + i(\mathrm{Im}a^{\mathrm{R}}\mathrm{Re}\bar{a}^{\mathrm{R}} - \mathrm{Re}a^{\mathrm{R}}\mathrm{Im}\bar{a}^{\mathrm{R}}) \\
&= w_r + iw_i
\end{aligned} \tag{D.6}
$$

Where

$$
w_r = \mathrm{Re}a^{\mathrm{R}}\mathrm{Re}\bar{a}^{\mathrm{R}} + \mathrm{Im}a^{\mathrm{R}}\mathrm{Im}\bar{a}^{\mathrm{R}}, \quad w_i = \mathrm{Im}a^{\mathrm{R}}\mathrm{Re}\bar{a}^{\mathrm{R}} - \mathrm{Re}a^{\mathrm{R}}\mathrm{Im}\bar{a}^{\mathrm{R}} \tag{D.7}
$$

Then

$$
\begin{aligned}
g_0^{\mathrm{R}} &= \frac{1 - w_r - iw_i}{1 + w_r + iw_i} \\
&= \frac{1}{w}(1 - w_r - iw_i)(1 + w_r - iw_i), \quad w = (1 + w_r)^2 + w_i^2
\end{aligned} \tag{D.8}
$$

$$
g_0^{\mathrm{R}} = \frac{1}{w}\left[(1 - w_r)(1 + w_r) - w_i^2\right] - \frac{i}{w}\left[(1 - w_r)w_i + w_i(1 + w_r)\right] \tag{D.9}
$$

Similarly,

$$
\begin{aligned}
f_0^{\mathrm{R}} &= \frac{2(\mathrm{Re}a^{\mathrm{R}} + i\mathrm{Im}a^{\mathrm{R}})}{1 + w_r + iw_i} \\
&= \frac{2}{w}(\mathrm{Re}a^{\mathrm{R}} + i\mathrm{Im}a^{\mathrm{R}})(1 + w_r - iw_i)
\end{aligned} \tag{D.10}
$$

Therefore,

$$
f_0^{\mathrm{R}} = \frac{2}{w}\left[\mathrm{Re}a^{\mathrm{R}}(1 + w_r) + \mathrm{Im}a^{\mathrm{R}}w_i\right] + \frac{2i}{w}\left[\mathrm{Im}a^{\mathrm{R}}(1 + w_r) - \mathrm{Re}a^{\mathrm{R}}w_i\right] \tag{D.11}
$$

D.3 Solutions near the bulk

Starting from the expansion

$$
a^{\mathrm{R}} \approx a^{\mathrm{R}(0)} + a^{\mathrm{R}(1)} \tag{D.12}
$$

Where $a^{\mathrm{R}(0)}$ is the solution for the homogeneous system and is given by

$$
a^{(0)} = \frac{\Delta\phi}{-i\varepsilon + \eta + \sqrt{(-i\varepsilon + \eta)^2 + \Delta^2\phi^2}} \tag{D.13}
$$

We further simply as follows; let

$$
\begin{aligned}
\sqrt{(-i\varepsilon + \eta)^2 + \Delta^2\phi^2} &= \sqrt{-\varepsilon^2 + \eta^2 + \Delta^2\phi^2 - 2i\varepsilon\eta} \\
&= \sqrt{w_{1r} + iw_{1i}} \\
&= re^{i\theta}
\end{aligned} \tag{D.14}
$$

Where we have used the following substitutions,

$$
w_{1r} = -\varepsilon^2 + \eta^2 + \Delta^2\phi^2, \quad w_{1i} = -2\varepsilon\eta. \tag{D.15}
$$

Then

$$w_{1r} + iw_{1i} = r^2 \mathrm{e}^{2i\theta}, \quad w_{1r} - iw_{1i} = r^2 \mathrm{e}^{-2i\theta}$$

$$r^4 = w_{1r}^2 + w_{1i}^2 \to r = (w_{1r}^2 + w_{1i}^2)^{1/4}, \quad r \geq 0 \tag{D.16}$$

$$w_{1r} = r^2 \cos 2\theta, \quad w_{1i} = r^2 \sin 2\theta$$

$$\tan\theta = \frac{w_{1i}}{w_{1r}} \to \theta = \frac{1}{2} \arctan \frac{w_{1i}}{w_{1r}} \tag{D.17}$$

$$\sqrt{w_{1r} + iw_{1i}} = (w_{1r}^2 + w_{1i}^2)^{\frac{1}{4}} \mathrm{e}^{\frac{1}{2} \arctan \frac{w_{1i}}{w_{1r}}} \tag{D.18}$$

We also write

$$a^{\mathrm{R}(0)} = \frac{\Delta\phi}{w_{2r} + iw_{2i}} \tag{D.19}$$

Where

$$w_{2r} = \eta + (w_{1r}^2 + w_{1i}^2)^{\frac{1}{4}} \cos\left(\frac{1}{2} \arctan \frac{w_{1i}}{w_{1r}}\right), \tag{D.20a}$$

$$w_{2i} = -\varepsilon + (w_{1r}^2 + w_{1i}^2)^{\frac{1}{4}} \sin\left(\frac{1}{2} \arctan \frac{w_{1i}}{w_{1r}}\right) \tag{D.20b}$$

$$a^{\mathrm{R}(0)} = \frac{\Delta\phi(w_{2r} - iw_{2i})}{w_2}, \quad w_2 = w_{2r}^2 + w_{2i}^2 \tag{D.21}$$

$$a^{\mathrm{R}(1)} = -\frac{v_{\mathrm{F}x}}{2\sqrt{(-i\varepsilon + \eta)^2 + \Delta^2\phi^2}} \frac{\partial a^{\mathrm{R}(0)}}{\partial x} \tag{D.22}$$

$$w_{3r} = (w_{1r}^2 + w_{1i}^2)^{\frac{1}{4}} \cos\left(\frac{1}{2} \arctan \frac{w_{1i}}{w_{1r}}\right), \tag{D.23a}$$

$$w_{3i} = (w_{1r}^2 + w_{1i}^2)^{\frac{1}{4}} \sin\left(\frac{1}{2} \arctan \frac{w_{1i}}{w_{1r}}\right) \tag{D.23b}$$

Furthermore, the correction term $a^{\mathrm{R}(1)}$ is expressed as

$$\begin{aligned} a^{\mathrm{R}(1)} &= -\frac{v_{\mathrm{F}x}}{2(w_{3r} + iw_{3i})} \frac{\partial a^{\mathrm{R}(0)}}{\partial x} \\ &= -\frac{v_{\mathrm{F}x}}{2w_3}(w_{3r} - iw_{3i}) \left(\frac{\partial \mathrm{Re} a^{\mathrm{R}(0)}}{\partial x} + i\frac{\partial \mathrm{Im} a^{\mathrm{R}(0)}}{\partial x}\right) \end{aligned} \tag{D.24}$$

$$w_3 = w_{3r}^2 + w_{3i}^2 \tag{D.25}$$

$$a^{\mathrm{R}(1)} = -\frac{v_{\mathrm{F}x}}{2w_3}\left(w_{3r}\frac{\partial \mathrm{Re}a^{\mathrm{R}(0)}}{\partial x} + w_{3i}\frac{\partial \mathrm{Im}a^{\mathrm{R}(0)}}{\partial x}\right) \tag{D.26}$$

$$-i\frac{v_{\mathrm{F}x}}{2w_3}\left(w_{3r}\frac{\partial \mathrm{Im}a^{\mathrm{R}(0)}}{\partial x} - w_{3i}\frac{\partial \mathrm{Re}a^{\mathrm{R}(0)}}{\partial x}\right) \tag{D.27}$$

$$\begin{aligned}
\frac{\partial a^{\mathrm{R}(0)}}{\partial x} &= -\frac{a^{\mathrm{R}(0)2}}{\sqrt{(-i\varepsilon+\eta)^2+\Delta^2\phi^2}}\frac{d\Delta}{dx}\phi + \frac{a^{\mathrm{R}(0)}}{\Delta}\frac{d\Delta}{dx} \\
&= -\frac{1}{w_3}(w_{3r}-iw_{3i})(\mathrm{Re}a^{\mathrm{R}(0)} + i\mathrm{Im}a^{\mathrm{R}(0)})^2\frac{d\Delta}{dx}\phi \\
&\quad + \frac{(\mathrm{Re}a^{\mathrm{R}(0)} + i\mathrm{Im}a^{\mathrm{R}(0)})}{\Delta}\frac{d\Delta}{dx} \\
&= -\frac{1}{w_3}(w_{3r}-iw_{3i})(\mathrm{Re}a^{\mathrm{R}(0)2} - \mathrm{Im}a^{\mathrm{R}(0)2} + 2i\mathrm{Re}a^{\mathrm{R}(0)}\mathrm{Im}a^{\mathrm{R}(0)})\frac{d\Delta}{dx}\phi \\
&\quad + \frac{\mathrm{Re}a^{\mathrm{R}(0)}}{\Delta}\frac{d\Delta}{dx} + i\frac{\mathrm{Im}a^{\mathrm{R}(0)}}{\Delta}\frac{d\Delta}{dx}
\end{aligned} \tag{D.28}$$

$$\begin{aligned}
\frac{\partial a^{\mathrm{R}(0)}}{\partial x} &= -\frac{1}{w_3}\left[w_{3r}(\mathrm{Re}a^{\mathrm{R}(0)2} - \mathrm{Im}a^{\mathrm{R}(0)2}) + 2w_{3i}\mathrm{Re}a^{\mathrm{R}(0)}\mathrm{Im}a^{\mathrm{R}(0)}\right]\frac{d\Delta}{dx}\phi \\
&\quad + \frac{\mathrm{Re}a^{\mathrm{R}(0)}}{\Delta}\frac{d\Delta}{dx} \\
&\quad - \frac{i}{w_3}\left[2w_{3r}\mathrm{Re}a^{\mathrm{R}(0)}\mathrm{Im}a^{\mathrm{R}(0)} - w_{3i}(\mathrm{Re}a^{\mathrm{R}(0)2} - \mathrm{Im}a^{\mathrm{R}(0)2})\right]\frac{d\Delta}{dx}\phi \\
&\quad + i\frac{\mathrm{Im}a^{\mathrm{R}(0)}}{\Delta}\frac{d\Delta}{dx}
\end{aligned} \tag{D.29}$$

D.4 Expression for $\partial a^{\mathrm{R}}/\partial p_{\mathrm{F}x}$

The derivatives $\frac{\partial}{\partial x}\frac{\partial a^{\mathrm{R}}}{\partial p_{\mathrm{F}x}}$, $\frac{\partial}{\partial x}\frac{\partial \mathrm{Re}a^{\mathrm{R}}}{\partial p_{\mathrm{F}x}}$ and $\frac{\partial}{\partial x}\frac{\partial \mathrm{Im}a^{\mathrm{R}}}{\partial p_{\mathrm{F}x}}$ are given by

$$v_{\mathrm{F}x}\frac{\partial}{\partial x}\frac{\partial a^{\mathrm{R}}}{\partial p_{\mathrm{F}x}} = -2(-i\varepsilon+\eta)\frac{\partial a^{\mathrm{R}}}{\partial p_{\mathrm{F}x}} - \Delta\frac{\partial \phi}{\partial p_{\mathrm{F}x}}a^{\mathrm{R}2} - 2\Delta\phi a^{\mathrm{R}}\frac{\partial a^{\mathrm{R}}}{\partial p_{\mathrm{F}x}} + \Delta\frac{\partial \phi}{\partial p_{\mathrm{F}x}} - \frac{\partial v_{\mathrm{F}x}}{\partial p_{\mathrm{F}x}}\frac{\partial a^{\mathrm{R}}}{\partial x}, \tag{D.30}$$

$$\begin{aligned}
v_{\mathrm{F}x}\frac{\partial}{\partial x}\frac{\partial \mathrm{Re}a^{\mathrm{R}}}{\partial p_{\mathrm{F}x}} &= -2\eta\frac{\partial \mathrm{Re}a^{\mathrm{R}}}{\partial p_{\mathrm{F}x}} - 2\varepsilon\frac{\partial \mathrm{Im}a^{\mathrm{R}}}{\partial p_{\mathrm{F}x}} - \Delta\frac{\partial \phi}{\partial p_{\mathrm{F}x}}(\mathrm{Re}a^{\mathrm{R}2} - \mathrm{Im}a^{\mathrm{R}2}) \\
&\quad - 2\Delta\phi\left(\mathrm{Re}a^{\mathrm{R}}\frac{\partial \mathrm{Re}a^{\mathrm{R}}}{\partial p_{\mathrm{F}x}} - \mathrm{Im}a^{\mathrm{R}}\frac{\partial \mathrm{Im}a^{\mathrm{R}}}{\partial p_{\mathrm{F}x}}\right) + \Delta\frac{\partial \phi}{\partial p_{\mathrm{F}x}} - \frac{\partial v_{\mathrm{F}x}}{\partial p_{\mathrm{F}x}}\frac{\partial \mathrm{Re}a^{\mathrm{R}}}{\partial x},
\end{aligned} \tag{D.31a}$$

and

$$v_{\mathrm{F}x}\frac{\partial}{\partial x}\frac{\partial \mathrm{Im}a^{\mathrm{R}}}{\partial p_{\mathrm{F}x}} = 2\varepsilon\frac{\partial \mathrm{Re}a^{\mathrm{R}}}{\partial p_{\mathrm{F}x}} - 2\eta\frac{\partial \mathrm{Im}a^{\mathrm{R}}}{\partial p_{\mathrm{F}x}} - 2\Delta\frac{\partial \phi}{\partial p_{\mathrm{F}x}}\mathrm{Re}a^{\mathrm{R}}\mathrm{Im}a^{\mathrm{R}} - 2\Delta\phi\left(\mathrm{Re}a^{\mathrm{R}}\frac{\partial \mathrm{Im}a^{\mathrm{R}}}{\partial p_{\mathrm{F}x}} + \mathrm{Im}a^{\mathrm{R}}\frac{\partial \mathrm{Re}a^{\mathrm{R}}}{\partial p_{\mathrm{F}x}}\right) - \frac{\partial v_{\mathrm{F}x}}{\partial p_{\mathrm{F}x}}\frac{\partial \mathrm{Im}a^{\mathrm{R}}}{\partial x} \tag{D.31b}$$

D.5 Spatial and momentum derivatives of the Green's functions

In the following, we calculate the variations of the Green's function in terms of space and momentum variables

$$\frac{\partial f_0^{\mathrm{R}}}{\partial x} = \frac{2}{(1+a^{\mathrm{R}}\bar{a}^{\mathrm{R}})}\left(\frac{\partial a^{\mathrm{R}}}{\partial x} - a^{\mathrm{R}2}\frac{\partial \bar{a}^{\mathrm{R}}}{\partial x}\right) \tag{D.32}$$

$$\begin{aligned}(1+a^{\mathrm{R}}\bar{a}^{\mathrm{R}})^2 &= (1+w_r+iw_i)^2 \\ &= w_{4r}+iw_{4i}\end{aligned} \tag{D.33}$$

Let

$$w_{4r} = (1+w_r)^2 - w_i^2, \quad w_{4i} = 2(1+w_r)w_i, \tag{D.34}$$

We then rewrite $\frac{\partial f_0^{\mathrm{R}}}{\partial x}$ as

$$\begin{aligned}a^{\mathrm{R}2}\frac{\partial \bar{a}^{\mathrm{R}}}{\partial x} &= (\mathrm{Re}a^{\mathrm{R}2} - \mathrm{Im}a^{\mathrm{R}2} + 2i\mathrm{Re}a^{\mathrm{R}}\mathrm{Im}a^{\mathrm{R}})\left(\frac{\partial \mathrm{Re}\bar{a}^{\mathrm{R}}}{\partial x} - i\frac{\partial \mathrm{Im}\bar{a}^{\mathrm{R}}}{\partial x}\right) \\ &= w_{5r}+iw_{5i}\end{aligned} \tag{D.35}$$

$$\begin{aligned}w_{5r} &= (\mathrm{Re}a^{\mathrm{R}2} - \mathrm{Im}a^{\mathrm{R}2})\frac{\partial \mathrm{Re}\bar{a}^{\mathrm{R}}}{\partial x} + 2\mathrm{Re}a^{\mathrm{R}}\mathrm{Im}a^{\mathrm{R}}\frac{\partial \mathrm{Im}\bar{a}^{\mathrm{R}}}{\partial x}, \\ w_{5i} &= 2\mathrm{Re}a^{\mathrm{R}}\mathrm{Im}a^{\mathrm{R}}\frac{\partial \mathrm{Re}\bar{a}^{\mathrm{R}}}{\partial x} - (\mathrm{Re}a^{\mathrm{R}2} - \mathrm{Im}a^{\mathrm{R}2})\frac{\partial \mathrm{Im}\bar{a}^{\mathrm{R}}}{\partial x}\end{aligned} \tag{D.36}$$

$$\begin{aligned}\frac{\partial f_0^{\mathrm{R}}}{\partial x} &= \frac{2}{w_{4r}+iw_{4i}}\left(\frac{\partial \mathrm{Re}a^{\mathrm{R}}}{\partial x} - w_{5r} + i\frac{\partial \mathrm{Im}a^{\mathrm{R}}}{\partial x} - iw_{5i}\right) \\ &= \frac{2}{w_4}(w_{4r}-iw_{4i})\left(\frac{\partial \mathrm{Re}a^{\mathrm{R}}}{\partial x} - w_{5r} + i\frac{\partial \mathrm{Im}a^{\mathrm{R}}}{\partial x} - iw_{5i}\right),\end{aligned} \tag{D.37}$$

Using

$$w_4 = w_{4r}^2 + w_{4i}^2, \tag{D.38}$$

we have

$$\begin{aligned}\frac{\partial f_0^{\mathrm{R}}}{\partial x} =& \frac{2}{w_4}\left[w_{4r}\left(\frac{\partial \mathrm{Re}a^{\mathrm{R}}}{\partial x} - w_{5r}\right) + w_{4i}\left(\frac{\partial \mathrm{Im}a^{\mathrm{R}}}{\partial x} - w_{5i}\right)\right] \\ &+ \frac{2i}{w_4}\left[w_{4r}\left(\frac{\partial \mathrm{Im}a^{\mathrm{R}}}{\partial x} - w_{5i}\right) - w_{4i}\left(\frac{\partial \mathrm{Re}a^{\mathrm{R}}}{\partial x} - w_{5r}\right)\right]\end{aligned} \tag{D.39}$$

$$\frac{\partial f_0^{\rm R}}{\partial p_{{\rm F}x}} = \frac{2}{(1+a^{\rm R}\bar{a}^{\rm R})}\left(\frac{\partial a^{\rm R}}{\partial p_{{\rm F}x}} - a^{\rm R2}\frac{\partial \bar{a}^{\rm R}}{\partial p_{{\rm F}x}}\right) \tag{D.40}$$

$$\begin{aligned} w_{6r} &= ({\rm Re}a^{\rm R2} - {\rm Im}a^{\rm R2})\frac{\partial {\rm Re}\bar{a}^{\rm R}}{\partial p_{{\rm F}x}} + 2{\rm Re}a^{\rm R}{\rm Im}a^{\rm R}\frac{\partial {\rm Im}\bar{a}^{\rm R}}{\partial p_{{\rm F}x}}, \\ w_{6i} &= 2{\rm Re}a^{\rm R}{\rm Im}a^{\rm R}\frac{\partial {\rm Re}\bar{a}^{\rm R}}{\partial p_{{\rm F}x}} - ({\rm Re}a^{\rm R2} - {\rm Im}a^{\rm R2})\frac{\partial {\rm Im}\bar{a}^{\rm R}}{\partial p_{{\rm F}x}} \end{aligned} \tag{D.41}$$

$$\begin{aligned} \frac{\partial f_0^{\rm R}}{\partial p_{{\rm F}x}} =& \frac{2}{w_4}\left[w_{4r}\left(\frac{\partial {\rm Re}a^{\rm R}}{\partial p_{{\rm F}x}} - w_{6r}\right) + w_{4i}\left(\frac{\partial {\rm Im}a^{\rm R}}{\partial p_{{\rm F}x}} - w_{6i}\right)\right] \\ &+ \frac{2i}{w_4}\left[w_{4r}\left(\frac{\partial {\rm Im}a^{\rm R}}{\partial p_{{\rm F}x}} - w_{6i}\right) - w_{4i}\left(\frac{\partial {\rm Re}a^{\rm R}}{\partial p_{{\rm F}x}} - w_{6r}\right)\right] \end{aligned} \tag{D.42}$$

We note the following relation:

$$\overline{\frac{\partial f_0^{\rm R}}{\partial p_{{\rm F}x}}} = -\frac{\partial \bar{f}_0^{\rm R}}{\partial p_{{\rm F}x}}. \tag{D.43}$$

D.6 Solution near the surface

We calculate the $p_{{\rm F}x}$ derivatives as follows;

$$\frac{\partial a^{\rm R}}{\partial p_{{\rm F}x}} \approx \frac{\partial a^{\rm R(0)}}{\partial p_{{\rm F}x}} + \frac{\partial a^{\rm R(1)}}{\partial p_{{\rm F}x}} \tag{D.44}$$

The first term is calculated as thus,

$$\begin{aligned} \frac{\partial a^{\rm R(0)}}{\partial p_{{\rm F}x}} &= -\frac{a^{\rm R(0)2}}{\sqrt{(-i\varepsilon+\eta)^2+\Delta^2\phi^2}}\Delta\frac{\partial \phi}{\partial p_{{\rm F}x}} + \frac{a^{\rm R(0)}}{\phi}\frac{\partial \phi}{\partial p_{{\rm F}x}} \\ &= -\frac{{\rm Re}a^{\rm R(0)2} - {\rm Im}a^{\rm R(0)2} + 2i{\rm Re}a^{\rm R(0)}{\rm Im}a^{\rm R(0)}}{w_{3r}+iw_{3i}}\Delta\frac{\partial \phi}{\partial p_{{\rm F}x}} \\ &+ \frac{{\rm Re}a^{\rm R(0)}}{\phi}\frac{\partial \phi}{\partial p_{{\rm F}x}} + i\frac{{\rm Im}a^{\rm R(0)}}{\phi}\frac{\partial \phi}{\partial p_{{\rm F}x}} \end{aligned} \tag{D.45}$$

$$\begin{aligned} \frac{\partial a^{\rm R(0)}}{\partial p_{{\rm F}x}} =& -\frac{1}{w_3}\left[w_{3r}({\rm Re}a^{\rm R(0)2} - {\rm Im}a^{\rm R(0)2}) + 2w_{3i}{\rm Re}a^{\rm R(0)}{\rm Im}a^{\rm R(0)}\right]\Delta\frac{\partial \phi}{\partial p_{{\rm F}x}} \\ &+ \frac{{\rm Re}a^{\rm R(0)}}{\phi}\frac{\partial \phi}{\partial p_{{\rm F}x}} \\ &- \frac{i}{w_3}\left[2w_{3r}{\rm Re}a^{\rm R(0)}{\rm Im}a^{\rm R(0)} - w_{3i}({\rm Re}a^{\rm R(0)2} - {\rm Im}a^{\rm R(0)2})\right]\Delta\frac{\partial \phi}{\partial p_{{\rm F}x}} \\ &+ i\frac{{\rm Im}a^{\rm R(0)}}{\phi}\frac{\partial \phi}{\partial p_{{\rm F}x}} \end{aligned} \tag{D.46}$$

while the derivative of the correction term is given by

$$\begin{aligned}\frac{\partial a^{\mathrm{R}(1)}}{\partial p_{\mathrm{F}x}} =&\frac{v_{\mathrm{F}x}\Delta^2\phi}{4\left[(-i\varepsilon+\eta)^2+\Delta^2\phi^2\right]^2}\frac{\partial\phi}{\partial p_{\mathrm{F}x}}\frac{\partial a^{\mathrm{R}(0)}}{\partial x}\\ &-\frac{1}{2\sqrt{(-i\varepsilon+\eta)^2+\Delta^2\phi^2}}\left(\frac{\partial v_{\mathrm{F}x}}{\partial p_{\mathrm{F}x}}\frac{\partial a^{\mathrm{R}(0)}}{\partial x}+v_{\mathrm{F}x}\frac{\partial^2 a^{\mathrm{R}(0)}}{\partial x\partial p_{\mathrm{F}x}}\right)\\ =&\frac{v_{\mathrm{F}x}\Delta^2\phi}{4(w_{1r}+iw_{1i})^2}\frac{\partial\phi}{\partial p_{\mathrm{F}x}}\frac{\partial a^{\mathrm{R}(0)}}{\partial x}-\frac{1}{2(w_{3r}+iw_{3i})}\left(\frac{\partial v_{\mathrm{F}x}}{\partial p_{\mathrm{F}x}}\frac{\partial a^{\mathrm{R}(0)}}{\partial x}+v_{\mathrm{F}x}\frac{\partial^2 a^{\mathrm{R}(0)}}{\partial x\partial p_{\mathrm{F}x}}\right),\end{aligned} \tag{D.47}$$

where

$$w_{7r}=w_{1r}^2-w_{1i}^2,\quad w_{7i}=2w_{1r}w_{1i},\quad w_7=w_{7r}^2+w_{7i}^2 \tag{D.48}$$

$$\begin{aligned}\frac{\partial a^{\mathrm{R}(1)}}{\partial p_{\mathrm{F}x}} =&\frac{v_{\mathrm{F}x}\Delta^2\phi}{4w_7}(w_{7r}-iw_{7i})\frac{\partial\phi}{\partial p_{\mathrm{F}x}}\left(\frac{\partial\mathrm{Re}a^{\mathrm{R}(0)}}{\partial x}+i\frac{\partial\mathrm{Im}a^{\mathrm{R}(0)}}{\partial x}\right)\\ &-\frac{w_{3r}-iw_{3i}}{2w_3}\frac{\partial v_{\mathrm{F}x}}{\partial p_{\mathrm{F}x}}\left(\frac{\partial\mathrm{Re}a^{\mathrm{R}(0)}}{\partial x}+i\frac{\partial\mathrm{Im}a^{\mathrm{R}(0)}}{\partial x}\right)\\ &-v_{\mathrm{F}x}\frac{w_{3r}-iw_{3i}}{2w_3}\left(\frac{\partial^2\mathrm{Re}a^{\mathrm{R}(0)}}{\partial x\partial p_{\mathrm{F}x}}+i\frac{\partial^2\mathrm{Im}a^{\mathrm{R}(0)}}{\partial x\partial p_{\mathrm{F}x}}\right)\end{aligned} \tag{D.49}$$

$$\begin{aligned}\frac{\partial a^{\mathrm{R}(1)}}{\partial p_{\mathrm{F}x}} =&\frac{v_{\mathrm{F}x}\Delta^2\phi}{4w_7}\frac{\partial\phi}{\partial p_{\mathrm{F}x}}\left(w_{7r}\frac{\partial\mathrm{Re}a^{\mathrm{R}(0)}}{\partial x}+w_{7i}\frac{\partial\mathrm{Im}a^{\mathrm{R}(0)}}{\partial x}\right)\\ &-\frac{1}{2w_3}\left[\frac{\partial v_{\mathrm{F}x}}{\partial p_{\mathrm{F}x}}\left(w_{3r}\frac{\partial\mathrm{Re}a^{\mathrm{R}(0)}}{\partial x}+w_{3i}\frac{\partial\mathrm{Im}a^{\mathrm{R}(0)}}{\partial x}\right)\right]\\ &-v_{\mathrm{F}x}\frac{1}{2w_3}\left(w_{3r}\frac{\partial^2\mathrm{Re}a^{\mathrm{R}(0)}}{\partial x\partial p_{\mathrm{F}x}}+w_{3i}\frac{\partial^2\mathrm{Im}a^{\mathrm{R}(0)}}{\partial x\partial p_{\mathrm{F}x}}\right)\\ &+i\frac{v_{\mathrm{F}x}\Delta^2\phi}{4w_7}\frac{\partial\phi}{\partial p_{\mathrm{F}x}}\left(w_{7r}\frac{\partial\mathrm{Im}a^{\mathrm{R}(0)}}{\partial x}-w_{7i}\frac{\partial\mathrm{Re}a^{\mathrm{R}(0)}}{\partial x}\right)\\ &-\frac{i}{2w_3}\left[\frac{\partial v_{\mathrm{F}x}}{\partial p_{\mathrm{F}x}}\left(w_{3r}\frac{\partial\mathrm{Im}a^{\mathrm{R}(0)}}{\partial x}-w_{3i}\frac{\partial\mathrm{Re}a^{\mathrm{R}(0)}}{\partial x}\right)\right]\\ &-v_{\mathrm{F}x}\frac{i}{2w_3}\left(w_{3r}\frac{\partial^2\mathrm{Im}a^{\mathrm{R}(0)}}{\partial x\partial p_{\mathrm{F}x}}-w_{3i}\frac{\partial^2\mathrm{Re}a^{\mathrm{R}(0)}}{\partial x\partial p_{\mathrm{F}x}}\right)\end{aligned} \tag{D.50}$$

We calculate the second derivative $\partial^2 a^{\mathrm{R}(0)}/\partial x \partial p_{\mathrm{F}x}$ as

$$\begin{aligned}\frac{\partial^2 a^{\mathrm{R}(0)}}{\partial x \partial p_{\mathrm{F}x}} =& \frac{a^{\mathrm{R}(0)2}}{[(-i\varepsilon+\eta)^2+\Delta^2\phi^2]^{3/2}}\Delta^2\phi^2\frac{d\Delta}{dx}\frac{\partial \phi}{\partial p_{\mathrm{F}x}} \\ &- 2\frac{a^{\mathrm{R}(0)}}{\sqrt{(-i\varepsilon+\eta)^2+\Delta^2\phi^2}}\frac{\partial a^{\mathrm{R}(0)}}{\partial x}\Delta\frac{\partial \phi}{\partial p_{\mathrm{F}x}} \\ &- \frac{a^{\mathrm{R}(0)2}}{\sqrt{(-i\varepsilon+\eta)^2+\Delta^2\phi^2}}\frac{d\Delta}{dx}\frac{\partial \phi}{\partial p_{\mathrm{F}x}} + \frac{\partial a^{\mathrm{R}(0)}}{\partial x}\frac{1}{\phi}\frac{\partial \phi}{\partial p_{\mathrm{F}x}} \\ =& \frac{a^{\mathrm{R}(0)2}}{(w_{1r}+iw_{1i})(w_{3r}+iw_{3i})}\Delta^2\phi^2\frac{d\Delta}{dx}\frac{\partial \phi}{\partial p_{\mathrm{F}x}} \\ &- 2\frac{a^{\mathrm{R}(0)}}{w_{3r}+iw_{3i}}\frac{\partial a^{\mathrm{R}(0)}}{\partial x}\Delta\frac{\partial \phi}{\partial p_{\mathrm{F}x}} \\ &- \frac{a^{\mathrm{R}(0)2}}{w_{3r}+iw_{3i}}\frac{d\Delta}{dx}\frac{\partial \phi}{\partial p_{\mathrm{F}x}} + \frac{\partial a^{\mathrm{R}(0)}}{\partial x}\frac{1}{\phi}\frac{\partial \phi}{\partial p_{\mathrm{F}x}} \end{aligned} \tag{D.51}$$

Using the substitutions

$$w_{8r} = w_{1r}w_{3r} - w_{1i}w_{3i}, \quad w_{8i} = w_{1r}w_{3i} + w_{1i}w_{3r}, \quad w_8 = w_{8r}^2 + w_{8i}^2, \tag{D.52}$$

we rewrite the it as

$$\begin{aligned}\frac{\partial^2 a^{\mathrm{R}(0)}}{\partial x \partial p_{\mathrm{F}x}} =& \frac{w_{8r}-iw_{8i}}{w_8}(\mathrm{Re}a^{\mathrm{R}(0)2} - \mathrm{Im}a^{\mathrm{R}(0)2} + 2i\mathrm{Re}a^{\mathrm{R}(0)}\mathrm{Im}a^{\mathrm{R}(0)})\Delta^2\phi^2\frac{d\Delta}{dx}\frac{\partial \phi}{\partial p_{\mathrm{F}x}} \\ &- 2\frac{w_{3r}-iw_{3i}}{w_3}\left(\mathrm{Re}a^{\mathrm{R}(0)}\frac{\partial \mathrm{Re}a^{\mathrm{R}(0)}}{\partial x} - \mathrm{Im}a^{\mathrm{R}(0)}\frac{\partial \mathrm{Im}a^{\mathrm{R}(0)}}{\partial x}\right. \\ &\qquad \left. + i\mathrm{Re}a^{\mathrm{R}(0)}\frac{\partial \mathrm{Im}a^{\mathrm{R}(0)}}{\partial x} + i\mathrm{Im}a^{\mathrm{R}(0)}\frac{\partial \mathrm{Re}a^{\mathrm{R}(0)}}{\partial x}\right)\Delta\frac{\partial \phi}{\partial p_{\mathrm{F}x}} \\ &- \frac{w_{3r}-iw_{3i}}{w_3}(\mathrm{Re}a^{\mathrm{R}(0)2} - \mathrm{Im}a^{\mathrm{R}(0)2} + 2i\mathrm{Re}a^{\mathrm{R}(0)}\mathrm{Im}a^{\mathrm{R}(0)})\frac{d\Delta}{dx}\frac{\partial \phi}{\partial p_{\mathrm{F}x}} \\ &+ \frac{\partial \mathrm{Re}a^{\mathrm{R}(0)}}{\partial x}\frac{1}{\phi}\frac{\partial \phi}{\partial p_{\mathrm{F}x}} + i\frac{\partial \mathrm{Im}a^{\mathrm{R}(0)}}{\partial x}\frac{1}{\phi}\frac{\partial \phi}{\partial p_{\mathrm{F}x}} \end{aligned} \tag{D.53}$$

Finally, it takes the form

$$
\begin{aligned}
\frac{\partial^2 a^{\mathrm{R}(0)}}{\partial x \partial p_{\mathrm{F}x}} =& \frac{1}{w_8}\left[w_{8r}(\mathrm{Re}a^{\mathrm{R}(0)2}-\mathrm{Im}a^{\mathrm{R}(0)2})+2w_{8i}\mathrm{Re}a^{\mathrm{R}(0)}\mathrm{Im}a^{\mathrm{R}(0)}\right]\Delta^2\phi^2\frac{d\Delta}{dx}\frac{\partial\phi}{\partial p_{\mathrm{F}x}}\\
&-\frac{2}{w_3}\left[w_{3r}\left(\mathrm{Re}a^{\mathrm{R}(0)}\frac{\partial \mathrm{Re}a^{\mathrm{R}(0)}}{\partial x}-\mathrm{Im}a^{\mathrm{R}(0)}\frac{\partial \mathrm{Im}a^{\mathrm{R}(0)}}{\partial x}\right)\right.\\
&\qquad\left.+w_{3i}\left(\mathrm{Re}a^{\mathrm{R}(0)}\frac{\partial \mathrm{Im}a^{\mathrm{R}(0)}}{\partial x}+\mathrm{Im}a^{\mathrm{R}(0)}\frac{\partial \mathrm{Re}a^{\mathrm{R}(0)}}{\partial x}\right)\right]\Delta\frac{\partial\phi}{\partial p_{\mathrm{F}x}}\\
&-\frac{1}{w_3}\left[w_{3r}(\mathrm{Re}a^{\mathrm{R}(0)2}-\mathrm{Im}a^{\mathrm{R}(0)2})+2w_{3i}\mathrm{Re}a^{\mathrm{R}(0)}\mathrm{Im}a^{\mathrm{R}(0)}\right]\frac{d\Delta}{dx}\frac{\partial\phi}{\partial p_{\mathrm{F}x}}\\
&+\frac{\partial \mathrm{Re}a^{\mathrm{R}(0)}}{\partial x}\frac{1}{\phi}\frac{\partial\phi}{\partial p_{\mathrm{F}x}}\\
&+\frac{i}{w_8}\left[2w_{8r}\mathrm{Re}a^{\mathrm{R}(0)}\mathrm{Im}a^{\mathrm{R}(0)}-w_{8i}(\mathrm{Re}a^{\mathrm{R}(0)2}-\mathrm{Im}a^{\mathrm{R}(0)2})\right]\Delta^2\phi^2\frac{d\Delta}{dx}\frac{\partial\phi}{\partial p_{\mathrm{F}x}}\\
&-\frac{2i}{w_3}\left[w_{3r}\left(\mathrm{Re}a^{\mathrm{R}(0)}\frac{\partial \mathrm{Im}a^{\mathrm{R}(0)}}{\partial x}+\mathrm{Im}a^{\mathrm{R}(0)}\frac{\partial \mathrm{Re}a^{\mathrm{R}(0)}}{\partial x}\right)\right.\\
&\qquad\left.-w_{3i}\left(\mathrm{Re}a^{\mathrm{R}(0)}\frac{\partial \mathrm{Re}a^{\mathrm{R}(0)}}{\partial x}-\mathrm{Im}a^{\mathrm{R}(0)}\frac{\partial \mathrm{Im}a^{\mathrm{R}(0)}}{\partial x}\right)\right]\Delta\frac{\partial\phi}{\partial p_{\mathrm{F}x}}\\
&-\frac{i}{w_3}\left[2w_{3r}\mathrm{Re}a^{\mathrm{R}(0)}\mathrm{Im}a^{\mathrm{R}(0)}-w_{3i}(\mathrm{Re}a^{\mathrm{R}(0)2}-\mathrm{Im}a^{\mathrm{R}(0)2})\right]\frac{d\Delta}{dx}\frac{\partial\phi}{\partial p_{\mathrm{F}x}}\\
&+i\frac{\partial \mathrm{Im}a^{\mathrm{R}(0)}}{\partial x}\frac{1}{\phi}\frac{\partial\phi}{\partial p_{\mathrm{F}x}}
\end{aligned}\tag{D.54}
$$

D.7 Expression for the LDOS

Using the expansion $g^{\mathrm{R}} = g_0^{\mathrm{R}} + g_1^{\mathrm{R}}$, the local density of states within the augmented quasiclassical theory is given by

$$
N_{\mathrm{s}} = N(0)\left\langle \mathrm{Re}g_0^{\mathrm{R}} + \mathrm{Re}g_1^{\mathrm{R}}\right\rangle_{\mathrm{F}} + N'(0)\varepsilon\left\langle \mathrm{Re}g_0^{\mathrm{R}}\right\rangle_{\mathrm{F}} - N'(0)\frac{\Delta}{2}\left\langle \mathrm{Im}f_0^{\mathrm{R}} + \mathrm{Im}\bar{f}_0^{\mathrm{R}}\right\rangle_{\mathrm{F}} \tag{D.55}
$$

Where g_1^{R} is the first-order quantum correction due to the PPG force and also due to the SDOS pressure, in terms of the quasiclassical parameter, $(k_{\mathrm{F}}\xi_0)^{-1}$.

D.8 g_1^{R} expression

Finally, we can calculate the $\frac{\partial g_1^{\mathrm{R}}}{\partial x}$ and $\frac{\partial \mathrm{Re}g_1^{\mathrm{R}}}{\partial x}$ using

$$
v_{\mathrm{F}x}\frac{\partial g_1^{\mathrm{R}}}{\partial x} = -\frac{i\delta}{2}\frac{d\Delta}{dx}\phi\frac{\partial f_0^{\mathrm{R}}}{\partial p_{\mathrm{F}x}} - \frac{i\delta}{2}\frac{d\Delta}{dx}\phi\frac{\partial \bar{f}_0^{\mathrm{R}}}{\partial p_{\mathrm{F}x}} + \frac{i\delta}{2}\Delta\frac{\partial\phi}{\partial p_{\mathrm{F}x}}\frac{\partial f_0^{\mathrm{R}}}{\partial x} + \frac{i\delta}{2}\Delta\frac{\partial\phi}{\partial p_{\mathrm{F}x}}\frac{\partial \bar{f}_0^{\mathrm{R}}}{\partial x} \tag{D.56}
$$

and

$$
v_{\mathrm{F}x}\frac{\partial \mathrm{Re}g_1^{\mathrm{R}}}{\partial x} = \frac{\delta}{2}\frac{d\Delta}{dx}\phi\frac{\partial \mathrm{Im}f_0^{\mathrm{R}}}{\partial p_{\mathrm{F}x}} - \frac{\delta}{2}\frac{d\Delta}{dx}\phi\frac{\partial \mathrm{Im}\bar{f}_0^{\mathrm{R}}}{\partial p_{\mathrm{F}x}} - \frac{\delta}{2}\Delta\frac{\partial\phi}{\partial p_{\mathrm{F}x}}\frac{\partial \mathrm{Im}f_0^{\mathrm{R}}}{\partial x} + \frac{\delta}{2}\Delta\frac{\partial\phi}{\partial p_{\mathrm{F}x}}\frac{\partial \mathrm{Im}\bar{f}_0^{\mathrm{R}}}{\partial x} \tag{D.57}
$$

References

[1] E. H. Hall, Am. J. Maths. **2**, 287 (1879).

[2] R. E. Prange and S. M. Girvin (eds.), *The Quantum Hall Effect* (Springer, New York, 1990).

[3] F. London, *Superfluids* (Dover, New York, 1961), Vol. 1, p. 56.

[4] T. Kita, Phys. Rev. B **64**, 054503 (2001).

[5] H. Ueki, W. Kohno, and T. Kita, J. Phys. Soc. Jpn. **85**, 064702 (2016).

[6] N. B. Kopnin, J. Low Temp. Phys. **97**, 157 (1994).

[7] E. Arahata and Y. Kato, J. Low. Temp. Phys. **175**, 364 (2014).

[8] M. Ohuchi, H. Ueki, and T. Kita, J. Phys. Soc. Jpn. **86**, 073702 (2017).

[9] D. I. Khomskii and F. V. Kusmartsev, Phys. Rev. B **46**, 14245 (1992).

[10] D. I. Khomskii and A. Freimuth, Phys. Rev. B **75**, 1384 (1995).

[11] H. Ueki, M. Ohuchi, and T. Kita, J. Phys. Soc. Jpn. **87**, 044704 (2018).

[12] G. Eilenberger, Z. Phys. **214**, 195 (1968).

[13] T. Kita, *Statistical Mechanics of Superconductivity* (Springer, Tokyo, 2015).

[14] T. Kita, Phys. Rev. B **79**, 024521 (2009).

[15] Y. Masaki, Phys. Rev. B **99**, 054512 (2019).

[16] W. Kohno, H. Ueki, and T. Kita, J. Phys. Soc. Jpn. **85**, 083705 (2016).

[17] W. Kohno, H. Ueki, and T. Kita, J. Phys. Soc. Jpn. **86**, 023702 (2017).

[18] A. Furusaki, M. Matsumoto, and M. Sigrist, Phys. Rev. B **64**, 054514 (2001).

[19] T. Emig, K. Samokhin, and S. Scheidl, Phys. Rev. B **56**, 8386 (1997).

[20] L. J. Buchholtz, M. Palumbo, D. Rainer, and J. A. Sauls, J.Low Temp. Phys. **101**, 1079 (1995); **101**, 1097 (1995).

[21] Y. Nagato and K. Nagai Phys. Rev. B **51**, 16254 (1995).

[22] X. Yan and H. Iyetomi Phys. Rev. B **57**, 7944 (1998).

[23] C. R. Hu, Phys. Rev. Lett. **72**, 1526 (1994).

[24] J. Yang and C. R. Hu, Phys. Rev. B **50**, 16766 (1994).

[25] M. Fogelström, D. Rainer, and J. A. Sauls Phys. Rev. Lett. **79**, 281 (1997).

[26] Y. Tanuma, Y. Tanaka, and M. Yamashiro, Phys. Rev. B **57**, 7997 (1998).

[27] T. Lofwander, V. S. Shumeiko, and G. Wendin, Supercond. Sci. Technol. **14**, R53 (2001).

[28] J. Geerk, X. X. Xi, and G. Linker, Z. Phys. **73**, 329 (1988).

[29] J. Lesueur, L. H. Greene, W. L. Feldmann, and A. Inam, Physica (Amsterdam) **191C**, 325 (1992).

[30] M. Covington, R. Scheuerer, K. Bloom, and L. H. Greene, Appl. Phys. Lett. **68**, 1717 (1996).

[31] L. Alff, A. Beck, R. Gross, A. Marx, S. Kleefisch, Th. Bauch, H. Sato, M. Naito, and G. Koren, Phys. Rev. B **58**, 11197 (1998).

[32] C. Caroli, P. G. de Gennes, and J. Matricon, Phys. Rev. Lett. **9**, 307 (1964).

[33] N. Hayashi, M. Ichioka, and K. Machida, J. Phys. Soc. Jpn. **67**, 3368 (1998).

[34] J.Bok and J. Klein, Phys. Rev. Lett. **20**, 660 (1968).

[35] T. D. Morris and J. B. Brown, Physica (Amsterdam) **55**, 760 (1971).

[36] H. Kontani, K. Kanki, and K. Ueda, Phys. Rev. B **59**, 14723 (1999).

[37] H. Kontani, *Transport Phenomena in Strongly Correlated Fermi Liquids* (Springer-Verlag Berlin and Heidelberg GmbH & Co. K, 2013).

[38] Y. Nagato, K. Nagai, and J. Hara, J. Low Temp. Phys. **93**, 33 (1993).

[39] N. Schopohl and K. Maki, Phys. Rev. B **52**, 490 (1995).

[40] N. Schopohl, arXiv:cond-mat/9804064.

[41] L. Kramer and W. Pesch, Z. Phys. **269**, 59 (1974).

[42] S. G. Doettinger, R. P. Huebener, and S. Kittelberger, Phys. Rev. B **55**, 6044 (1997).

[43] A. Peronio and F. J. Giessibl, Phys. Rev. B **94**, 094503 (2016).

[44] Y. Nagato, S. Higashitani, K. Yamada, and K. Nagai, J. Low Temp. Phys. **103**, 1 (1996).

[45] S.-I. Suzuki and Y. Asano, Phys. Rev. B **94**, 155302 (2016).

[46] X. Wang, Z. Wang, and C. Kallin, Phys. Rev. B **98**, 094501 (2018).

[47] L. P. Gor'kov, Zh. Eksp. Teor. Fiz. **36**, 1918 (1959) [Sov. Phys. JETP **9**, 1364 (1959)]; Zh. Eksp. Teor. Fiz. **37**, 1407 (1959) [Sov. Phys. JETP **10**, 998 (1960)].

[48] E. P. Wigner, Phys. Rev. **40**, 749 (1932).